UNIVERSITA' DEGLI STUDI DI MILANO-BICOCCA

Facoltà di Scienze MM. FF. NN.

Dipartimento di Biotecnologie e Bioscienze

Dottorato di Ricerca in Biotecnologie Industriali - XXIII Ciclo

Nutritional modulation of cell size at S phase initiation in the budding yeast *Saccharomyces Cerevisiae*: a role for glucose sensing and the cyclin dependent kinase inhibitor *FAR1*

Laura Gotti

TUTOR: Prof. Marco Vanoni

Anno Accademico 2009-2010

Dottorato di Ricerca in Biotecnologie Industriali – XXIII ciclo

Index

Index

Introduction

CELL CYCLE EVENTS

The discovery that we are all made of cells (Schleiden, 1838; Schwann, 1839) was possibly the most important biological discovery of the 19th century. All living organisms on this planet descend through an unbroken series of divisions from an ancestral cell that came into being over a billion years ago.

In eukaryotes, cell cycle is conventionally divided in temporally distinct phases: G_1 (Gap1) phase precedes the initiation of chromosomal DNA replication; during S phase the replication of genetic material takes place; a G_2 (Gap2) phase then follows and a final M phase in which mitosis, nuclear division and cytokinesis occur (figure 1). Thus two main cellular events, DNA replication and mitosis are temporally separated by two gap phases.

In yeast a regulatory area of the cell cycle, called Start, is positioned immediately before beginning of S phase, at the G_1-S boundary. Start is the set of events, that commits a cell to a new round of division. Immediately after Start, a number of semi-independent, cell cycle-specific processes are set in motion which inevitably lead to division. These processes include budding, DNA synthesis, and spindle pole body duplication. Budding is the characteristic way of *S. cerevisiae* of dividing: a bud emerges from the mother cell, it grows attached to it until it reaches a certain size and then it detaches after cytokinesis as a smaller cell. So cell division in budding yeast is asymmetric and initiation of DNA replication coincides with emergence of the bud.

At Start, a yeast cell coordinates growth with division. On average, there must be exactly one cell division for each doubling in cell mass; otherwise, cells would become inexorably larger or smaller. Start is also important in choosing between different developmental fates, such as mitotic division or mating. Before Start, environmental signals can direct a cell (if aploid) to mate or (if diploid) to sporulate, but after Start, cell is committed to mitosis (figure 1).

Originally Start has been defined in an operationally way as the position of arrest of different conditions and mutations, namely nutrient limitation, mating pheromone exposure, and a number of cdc (cell division cycle) mutations at the restrictive temperature (Hartwell et al., 1974).

At least two different steps regarding Start were considered: Start A and Start B. Progress through Start A requires functioning of the RAS-adenylate cyclase pathway, which regulates the production of cyclic AMP (cAMP). Instead, the completion of Start B is critically dependent on activation of the cyclin dependent kinase (Cdk) Cdc28. Both these two sub-steps of Start are defined by different arrest phenotype: Start A mutant morphology resembles that of cells arrested under conditions of limited nutrient availability; Start B mutant morphology is characteristic of cells that have arrested in response to treatment with mating pheromone (Sherlock and Rosamond, 1993).
Start A functions are necessary to execute Start B, the true cell cycle commitment point. At Start B cells block cycle in response to mating factors but cytoplasmic growth proceeds unaffected (Baroni et al., 1994).

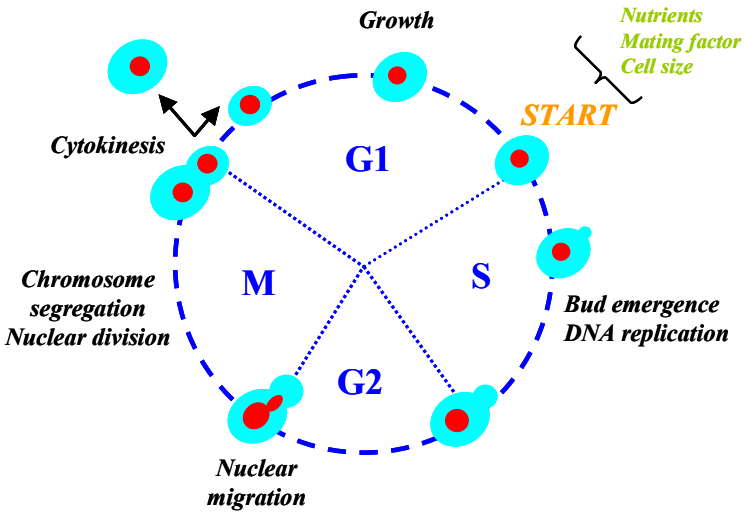

Figure 1. **The cell division cycle in budding yeast.**

CELL CYCLE REGULATION IN S. CEREVISIAE: THE CYCLIN DEPENDENT KINASE Cdc28 (Cdk1)

As the name implies, the Cdks are protein kinases that are dependent for their activity on the binding of a cyclin subunit. Full activation of Cdks generally requires two events: cyclin binding and stimulatory phosphorylation. This activation is opposed by the binding of inhibitory proteins, the Ckis (Cdk Inhibitors), and by inhibitory phosphorylation events. Regulators of Cdk activity are under complex transcriptional, translational, and proteolytic controls that vary from species to species.

S. cerevisiae possesses at least four Cdks other than Cdc28: Pho85, Kin28p Srb10, and Ctk1. Cdc28 is the best studied Cdk by far and it is the central regulator of the major events of the yeast cell division cycle; the gene encoding Cdc28 is essential and most of the original discovered *cdc28* mutants arrest cell cycle progression at Start when shifted to restrictive conditions (Hartwell, 1974).
The complexes of Pho85 with Pcl1 and Pcl2 cyclins play a role in G_1 passage: Pho85 is required for commitment in cell cycle in particular conditions, i.e. absence of G_1 specific activator subunits of Cdc28, the cyclins Cln1 and Cln2 (Measday et al., 1997). The other Cdks are all involved in regulating transcription (Lee and Greenleaf 1991 Cismowski et al., 1995).

Cdc28 is subject to mechanisms of regulation that can be divided in the following: activation by cyclins, activation by phosphorylation, inhibition by stoichiometric inhibitors cyclin dependent kinase inhibitors (Cki), inhibition by phosphorylation.

Activation by cyclins

Cyclin-dependent kinases (Cdks) control progression through the eukaryotic cell cycle. Cdks are serine and threonine kinases, and their actions are dependent on associations with their activating subunits, cyclins.
Cyclin abundance is regulated by protein synthesis and degradation; the activity of Cdks is therefore regulated to a large degree by the presence of different cyclins. In the budding yeast *S. cerevisiae*, a single Cdk, Cdc28 (also call Cdk1), associates with multiple cyclins to regulate the cell cycle.
Cyclin specificity can be deduced from a genetic requirement for a specific subset of cyclins for a cell cycle event to occur (figure 2).

For example, advancement through G_1 phase of the cell cycle, which involves bud emergence, spindle pole body (SPB) duplication and the activation of subsequently expressed cyclins, requires at least one of the G_1-phase cyclins Cln1, Cln2 or Cln3.

In the absence of *CLN1-3*, G_1 arrest occurs. Following Cln function, efficient initiation of DNA replication and progression through S phase requires the early-expressed B-type cyclins Clb5 and Clb6. In their absence, the B-type cyclins Clb1-4 will drive a late initiation of DNA replication.
The B-type cyclins Clb1-4 are required for mitotic events, such as spindle morphogenesis; these cyclins also prevent mitotic exit and cytokinesis, and therefore, mitotic cyclin activity must be down regulated for cell division to be completed.

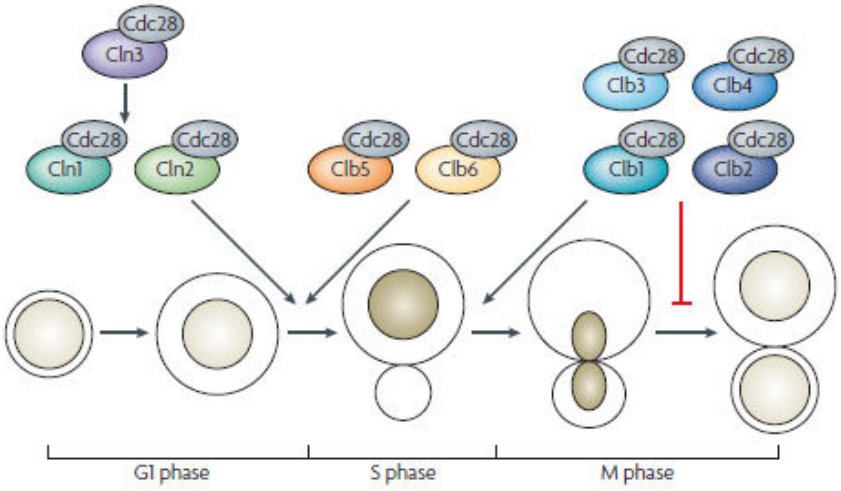

Figure 2. **Cyclins in the budding yeast cell cycle.**
Budding yeast cyclins activate a single cyclin-dependent kinase (Cdc28). The G_1-phase cyclins (Cln1, Cln2 and Cln3) promote bud emergence, spindle pole body duplication (not shown) and activation of the B-type cyclins. The S-phase cyclins (Clb5 and Clb6) advance DNA replication (shaded nucleus), and the M-phase cyclins (Clb1, Clb2, Clb3 and Clb4) promote spindle formation and the initiation of mitosis. Mitotic cyclins inhibit mitotic exit and cell division. Following cytokinesis, a mother and daughter cell are generated
(From Bloom and Cross, 2007).

Transcriptional regulation of cyclins

A crucial mechanism for cyclin specificity is the differential regulation of G_1 and B-type cyclins at the level of transcription during the cell cycle. Transcription of the *CLN3* gene is detectable throughout the cell cycle, but peaks in late M-early G_1, whereas the transcription of the *CLN1* and *CLN2* genes peaks during G_1-S. Transcription of the *CLB5* and *CLB6* genes also peak at G_1-S, followed by the transcription of the *CLB3* and *CLB4* genes and then the transcription of the *CLB1* and *CLB2* genes.
Transcription of early-expressed cyclins is largely controlled by the heterodimeric transcription factor SBF, which is composed of Swi4 and Swi6, and the related MBF transcription factor, which is composed of Mbp1 and Swi6.

Cln3-Cdc28 phosphorylates Whi5, a transcriptional repressor of SBF, to induce its nuclear export and allows for *CLN1* and *CLN2* transcription to be induced (Costanzo, et al.2004; de Bruin et al., 2004).
The phosphorylation of Whi5 by Cln3-Cdc28 early in the cell cycle probably reflects, at least in part, the fact that Cln3 is the only cyclin that is expressed at this time. Cln1-, Cln2- and Clb5-directed Cdc28 activity can also phosphorylate Whi5, which has the potential to provide a positive-feedback loop for their expression (Dirick and Nasmyth 1991) (figure 3).

An additional level of cyclin-specific regulation of SBF and MBF is provided by Clb6-Cdc28, which phosphorylates Swi6 to promote its nuclear export. Biochemical evidence indicates that this is due to the intrinsic specificity of Clb6, although the responsible sequences in Clb6 have not been mapped. Therefore, the ability of different cyclins to bind to specific targets is an additional cyclin-specific mechanism for transcriptional control.
Later in the cell cycle, Clb2 can specifically inactivate SBF-mediated gene expression, which correlates with the ability of Clb2 to bind to Swi4 (Amon et al., 1993).
Clb3 and Clb4, are much less capable of turning off SBF, which indicates some intrinsic difference in the protein structure of Clb2 (Cross et al., 2002).
The transcription factor Mcm1 recruits the forkhead transcription factor Fkh2 and the co-activator Ndd1 to regulate the expression of *CLB2*.
Clb2-Cdc28 phosphorylates Ndd1, which is important for its recruitment to the *CLB2* gene promoter (Reynolds et al., 2003; Darieva, et al., 2003) and phosphorylates Fkh2, which enhances the interaction of Fkh2 with Ndd1.

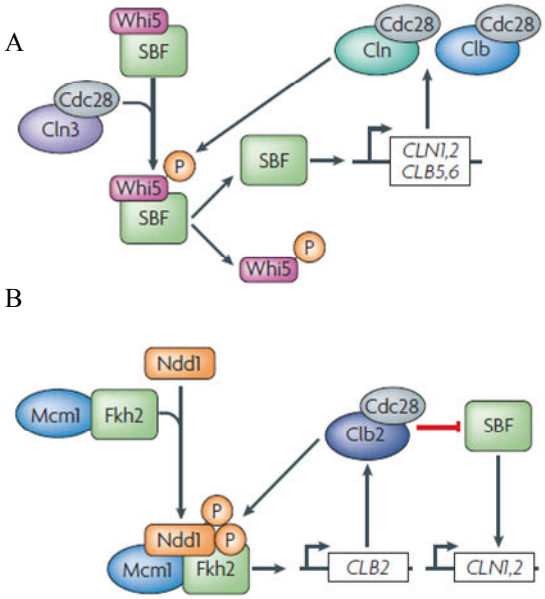

Figure 3. **Transcriptional regulation of cyclins.**
A) The transcription repressor Whi5 inhibits the activity of the SBF transcription factor. Phosphorylation of Whi5 by Cln3-Cdc28 induces the nuclear export of Whi5 and activates SBF, which induces the transcription of the genes that encode Cln1, Cln2, Clb5 and Clb6. Cln-Cdc28 and Clb-Cdc28 phosphorylate Whi5, which might provide a positive-feedback loop.
B) The co-activator Ndd1 recruits minichromosome maintenance-1 (Mcm1) and the transcription factor Fkh2 for the activation of the gene that encodes Clb2. Phosphorylation of Ndd1 and Fkh2 by Clb2-Cdc28 promotes Ndd1-dependent recruitment of Mcm1-Fkh2 to the promoter of *CLB2*. Clb2-Cdc28 also phosphorylates and inhibits SBF to repress the transcription of G_1-phase cyclins.
(From Bloom and Cross, 2007).

Activation by phosphorylation

The crystal structure of human Cdk2, critical for G_1- and S-phase progression, has been solved and has been taken as a model for other Cdks, including Cdc28.
Full activation of Cdk-cyclin complexes requires phosphorylation in the so called T loop at position 169 (T) of Cdc28 (de Bondt 1993). The T-loop is a site for autophosphorylation in many protein kinases but not in Cdks. Phosphorylation at this position in a Cdk requires a Cdk-activating kinase (CAK). In *S. cerevisiae* the gene *CAK1* encodes a Cdk activating kinase (Kaldis, 1996). A non phosphorylatable Cdc28-T169A mutant cannot be activated in vitro and is not able to support cell division in vivo. The activation mechanisms described above are opposed by the binding of inhibitory proteins, the Ckis.

Inhibition by specific inhibitors

The Cdks inhibitors (Cki) oppose the action of the cyclins. Two important Ckis are present in budding yeast: *FAR1* an *SIC1* gene products.
The Far1 protein is involved in mating factor pathway regulation, in fact activation of the pheromone response pathway stimulates association of Far1 with all three Cln-Cdc28 complexes (Peter et al., 1993); thus the Far1 Cki is an essential component of the G_1 arrest necessary for mating, and links the mating signal transduction pathway with the cell cycle machinery. Far1 is cell-cycle-regulated, its transcription levels has a peak at the M-G_1 boundary and this suggests Far1 has a role in cell cycle progression independent from mating (Fu et al., 2003; Alberghina et al., 2004).

Sic1 protein has a complementary specificity from Far1: it inhibits Clb-Cdc28 complexes and its activity is due to its ability to exclude substrates from the Cdc28 active site (Schwob et al., 1994). *SIC1* gene is not essential, but cultures of cells deleted in this gene have a high percentage of G_2 arrested cells. Sic1 has the role to prevent premature initiation of DNA replication by inhibiting Clb5- and Clb6-Cdc28 complexes until Sic1 itself is destroyed by a ubiquitin dependent mechanism.

Inhibition by phosphorylation

Finally, Cdc28 is also inhibited by phosphorylation on specific residues: T18 and Y19 (Berry and Gould, 1996). These phosphorylation events are controlled by multiple, dually specific protein kinases and phosphatases which, in turn, are under complex and not well-understood controls.
Combined action of Clns, Clbs and Ckis results in an oscillation of two main kinase activities: the one associated with Cln-Cdc28 complexes in G_1 phase and the other with Clb-Cdc28 complexes from S phase to mitosis.

THE CYCLIN CLN3

The most upstream activator of Start is Cln3 (Nash et al., 1988; Dirick et al., 1995), a G_1 cyclin that, together with the cyclin-dependent kinase Cdc28, activates two heterodimeric transcription factors, SBF (Swi6-Swi4) and MBF (Swi6-Mbp1) (Nasmyth, 1996).
The Cdc28-Cln3 complex relieves SBF, and perhaps MBF as well, from Whi5 inhibition in the nucleus (Costanzo et al., 2004; de Bruin et al., 2004), creating a transcriptional wave that triggers budding and S phase entry (Futcher, 2002). The Cln3 cyclin is a low abundant and very unstable protein (Tyers et al., 1993) whose levels respond very rapidly to nutritional changes by different regulatory mechanisms (Barbet et al., 1996; Schneider et al., 2004), allowing the cell to adjust proliferation requirements to a changing environment. However, Cln3 expression is not sharply regulated through the cell cycle, and it is already present in early G_1 cells (Tyers et al., 1993). Thus, when nutritional and other external signals are kept constant, posttranslational mechanisms must exist that withhold the activity of the Cdc28-Cln3 complex until a critical cell size is reached at Start.
Cln3 contains a bipartite nuclear localization signal (NLS) at the C terminus that is sufficient for nuclear import (Edgington and Futcher, 2001; Miller and Cross, 2001), and it is generally assumed that Cln3 triggers Start when it reaches a critical level in the nucleus.

In contrast with other cyclins, *CLN3* mRNA is transcribed at rather constant, low level throughout the cell cycle, with only a minor peak at the M-G_1 boundary, which depends on Mcm1 (MacKay et al., 2001; McInerny et al., 1997). Hyperstabilization of Cln3 causes not only a dramatic decrease in the cell size required for budding and entry into S phase but also to resistance to mating pheromone-induced G_1 arrest (Cross, 1988; Nash et al., 1988).

Multiple signal transduction pathways that control cell cycle progression converge to regulate Cln3 transcription, translation, stability, and activity. *CLN3* transcription is maintained at rather constant level throughout the cell cycle but displays some cell cycle periodicity that depends on early cell cycle boxes (ECB) sites upstream of the *CLN3* promoter (Mai et al., 2002; McInerny et al., 1997).
CLN3 mRNA levels are high during exponential growth on glucose but dramatically drops at the diauxic shift and it further declines during stationary phase cells (Parviz et al., 1998a).
Glucose induces *CLN3* transcription (Parviz et al., 1998) through a mechanism that requires glucose metabolism but that is not affected by mutations in all the known glucose sensing pathways (Parviz et al., 1998a; Newcomb et al., 2003).

Cln3 nuclear translocation is regulated by a surprisingly complex mechanism (figure 4). In early G_1, most of Cln3 is retained on the cytoplasmic face of the endoplasmic reticulum (ER) to prevent its nuclear accumulation (Verges et al., 2007). Efficient binding of Cln3 to the ER requires Cdc28, which seems to act as an adaptor between Cln3 and ER-scaffold structures, and Whi3, a protein originally identified as involved in cell size regulation (Nash et al., 2001). Whi3 sequesters the *CLN3* mRNA to confine its translation to specific sites of the ER, where also Cdc28 is recruited via interaction with Whi3 (Verges et al., 2007; Wang et al., 2004; Garì et al., 2001).

The newly formed Cdc28-Cln3 complexes are retained onto the ER by the interaction between the "Ji" domain of Cln3 and Ssa1 and Ssa2, two of the most important Hsp70 chaperones in yeast. The "j domain" is a key signature of the Hsp70-cochaperone regulators, but the one present in Cln3 is likely an inhibitory version (hence Ji), since it lacks the HPDK tetrapeptide essential to trigger the ATPase activity of Hsp70 chaperones (Verges et al., 2007): according to the proposed model, the Ji domain of Cln3 would hinder the Hsp70 chaperone cycle and effectively lock Ssa1 and Ssa2 into a tight complexes with Cdc28-Cln3 onto the ER, thus preventing unscheduled nuclear import of Cln3 in early G_1. The J chaperone seems to play a key and limiting role in the release of Cln3 from the ER in late G_1 cells and in the subsequent nuclear accumulation of the cyclin.

Ydj1 amount increase linearly during the G_1 phase, eventually achieving a sufficient level to trigger the ATPase activity of Ssa1,2 and unlock the complex. The released Cln3 then freely accumulates in the nucleus to initiate the G_1-S transition (Verges et al., 2007; Aldea et al., 2007). Thus, the Cln3 retention on the ER would serve to prevent an inappropriate activation of the Start transcriptional program until the cell have reached a critical size, which would coincide with the achievement of a relative surplus of chaperone folding activity (Verges et al., 2007; Aldea et al., 2007).
Later, as cells proceed into S phase, a change in the rate of protein synthesis (presumably as a direct consequence of the wave of late G_1 transcription) would once more reduce chaperone availability, again resulting in Cln3 retention at the ER (Verges et al., 2007; Aldea et al., 2007).

Since they have already reached enough Ydj1 levels in the previous cycle, mother cells would enter a new round of mitotic division soon after citokinesis if the growth rate remains unaltered. Therefore, in cooperation with other mechanisms that have been proposed to selectively reduce Cln3 expression in daughter cells (Laabs et al., 2003), this model may also explain one of the key features of *S. cerevisiae* cell cycle: asymmetrical division (Aldea et al., 2007).

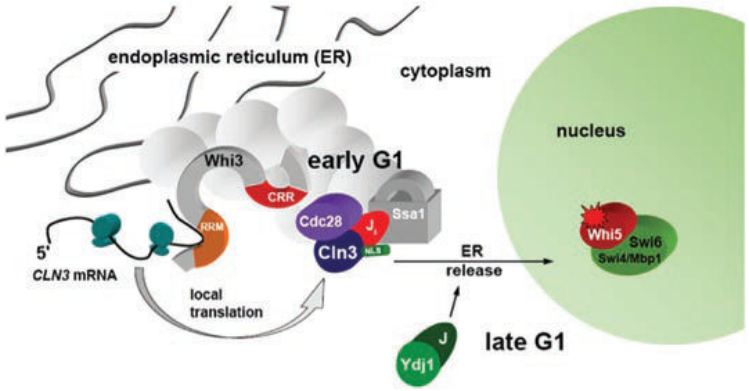

Figure 4. **Cyclin Cln3 is retained at the ER in early G_1 and released by the Ydj1 chaperone to trigger cell cycle entry.**
Whi3 contains an RNA-recognition motif (RRM) that binds the *CLN3* mRNA and a Cdc28-recruitment region (CRR) to locally retain newly formed Cdc28-Cln3 complexes. By inhibiting their ATPase-dependent conformational cycle, the Ji domain of Cln3 would lock Ssa1,2 chaperones into a tightly associated ER complex with Cdc28 in early G_1, which would prevent uncontrolled nuclear import of Cln3. In late G_1, once a relative surplus of Ydj1 (and most likely other folding activities) is achieved, ATPase activation by Ydj1 would unlock the Ssa1,2 complex, thus releasing Cln3 from the ER and allowing its nuclear accumulation to phosphorylate Whi5 and trigger Start.
(From Aldea et al., 2007).

THE CYCLINS CLN1 AND CLN2

CLN1 and *CLN2* were originally identified as high-copy-number suppressors of *cdc28-4*ts mutations (Hadwiger et al., 1989). These cyclins share a high degree of identity (~60%), whereas they are only distantly related to Cln3 (Nash et al. 1988; Hadwiger et al. 1989). They are able to bind Cdc28 and activate its protein kinase that is maximal at Start (Tyers et al., 1993), suggesting a role in commitment to the mitotic division process.

Individual gene knockouts do not have dramatic phenotypes, double *cln1Δ cln2Δ* mutant cells grow slowly, are aberrantly shaped (Hadwiger et al., 1989) and have delayed times of bud emergence and DNA synthesis initiation (Dirick et al., 1995*;* Pavletich and Pabo, 1991).

Control of *CLN1* and *CLN2* transcription plays a crucial part in the proper execution of Start. Cln1 and Cln2 hyperstable alleles accelerate the execution of Start, thus shortening G_1 phase length and decreasing the minimal cell size required for budding (Cross, 1988; Nash et al., 1988). Similarly, their overexpression leads to premature cell cycle entry and reduce the mean cell size (Lew et al. 1992).

A Recent study has confirmed that Cln1 and Cln2 form a potent feedback loop to stimulate the transcription of their own encoding genes: this mechanism operates by accelerating the nuclear exclusion of Whi5 and it is essential for the synchronous transcription of the G_1-S regulon (Stokheim et al., 2008; Dirick and Nasmith, 1995).

Cln1 and Cln2 are largely cytoplasmic, their function is compromised when a nuclear export signal is added, suggesting that the two cyclins have also important roles in the nucleus (Bloom and Cross, 2007; Miller and Cross, 2001).
The subcellular localization of Cln2 is regulated by Cdc28- mediated phosphorylation: when the Cdc28 consensus phosphorylation sites in Cln2 are mutated, Cln2 is exclusively nuclear. Therefore, the phosphorylation event may conceal a nuclear localization signal or, alternatively, expose a nuclear export signal (Bloom and Cross, 2007; Miller and Cross, 2001).

The mechanism by which Cln1 and Cln2 is involved in morphogenesis and bud emergence is not completely clear (Mendenhall and Hodges, 1998): the process is apparently mediated by a mechanism involving cytoplasmic Cln1 and Cln2 (Polymenis and Schmidt, 1999; Miller and Cross, 2000) and other members of the G_1-S regulon, such as the cyclins Pcl1 and Pcl2 that regulate the activity of the Pho85 Cdk (Moffat et al., 2004).

The dual role of Cln1 and Cln2 (in promoting the G_1-S transcriptional program and in directly driving bud emergence) provides a compact solution to ensure efficient and timely morphogenesis and synchronous expression of the G_1-S regulon (Skotheim et al., 2008).
Cln1 and Cln2 indirectly participate to DNA synthesis by promoting the targeted degradation of Sic1 (Verma et al., 1997; Nash et al., 2001b) and inactivating Cdh1, two negative regulators of B-type cyclins (Zachariae et al., 1998; Schwab et al., 1997; Visintin et al., 1997).

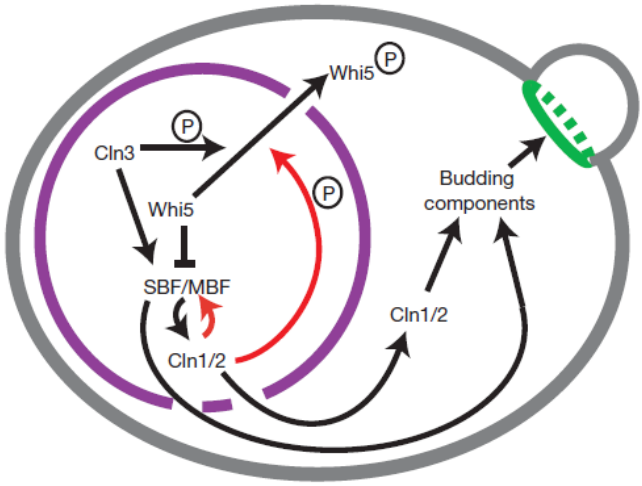

Figure 5. **Function of nuclear Cln2 and a model for Start regulation by positive feedback**. Model for regulon activation and bud emergence; red lines indicate pathways generating positive feedback.
(From Stokheim et al., 2008).

THE CYCLINS CLB5 AND CLB6

CLB5 encodes for a protein of 435 amino acids (50.4 kDa) that shares 49.7% identity with the product of *CLB6* (380 amino acids 44.1 kDa).
Both have a specific role in S-phase entry, in that they are primarily responsible for initiating DNA replication.
Transcription of *CLB5* and *CLB6* peak at G_1-S, followed by the transcription of *CLB3* and *CLB4* and then by the transcription of *CLB1* and *CLB2* (Bloom & Cross, 2007). The transcriptional waves are autoregulatory: *CLN3* drives the expression of *CLN1* and *CLN2,* which activate Clb5 and Clb6 by removing the Sic1 inhibitor and thus indirectly promoting the expression of the mitotic B-type cyclins. Once *CLBs* are expressed, they repress CLN1 and CLN2 transcription. This feedback loop ensures the periodicity of cyclin expression (Futcher et al., 1996).

Deletion of *CLB6* alone has little or no phenotype, deletion of *CLB5* causes a lengthening of S-phase, deletion of both genes delays entry into S-phase relative to bud emergence and *CLN2* activation. Strains lacking *CLB5* grow slightly slower than wild type strains, and their cells are larger (Mendenhall and Hodge, 1998).

Analysis of DNA contents of cell populations by DNA flow cytometry (FACS) has shown that progression through S-phase is retarded in *clb5Δ* strains (Schwob and Nasmyth, 1993). *Clb5Δ clb6Δ* mutant cells are viable but, like *clb5*Δ mutant cells, are large and grow somewhat slower than wild type cells. There is considerable overlap in the functional specificities of S and M cyclins in yeast. In the case of lacking both Clb5 and Clb6 S-phase is trigged by Clb3 and Clb4.

THE CYCLIN DEPENDENT KINASE INHIBITOR FAR1

FAR1 has been discovered as a gene regulating the cell cycle arrest induced by mating pheromone, specifically as an inhibitor of G_1 cyclin Cln2 (Chang and Herskowitz, 1990). Successive work established that Far1 inhibition is not restricted to Cln2 only but operates also on Cln1 and Cln3.
The inhibition is specific for G_1 cyclins since Far1 is not able to inhibit Clb5-Cdc28 and Clb2-Cdc28 complexes in vitro (Peter and Herskowitz, 1994).

Transcription of *FAR1* gene is cell cycle regulated, with a peak near the M-G_1 transition. Both Cln1-Cdc28 and Cln2-Cdc28 complexes are found to be bound to Far1 in cells not exposed to pheromone and *far1Δ* strains have a reduced G_1 phase compared to wild type (Lim et al., 1996).
Moreover, *FAR1* deletion can rescue the G_1 arrest of a *cdc4*8-*td* mutant (Fu et al., 2003). These data suggests that Far1 may have a cell cycle function independent of its role in mating.
Far1 is an unstable protein and is degraded via a ubiquitin dependent mechanism: phosphorylation on specific sites by Cln2-Cdc28 kinase activity is a targeting signal for degradation.
A recombinant Far1 mutant, lacking a Cdc28 phosphorylation site at position 87 (Serine87), inhibits Cln1-Cdc28 and Cln2-Cdc28 complexes *in vitro* (Peter and Herskowitz, 1994) and results in a hyperstable gene product *in vivo*. Expression of FAR1-22S87P results in constitutive, pheromone-independent cell cycle arrest and seems to cause arrest in cell cycle intervals past Start (Henchoz et al., 1997).

Inhibition of Cln3-Cdc28 complexes by Far1 is very sensitive to the relative levels of Cln3 and Far1; mutations or genetic constructs that increase Cln3 production or stability are mating-pheromone resistant and this resistance is bypassed by overproduction or stabilization of Far1 (Henchoz et al., 1997). Thus Far1 is a rapidly acting inhibitor of Cln1-Cdc28 and Cln2-Cdc28 complexes, but is less potent and acts more slowly against Cln3-Cdc28. Actually, more on Far1 mechanisms of action in inhibiting the G_1 phase Cln-Cdc28 complexes must be uncovered since some results are sometimes in contradiction. In fact, Far1-associated Cdc28-Cln2 complexes seems to be moderately inhibited in immunoprecipitation kinase assays, suggesting unconventional inhibitory mechanisms of Far1, but an alternative mode of action has not been proposed (Gartner et al., 1998).
Relative to the size regulation during cell cycle it should recalled that G_2/M transcription of *FAR1* is dependent on the transcription factor Mcm1, the same regulating Cln3 transcription, and that higher levels of Far1 results in larger cells (Oehlen et al., 1996).

Besides its well established role in the response to pheromone, recent evidences suggest that Far1 may also regulate cell cycle progression in mitotic cells (Alberghina et al., 2004; Fu et al., 2003).
In particular, it has been proposed that Far1, together with the G_1 cyclin Cln3, may be part of a nutritionally modulated cell sizer plus timer mechanism that controls the entry into S phase (Alberghina et al., 2004; Barberis et al., 2007; Di Talia et al., 2007). Each threshold consists of an activator and an associated inhibitor blocking its function. The first one involves the G_1 cyclin Cln3, the Cdk inhibitor (Cki) Far1 and the cyclin-dependent kinase Cdc28, whereas the second one comprises the S phase cyclin Clb5 (and Clb6), the Cki Sic1 and Cdc28 (Alberghina et al., 2009; Alberghina et al., 2004; Barberis et al., 2007).
In the first threshold, that is as the actual cell sizer, Cln3 has to overcome Far1 in order to trigger Cln-Cdc28 activation, which is in turn required for SBF- and MBF-dependent transcription.

Carbon source affects the expression level of the components of both thresholds: for instance, Cln3 and Far1 levels are higher in cells growing on glucose than on ethanol (Alberghina et al., 2004; Hall et al., 1998), whereas Sic1 content is higher in non-fermentable carbon sources (Rossi et al., 2005). The two thresholds cooperate to set the critical cell size according to the available carbon source: consistently with this notion, when both the thresholds are inactivated yeast cells loose the capacity to increase their size in presence of glucose (Alberghina et al., 2004).

THE CYCLIN DEPENDENT KINASE INHIBITOR SIC1

Sic1 is a potent stoichiometric inhibitor of Cdc28-Clbs complexes that prevents premature DNA replication and ensures correct timing for the G_1-S transition, thus maintaining genome integrity (Schwob, 2004).
SIC1 transcription is dependent on the Swi5 transcription factor and peaks at the G_1-M-phase border (Toyn et al., 1997). Its expression is confined from late mitosis to the G_1-S phase transition (Donovan et al., 1994; Verma et al., 1997). During G_1 phase Sic1 protein is stable and inhibits the newly formed Clb5,6-Cdc28 complexes, preventing a premature entry into S phase.
Sic1 binding motif to Clbs-Cdk complexes has been mapped to the C-terminal half of the inhibitor.
At Start, Cln1,2-Cdc28 complexes phosphorylate Sic1 on multiple sites, allowing the recognition of the inhibitor by the SCF^{Cdc4} ubiquitin ligase and its subsequent proteolytic degradation (Verma et al., 1997). Sic1 proteolysis requires phosphorylation of at least six of the nine Cln1,2-Cdc28 consensus sites (Nash et al., 2001b).

The removal of Sic1 relieves the inhibition from Clb5,6-Cdc28 complexes allowing the entry into S phase and the onset of DNA replication (Schwob; 2004). Apparently, Sic1 degradation is the only essential function of the G_1 cyclins*:* consistently*,* a *cln1Δ cln2Δ cln3Δ sic1Δ* multiple null mutant is viable (Epstein and Cross, 1994; Schneider et al., 1996, Tyers, 1996).
SIC1 is a nonessential gene (Donovan et al., 1994; Nugrobo et al., 1994), although *sic1Δ* null cells often undergo a permanent G_2 arrest (Nugrobo et al., 1994). Loss of *SIC1* causes premature DNA replication from fewer origins, extension of the S phase length and inefficient separation of sister chromatids during anaphase (Lengronne and Schwob, 2002); conversely, in strains expressing Sic1 variants resistant to proteolysis DNA synthesis is delayed, indicating that the timing of Sic1 degradation is crucial for the onset of DNA replication (Schwob, 2004).

The amount of Sic1 is modulated by nutrient availability, in particular by the carbon source: Sic1 content is higher in cells cultivated in ethanol than in glucose grown cells (Rossi et al., 2005). Furthermore, rapamycin treatment induces a G_1 arrest by a dual mechanism consisting of downregulation of the G_1-cyclins Cln1-3 and upregulation of Sic1 (Zinzalla et al., 2007).

Sub-cellular localization of Sic1 is also carbon source modulated: in glucose grown cells, Sic1 is mainly nuclear, whereas a sizeable amount of the inhibitor is detected also in the cytoplasm during growth on ethanol (Rossi et al., 2005). Nuclear import of Sic1 is dependent upon a bipartite localization sequence and is essential for correct cell cycle progression in a carbon-source dependent manner (Rossi et al., 2005).

Similarly to Cip-Kip proteins (Sic1 mammalian counterparts (Barberis et al., 2005)) Sic1 facilitates nuclear accumulation of its cognate cyclin Clb5 (and possibly Clb6), thus playing also a positive role in promoting the G_1-S transition (Rossi et al., 2005). Consistent with this notion, phenotypes of cells expressing a nuclear exporting signal (NES) fused to Sic1 are more severe than those observed in *sic1Δ* null mutants, indicating that when excluded from the nucleus Sic1 can act as a cytoplasmic retention device for Clb5-Cdc28 complexes and thus reduce the Clb5 nuclear pool.
The aberrant morphologies observed in cells expressing the NES-Sic1 fusion are similar to those observed in strains expressing stabilized versions of Sic1 (Schwob, 2004; Petrosky and Deshaies, 2003) or in *cdc34-ts* strains at the restrictive temperature, in which Sic1 cannot be degraded due to the inactivation of the catalytic subunit of the SCF complex (Schwob, 2004).

In addition to Cln- and Clb-Cc28 complexes, Sic1 can be phosphorylated by other kinases, such as the Pcl1-Pho85 complex (Nishizawa et al., 1998) or CK2 (Coccetti et al., 2004; Coccetti et al., 2006; Tripodi et al., 2007).
Loss of the CK2 phosphorylation site (Ser201) alters the coordination between growth and cell cycle progression by increasing the critical size at the onset of DNA replication (Coccetti et al., 2004).

CHECKING CELL SIZE IN THE BUDDING YEAST

Cell size is generally considered as the outcome of complex parallel processes more or less interconnected and/or interdependent that, in turn, transmit different sorts of intrinsic and extrinsic information.
Among these processes, cell growth and cell cycle are particularly relevant as they likely apply to all cellular models. The budding yeast displays two of the most universal credentials regarding cell size control: (1) a critical size threshold for cell cycle progression, (Hartwell et al., 1977; Johnston et al., 1977) and (2) a constant mass/ploidy ratio (Mortimer 1958). In this organism the importance of cell size control is particularly obvious in fact cytokinesis is asymmetric with respect to cell mass, producing a large mother cell and a smaller daughter cell.

As defined by Hartwell (Hartwell et al., 1974) and colleagues, coordination between cell growth and the cell cycle occurs at Start, a short interval in late G_1 phase during which the yeast commits to division. Passing Start requires that cells first obtain a critical cell size, such that large mother cells traverse a minimal G_1 phase while small daughter cells spend a long time in G_1 phase growing to the threshold size (Johnston et al., 1977; Hartwell et al., 1977). Although *ipso facto* larger than the critical cell size, mother cells do arrest prior to Start in response to nutrient starvation, mating pheromones, or translation deficiencies (Unger and Hartwell 1976; Hartwell et al., 1977). Following Start, the cell cycle progresses until the subsequent G_1 phase even if cells are subjected to nutrient starvation, mating pheromones (if haploid), and signals that initiate meiosis (if diploid) (Hartwell et al., 1974). Therefore, in addition to maintaining average size over the generations, the size requirement at Start ensures that the yeast possesses enough resources to complete the crucial processes of genome duplication and segregation.
Start is a series of events that culminate in S phase entry (figure 6).

The earliest known Start event is the onset of transcriptional activation by the SBF (Swi4-Swi6) and MBF (Mbp1-Swi6) complexes, which drive expression of ~200 genes (Futcher, 2002). This regulon contains numerous genes involved in DNA synthesis and repair, but the key transcripts are the G_1 cyclins *CLN1* and *CLN2* and the B-type cyclins *CLB5* and *CLB6* (Nasmyth, 1996). Cln1 and Cln2 bind to and activate Cdc28, the primary Cdk that controls cell cycle progression in budding yeast. Cln1/2-Cdc28 complexes trigger bud emergence and inactivate Sic1 and Cdh1, two key inhibitors of Clb-Cdc28 activity. Once derepressed, Clb-Cdc28 complexes immediately initiate DNA replication (Nasmyth, 1996). The onset of SBF and MBF mediated transcription requires that cells attain a critical cell size. A third G_1 cyclin, Cln3, is a highly unstable, rate-limiting activator of Start (Sudbery,et al., 1980; Nash et al.,1988).

CLN3 appears to function in parallel to the *BCK2* gene and strains with deletions of both genes are inviable due to permanent G_1 arrest (Wijnen and Futcher, 1999). In contrast, *CLN1* and *CLN2* have no effect on the timing of the SBF and MBF transcriptional program (Stuart and Wittenberg 1995; Dirick et al., 1995). Although *CLN1* and *CLN2* do not control SBF and MBF, they do control how long the Start interval lasts, because critical concentrations of Cln-Cdc28 activity are required for the phosphorylation of Cdh1, Sic1, and targets at the incipient bud site, such as Cdc24 (Stuart and Wittenberg 1995 Moffat and Andrews 2004) (figure 6A).

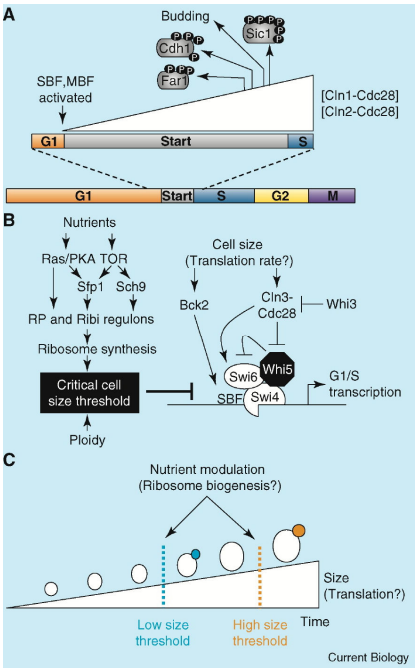

Figure 6. **Start in the budding yeast *S. cerevisiae*.**
A) Start is a short interval during which Cln1/2-Cdc28 activity is elaborated. Phosphorylation of Far1, Cdh1, Sic1, and Cdc24 allows DNA replication and bud emergence to be initiated.
B) A current model of Start entry. Activation of SBF and MBF (not shown) results from the dissociation of the Whi5 repressor upon Cln3-Cdc28 phosphorylation of Whi5 and perhaps Swi6. Cln3, and perhaps Bck2, abundance may be proportional to translation rate and must overcome a poorly understood size threshold. The size threshold is increased by cell ploidy and rich nutrients, perhaps via Ras-PKA, Sfp1, and Sch9 mediated control of ribosome biogenesis rates.
C) The mechanism that sets the critical cell size threshold in response to nutrients (possibly ribosome biogenesis rates) appears to be distinct from the mechanism that actually determines cell size (possibly the translation of an unstable sizer). The latter increases over time as cells accumulate biosynthetic capacity, whereas the former is determined by current nutrient conditions and ploidy
(From Jorgensen and Tyers, 2004).

Additional players have also emerged as interaction partners of known Start factors (Ho et al., 1999 ; de Bruin et al., 2004).
One new regulator, Whi5, is the key G_1 target of Cln3-Cdc28 and is thus a linchpin in the Start hierarchy (Jorgensen et al., 2002; de Bruin et al., 2004; Costanzo et al., 2004). In early G_1 phase cells, Whi5 binds to and represses promoter-bound SBF and MBF (de Bruin et al., 2004; Costanzo et al., 2004). Multi-site phosphorylation of Whi5 by Cln3-Cdc28 dissociates Whi5 from SBF-MBF, drives Whi5 into the cytoplasm, and induces the expression of Start specific transcripts (de Bruin et al., 2004; Costanzo et al., 2004).

Bck2 activates SBF-MBF by an unknown mechanism that is independent of Cdc28 or Whi5 (Wijnen, and Futcher 1999; Jorgensen et al., 2002).
But what is the actual cell sizing mechanism? Though not conclusive, there is evidence that budding yeast assess their size by measuring the overall translation rate. This model unifies the volume, nutrient and translation requirements for Start. In support of this model, budding yeast growing in a stable nutrient environment have an overall translation rate that correlates with cell volume (Elliott and McLaughlin, 1978). Nutrient-sensing pathways control not only the rate at which ribosomes are produced and the cytoplasmic ribosome concentration, but also the rate at which ribosomes function (Warner, 1999; Cherkasova and Hinnebusch, 2003).

As passage through Start is highly sensitive to Cln3 dosage, a critical translation rate of Cln3 might trigger Start (Nash et al., 1988; Tyers et al., 1993; Futcher, 1996). But the relative amount Cln3 protein does not appear to increase as cells approach Start (Tyers et al., 1993). Instead, the relative abundance of Cln3 oscillates only weakly, peaking in early G_1 when daughter cells are smallest due to a transcriptional induction (Tyers et al., 1993; McInerny et al., 1997). Because Cln3 localizes to the nucleus and is very unstable (Tyers et al., 1992 Edgington and Futcher, 2001), the nuclear concentration of Cln3-Cdc28 might reflect the overall rate of Cln3 translation, which steadily increases as cells grow larger and acquire more ribosomes (Futcher, 1996). An important requirement of this model is that the nuclear volume remains constant during G_1 phase, because the nuclear volume would be the metric against which the protein synthetic rate is measured.
It has recently been observed, however, that nuclear volume increases as cells grow during G_1 phase, such that the nucleo-cytoplasmic volume ratio does not appreciably decrease prior to Start (Gasser, 2002).

NUTRIENT MODULATION OF CRITICAL CELL SIZE

Since cells in a culture remain the same size over multiple generations, the duration of all the sequential events directing duplication and segregation of the cell's genetic material (the cell cycle) must in general match the amount of time required for the continuous increase in cell mass to double the no genetic components of the cell (the growth cycle).
Since the minimal amount of time required to complete all the events in the cell cycle is less than that needed to duplicate the mass of the cell, cells can maintain a constant size by requiring that progress through the cell cycle be dependent on duplicating the cell's mass.
Classic studies showed that yeast cells execute this feat by making the transition from G_1 to S, a step termed "Start," dependent on the cell attaining an appropriate "size" (Johnston et al., 1977). Thus, budding yeast cells growing slowly due to limited nutrient availability extend their G_1 phase to allow time for growth to this appropriate size. That means that the critical size threshold is large for budding yeast growing in rich nutrients and small for those grown in poor nutrients (Lorincz and Carter, 1979) (figure 6).
More recent studies using nutrient-limited chemostats reinforced these observations by documenting that the fraction of unbudded cells, i.e., those in G_1, in cultures limited for glucose, ammonia, sulfate, or phosphate is proportional to the doubling time of the culture (Brauer et al., 2008).

The nutrient modulation of size thresholds was first characterized in fission yeast (Fantes and Nurse, 1977), but hints had been observed earlier in budding yeast (Wehr and Parks, 1969). Given that overall translation rates appear to report cell size to the Start machinery and that yeast growing in rich nutrient conditions have higher ribosome concentrations (Kief and Warner, 1981), one might naively expect that yeast growing in rich nutrients would achieve the critical translation rate (and pass Start) with less cell volume than yeast growing in poor nutrients. Because the opposite is true, the existence of a powerful nutrient repression of Start is inferred.
As the threshold is reset very quickly (Lorincz and Carter, 1979), nutrients must exert a continual repression of Start through G_1 phase. It is frequently argued that nutrients modulate the critical cell size threshold via Cln3, as its abundance is greatly diminished in cells growing in poor media due to transcriptional and translational controls (Tokiwa, 1995; Newcomb et al., 2003). This 'Cln3 abundance model' successfully explains the effects nutrients have on the length of G_1 phase, i.e., in poor nutrients yeast spend more time in G_1 phase. However, the model cannot explain why in these conditions a smaller critical cell size is required to pass Start.

With respect to critical cell size, the Cln3 abundance model of nutrient modulation breaks down: in poor nutrients, yeast have the lowest levels of Cln3 yet pass Start with the least amount of mass and translational capacity. Shifting cells into glucose delays Start relative to cell size despite increases in Cln3 abundance (Lorincz and Carter, 1979; Tokiwa, 1995; Newcomb et al., 2003). From this perspective, nutrient modulation of the critical cell size threshold is even more remarkable, as not only must the yeast growing in poor nutrients enter Start with less translational capacity but it does so with much less Cln3. Consistently, poor nutrient conditions partially suppress the Cdc28 requirement at Start (Shuster, 1982). A final problem with the Cln3 abundance model is that the size of *WHI1-1* and *cln3*Δ cells responds appropriately to nutrient modulation (Nash et al.,1988, Jorgensen et al., 2004).

In fact, nutrient modulation appears to be independent of all known upstream regulators of SBF-MBF (Jorgensen et al., 2004). These results suggest that an uncharacterized pathway(s) signals from nutrients to increase the critical cell size threshold. Nutrient modulation of Start entry appears to involve at least three main conduits. Activation of the Ras-PKA signaling pathway, either by glucose or mutation, increases critical cell size and is accompanied by a transient reduction in SBF-dependent transcription (Baroni et al., 1989; Baroni et al., 1994). A genome-wide size screen identified the zinc-finger transcription factor Sfp1 and the Akt-like kinase Sch9 as two other effectors of nutrient modulation.

In fact the most significant advances in the last decade regarding cell size control have originated from genome-wide screens for small single-gene deletants in budding yeast, (Jorgensen et al., 2002; Zhang et al., 2002) which demonstrated that ribosome biogenesis is *per se* a negative regulator of Start. So, Ras-PKA, Sfp1, and Sch9 all activate the transcription of ribosomal protein (RP) and ribosome biogenesis (*Ribi* or *RRB*) genes in response to nutrient signals (Jorgensen et al., 2002; Jorgensen et al., 2004; Klein and Struhl, 1994; Marion et al., 2004). Furthermore, the same genome-wide screen for cell size revealed that at least 15 *Ribi* genes encode potential Start repressors. All of these observations can be unified by a model in which the rate of ribosome biogenesis, which is proportional to nutrient quality, represses SBF-MBF, thereby linking nutrients to the critical cell size threshold (figure 6B).

In this model, for any cell in G_1 phase, the current rate of ribosome biogenesis modulates the critical cell size set point, while the overall translation rate (an integral of all past ribosome biogenesis) reports cell size (figure 6C). This model has the appealing property that future changes in overall translation rate are anticipated at an early juncture and the cell size threshold can be reset accordingly.

THE CRITICAL CELL SIZE AS AN EMERGENT PROPERTY OF G_1-S TRANSITION

Recently, Barberis and colleagues have developed a new mathematical model which describes the molecular events taking place at the G_1-S transition (Barberis et al., 2007). Many diverse experimental evidences have been integrated into a concise mathematical model through a set of ordinary differential equations. These equations describe the temporal change of the concentrations of proteins and complexes involved in the G_1-S network.
As a distinguishing feature, the model proposes that two sequential, nutrient modulated thresholds control the entry into S phase (Alberghina et al., 2004; Barberis et al., 2007; Vanoni et al., 2005).

Basically, a molecular "threshold" is given by the interplay between an "activator" and an inhibitor blocking its activity: when the number of molecules of the activator exceeds that of the inhibitor, the threshold is overcome. As previously describe, the first threshold regulating the G_1-S transition involves the G_1 cyclin Cln3, Far1 and the Cdc28, whereas the second one comprises the S phase cyclin Clb5 (and Clb6), Sic1 and Cdc28.
According to the model, the Cln3-Far1 threshold is set by the amount of Far1, which is mostly inherited by newborn cells at the end of the previous mitotic cycle and remains roughly constant during the G_1 phase.
It is assumed that Far1 binds to and inhibits the nuclear Cdc28-Cln3 complexes in early G_1 phase, when it is present in substantial excess relative to Cln3 (Alberghina et al., 2004; Vanoni et al., 2005; Barberis et al., 2007). As cells grows during G_1 phase, Cln3 accumulates proportionally to cell mass until it exceeds Far1 levels, thus allowing to overcome the first threshold regulating the G_1-S transition (Alberghina et al., 2004; Vanoni et al., 2005; Barberis et al., 2007). The overcoming of this threshold is made irreversible by Cln3-Cdc28-primed Far1 degradation (Henchoz et al., 1997; Alberghina et al., 2004). Once free from Far1 inhibition, Cln3-Cdc28 complexes trigger the SBF-MBF transcriptional program by inactivating the Whi5 inhibitor, which abandons the nucleus (Costanzo et al., 2004; de Bruin et al., 2004).

The irreversible overcoming of the second threshold requires the elimination of Sic1: the growing pool of Cdc28-Cln1,2 phosphorylates the inhibitor on multiple site, promoting its degradation via an ubiquitin mediated mechanism, (Nash et al., 2001). The now active Cdc28-Clb5,6 complexes drive the entry into S phase by promoting the onset of DNA replication (Verma et al., 1997; Deshalis and Ferrel, 2001; Toone et al., 1997).

In the model (Barberis et al., 2007), nutrient-dependent control of the G_1 to S transition is distributed over the two described sequential thresholds, each one able to integrate cell signaling information coming from external and internal conditions (Alberghina et al., 2004; Vanoni et al., 2005).
When one or both components of each threshold are inactivated, cells largely retain their ability to modulate their size according to carbon source availability. In contrast, concurrent loss of either *CLN3* or *FAR1* (first threshold) and *SIC1* (second threshold), abolishes glucose modulation of cell size (Alberghina et al., 2004). Consistently, nutrient status (and in particular the quantity and quality of available carbon source) influences the components of the two thresholds at the level protein abundance and sub-cellular localization. For instance, Cln3 and Far1 levels are higher in cells growing on glucose than in cell cultivated on ethanol (Hall et al., 1998; Alberghina et al., 2004). On the contrary, Sic1 content is higher in ethanol growing cells; the sub-cellular localization of Sic1 is also carbon source-modulated: the inhibitor is mostly nuclear in cells grown in glucose- media, whereas a sizeable amount of Sic1 is detected also in the cytoplasm during growth on ethanol (Rossi et al., 2005).

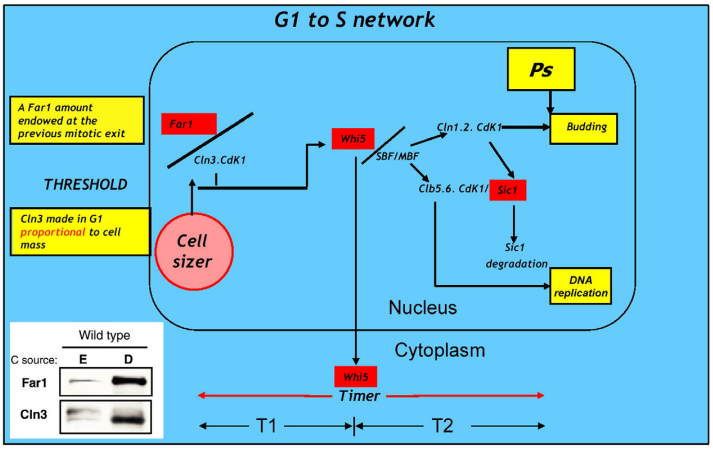

Figure 7. The design principle underlying the G_1 to S transition is sizer plus timer. It is given by three couples of interactors in each of which an inhibitor is present. The inhibitory proteins Far1, Whi5 and Sic1 are shown in red boxes. The sizer is given by the overcoming of the inhibitor effect of Far1 by the building up of Cln3, made during G_1 in a way proportional to cell mass. The duration of the timer (that is divided in two periods T1 and T2) is given by the time required to develop all the biochemical events from the overcoming of the sizer to the onset of DNA replication and budding. Ps is the size that the cell achieved at the onset of S phase. In the inset there is shown a western blot showing relative amounts of Far1 and Cln3 in exponentially growing cells on ethanol, E, and glucose, D.
(From Alberghina et al., 2009)

A simulation analysis performed with the model described above has provided a novel, intriguing conclusion: the critical cell size required for entry into S phase (as defined by the parameter Ps, the protein content at the onset of DNA replication) is an emergent property of the G_1-S network and is strongly influenced by growth rate (Barberis et al. 2007; Alberghina et al., 2009). In other words, Ps is a property that individual components of the G_1-S network do not possess but that emerges from their interaction. The setting of the critical cells size (Ps) is carried out by a mechanism consisting of a "sizer "plus a "timer" (figure 7).
The Far1/Cln3 threshold acts essentially as a growth-sensitive sizer, which is activated at similar cell size both in cells growing in rich or poor media: in fact, the Cln3/Far1 ratio remains almost equimolecular in the various growth conditions, since both Cln3 and Far1 levels increase or decrease accordingly to the growth rate (Hall et al., 1998; Alberghina et al., 2004; Alberghina et al., 2009; Barberis et al., 2007). The first Cln3/Far1 threshold and the second one involving Clb5,6 and Sic1 are temporally spaced ("timer") (Barberis et al., 2007): therefore, the actual value of Ps depends not only on the Cln3/Far1 "sizer", but also on the length of the "timer", which is the period elapsing between the passage through the first threshold and the overcoming of the second one (Barberis et al., 2007).
The growth rate (which depends on nutrient availability and quality) is a major factor in determining the critical size required for budding and DNA replication (Ps): in fact, since it is the overcoming of the second threshold that actually sets Ps, its value will be much higher in fast growing cells.

In other models of the yeast cell cycle previously proposed, the G_1-S transition is controlled by a single event: a cell sizer is operative only at low-growth rates, whereas an oscillator mechanism is active at fast-growth rates (Chen et al., 2004; Csikasz-Nagy et al., 2006).
In the model presented by Barberis and colleagues, a sizer mechanism is operative at all growth rates, and the presence of two distinct, temporally spaced, thresholds cooperating to set the critical size (Ps) introduces a delay that is sensitive to the growth rate (Barberis et al., 2007).
The existence of a "sizer plus timer mechanism" regulating the G_1-S transition has been confirmed in a work by Di Talia and colleagues (Di Talia et al., 2007). In this study, several of the predictions offered by the mathematical model have been experimentally verified, thus further supporting the soundness of the model by Barberis and colleagues (Alberghina et al., 2009).

NUTRIENT SENSING THROUGH THE PLASMA MEMBRANE

Glucose is the principal carbon and energy source for most cells, and many organisms have evolved sophisticated means for sensing glucose and utilizing it efficiently. Yeast cells can sense glucose and utilize it efficiently over a broad range of concentrations. Accordingly, yeasts have evolved sophisticated mechanisms for sensing the amount of glucose available and responding appropriately (reviewed in Gelade et al., 2003).

The budding yeast *Saccharomyces. cerevisiae* has an unusual lifestyle: it prefers to ferment rather than oxidize glucose, even when oxygen is abundant (Lagunas, 1979; Lagunas, 1986).
Glucose is metabolized through glycolysis to pyruvate, which has two fates (figure 8). In the presence of oxygen, most organisms convert pyruvate to carbon dioxide and water (via the tricarboxylic acid cycle), generating many ATPs (up to 36 per molecule of glucose used, according to the textbooks, but fewer are actually produced) via oxidative phosphorylation. Only when oxygen becomes limiting do most cells resort to fermentation, because it yields only 2 ATPs per molecule of glucose via 'substrate-level phosphorylation' of ADP. *Saccharomyces cerevisiae* is one of the few organisms that prefers to ferment glucose, even when oxygen is abundant. The resulting low yield of ATP production demands that yeasts aggressively utilize the available carbon at the expense of their more efficient competitors (Pfeiffer et al., 2001).

The tendency of most types of cells to resort to fermentation only when oxygen becomes limiting is known as the 'Pasteur effect', named after its discoverer (Pasteur, 1861). The contrasting lifestyle of yeast cells, their propensity to carry out aerobic fermentation, is called the 'Crabtree effect' after the oncologist who discovered this phenomenon in mammalian tumors cells in the 1920s (Crabtree, 1929).

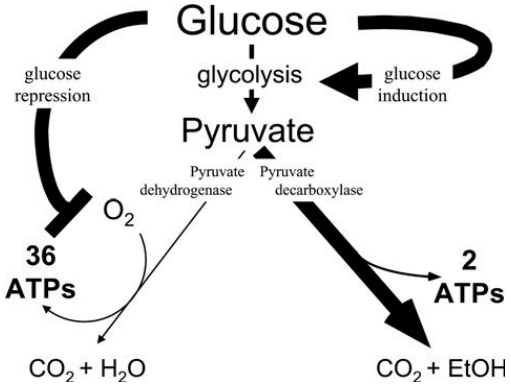

Figure 8. **Simplified diagram of glucose metabolism in yeast.**
(From Johnston and Kim, 2005)

Two major factors contribute to yeasts' propensity to ferment glucose even when oxygen is abundant. First, the enzyme catalysing the first step of pyruvate reduction (pyruvate decarboxylase) has more capacity than its counterpart that catalyses the first step of pyruvate oxidation (pyruvate dehydrogenase) (Kappeli, 1986). Secondly, the many enzymes necessary for glucose oxidation (e.g., electron transport chain proteins in the mitochondria, tricarboxylic acid cycle enzymes) are present at low levels in glucose-grown cells because glucose represses expression of their genes (Polakis et al., 1964).

The ability of glucose to repress the expression of genes that are not required for glucose fermentation is mediated through the actions of two key regulatory proteins: Snf1, a protein kinase; and Mig1, a transcriptional repressor (Carlson, 1999; Gelade, et al., 2003).
Mig1 binds to the promoters of glucose-repressed genes when glucose is present in the environment (figure 9). Mig1 activity is controlled by regulating its sub-cellular localization: in the presence of glucose, Mig1 is nuclear, but it occurs in the cytoplasm when glucose is depleted (DeVit and Johnston, 1999).

This glucose regulated localization is controlled by the Snf1 protein kinase. Glucose inhibits the activity of Snf1, which results in dephosphorylation, nuclear localization and repression of Mig1. Under conditions of glucose deficiency, Snf1 is active and phosphorylates Mig1 to promote its cytoplasmic localization and so de-represses glucose-repressed genes.

Because glucose fermentation yields only two molecules of ATP per molecule of glucose metabolized, yeast need high concentrations of glycolytic enzymes to support fermentative growth. Consequently, genes that encode these enzymes are induced in yeast in response to glucose.
This induction is particularly well characterized for the glucose-transporter genes. The sensing components of this pathway are two plasma-membrane proteins, Snf3 and Rgt2, which are paralogs of the hexose transporter genes (figure 9).

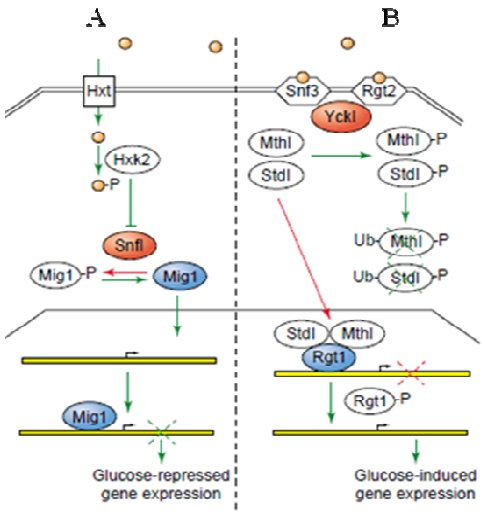

Figure 9. **The two glucose-signaling pathways in S. cerevisiae**.
Green arrows indicate processes that are activated by glucose and red arrows indicate processes that are active in the absence of glucose. Blue-shaded proteins represent transcriptional repressors, and red-shaded proteins are protein kinases. Glucose molecules are indicated by orange circles.
A) The repression of genes that are not required for fermentative growth on glucose. Signaling in this pathway requires Hxk2, which acts through an unknown pathway to inhibit Snf1. In the presence of inactive Snf1, Mig1 becomes dephosphorylated and can translocate to the nucleus to repress expression of specific genes.
B) The pathway involved in induction of gene expression in the presence of glucose. Snf3 and Rgt2 act as 'glucose receptors' that activate the protein kinase Yck1. This then phosphorylates two proteins, Mth1 and Std1, which are required for repression by Rgt1. When phosphorylated, these proteins become ubiquitinylated and degraded. This results in phosphorylation of Rgt1 and its release from DNA-regulatory sites.
(From Howard, 2005).

The glucose transporters of the budding yeast

It is well know that *Saccharomyces cerevisiae* has 20 genes that encode proteins similar to glucose (hexose) transporters (*HXT1* to *HXT17*, *GAL2*, *SNF3*, and *RGT2*) (Bisson and Fraenkel, 1984; Boles and Hollenberg 1997; Kruckeberg, 1996). These Hxt proteins belong to the major facilitator superfamily (MFS) of transporters (Maeda et al., 1994.). It has the largest number of MFS transporters of any organism. MFS proteins transport their substrates by passive, energy-independent facilitated diffusion, with glucose moving down a concentration gradient (Bisson and Fraenkel, 1984).
Two uptake systems were described in *S. cerevisiae*: a constitutive, low-affinity system (high *Km*, 15 to 20 mM) and a glucose-repressed, high-affinity system (low *Km*, 1 to 2 mM) (Bisson and Fraenkel. 1983; Bisson and Fraenke, 1984). None of these transporters are essential for growth on glucose, indicating their functional redundancy.
Of the 20 members of the *HXT* gene family, only 7 are known to encode functional glucose transporters. A strain lacking these seven *HXT* genes (*HXT1* through *HXT7*, called the *hxt* null mutant [*hxt1*Δ *hxt7*Δ]) is unable to grow on glucose, fructose, or mannose and has no glycolytic flux (Boles and Hollenberg 1997; Lian, and Gaber. 1996). Introduction of any one of the seven *HXT* genes into the *hxt* null mutant is sufficient to allow it to grow on glucose.
HXT2, *HXT6*, or *HXT7* are sufficient for growth on 0.1% glucose, suggesting that they encode high-affinity transporters whereas *HXT1*, *HXT3*, or *HXT4* enable growth only on higher glucose concentrations (more than 1%), suggesting that these genes encode low-affinity glucose transporters.

Three key components of the pathway responsible for glucose induction of HXT gene expression have been identified: (i) the glucose sensors Snf3 and Rgt2, which are plasma membrane proteins that sense the presence of extracellular glucose and generate an intracellular signal for induction of HXT gene expression; (ii) the Rgt1 repressor, a C6 zinc finger DNA binding protein that binds to the promoters of the HXT genes and represses their transcription in the absence of glucose and activates HXT1 transcription when high levels of glucose are present; and (iii) Grr1, which is required for glucose regulation of Rgt1 function and is a component of the SCF^{Grr1} complex of proteins that have been implicated in protein modification by ubiquitin.

GLUCOSE INDUCED SIGNALING

Snf3-Rgt2 signaling transduction pathway

Snf3 and Rgt2 are about 70% similar to each other but are less than 30% similar to the other members of the Hxt family (Boles and Hollenberg 1997; Kruckeberg, 1996; Ozcan, et al., 1996). They appear not to transport glucose but to serve as sensors of extracellular glucose that generate the intracellular signal for induction of *HXT1* to *HXT4* expression. Both genes are expressed at very low levels: about 100- to 300-fold lower than the *HXT1* to *HXT4* genes (Ozcan, et al., 1996). Consistent with its proposed role as a high-affinity glucose sensor, *SNF3* transcription is repressed at high concentrations of glucose (Marshall-Carlson, et al., 1990**;** Neigeborn et al., 1986; Ozcan, and Johnston, 1995). Rgt2 is proposed to function as a low-affinity glucose sensor, and consistent with this role, its expression is independent of the glucose concentration (Ozcan, et al., 1996).

SNF3 and *RGT2* encode proteins with 12 predicted transmembrane-spanning domains that are about 60% identical to each other. They are the most divergent members of the glucose transporter protein family, being only 26 to 30% identical to the other Hxt proteins (Celenza et al., 1988; Marshall-Carlson, et al., 1990; Ozcan, et al., 1996).
SNF3 was identified as a mutant that does not grow on sucrose or raffinose (Neigeborn and Carlson;1984); *RGT2* mutations were obtained as dominant suppressors of the raffinose growth defect of *snf3Δ* mutants (Marshall et al., Carlson, 1991).
Mutants of *snf3Δ* were found to be defective in high-affinity glucose transport, which initially led to the conclusion that Snf3 is a high-affinity glucose transporter (Celenza et al., 1988). This was supported by the observation that multiple copies of *HXT1* and *HXT2* restore the raffinose growth defect of *snf3Δ* mutants (Kruckeberg and Bisson. 1990). However, several subsequent pieces of evidence led to the view that Snf3 has a regulatory rather than a metabolic role in glucose transport. First, *SNF3* is expressed at a very low level relative to other glucose transporter genes (about 300-fold less than *HXT1*) (Neigeborn et al., 1986; Ozcan, et al., 1996). Second, *SNF3* has a negative effect on the growth of an *hxt1-hxt4*Δ strain on intermediate levels (0.5%) of glucose, rather than the positive effect that would be expected for a glucose transporter (Ko et al., 1993). Third, analysis of transport kinetics in a *snf3*Δ mutant suggested that the decrease in high-affinity glucose uptake is not due to loss of a single transporter (Coons et al., 1995). Finally, Snf3 was found to be required for induction of transcription of the *HXT2*, *HXT3*, and *HXT4* genes by low levels of glucose (Ozcan, and Johnston, 1995).

This last observation strongly suggests that *snf3Δ* mutants are defective in high affinity glucose transport because they are unable to express genes encoding high-affinity glucose transporters.
Three key pieces of evidence suggest that Snf3 and Rgt2 are not glucose transporters but glucose receptors that bind glucose outside the cell and generate a signal inside the cell for induction of *HXT* gene expression (Ozcan, et al., 1996). First, they are required for glucose induction of expression of several *HXT* genes. Snf3 is required for induction of *HXT2* and *HXT4* expression by low levels of glucose but not for induction of *HXT1* expression by high levels of glucose. This suggests that it functions as a sensor of low levels of glucose. This conclusion is consistent with the observation that transcription of *SNF3* is maximal when glucose levels are low (*SNF3* expression is repressed about fivefold by high levels of glucose) (Ozcan, et al., 1996).

Rgt2, on the other hand, appears to be a sensor of high levels of glucose, because it is required for maximal induction of *HXT1* expression by high concentrations of glucose but not for induction of *HXT2* and *HXT4* expression by low levels of glucose. It is appropriate, then, that *RGT2* is expressed in cells growing on high levels of glucose (it is expressed constitutively, being neither repressed nor induced by glucose) (Ozcan, et al., 1996). Second, Snf3 and Rgt2 are apparently unable to transport glucose. Expression of *SNF3* or *RGT2* in the *hxt* null mutant (*hxt1-hxt7*Δ) does not provide growth of this mutant on glucose, even when they are overexpressed from high-copy number plasmids (Lian, and Gaber. 1996; Ozcan et al., 1998). Thus, in contrast to the Hxt proteins, Snf3 and Rgt2 appear to have little or no ability to transport glucose.
Perhaps the most compelling observation that supports the view that Snf3 and Rgt2 are glucose sensors comes from the identification of a dominant mutation in these genes (*RGT2-1* and *SNF3-1*) that causes constitutive expression of *HXT1* to *HXT4* (i.e., in the absence of the inducer glucose) (Ozcan, et al., 1996). It is possible imagine that this mutation converts Snf3 and Rgt2 into their glucose-bound forms, thereby causing them always to generate the glucose signal that activates *HXT* expression. This and several other observations (Coons et al., 1997; Lian, and Gaber. 1996; Vagnoli et al., 1998) led to the proposal that Snf3 and Rgt2 are membrane receptors that bind glucose outside the cell and generate a signal inside the cell for activation of gene expression (Ozcan et al., 199; Ozcan, et al., 1996).
In this view, glucose signaling by Snf3 and Rgt2 is a receptor-mediated process similar to hormone signaling in mammalian cells.

Two observations indicate that the cytoplasmic tails of Snf3 and Rgt2 are involved in generating the signal for induction of *HXT* expression upon glucose binding. First, the tails are required for glucose induction of *HXT* expression: the Snf3 tail is required for low glucose induction of *HXT2* and *HXT4* expression (Coons et al., 1997; Ozcan et al., 1998; Vagnoli et al., 1998), and the Rgt2 tail is required for high glucose induction of *HXT1* expression (Ozcan et al., 1998). Second, the cytoplasmic tail of Snf3 is sufficient for glucose-inducible signaling: attaching it to the Hxt1 or Hxt2 glucose transporters creates a chimeric protein that is able to complement the defect in glucose induction of *HXT* gene expression of *snf3Δ* and *rgt2Δ* mutants. That is, these modified glucose transporters sense glucose and generate an intracellular signal for induction of *HXT* expression.
Another observation that implicates the C-terminal tail of Snf3 in glucose signaling is that overexpression of just the Snf3 tail suppresses the growth defect of *snf3Δ* mutants on low levels of glucose (Coons et al., 1997) and seems to restore the low glucose induction defect of the *snf3Δ* mutant (Vagnoli et al., 1998).

Glucose sensing and cAMP pathway

In *S. cerevisiae* the cAMP-PKA pathway plays a major role in the control of metabolism, in the cell stress resistance and proliferation, in particular in connection with the available nutrient conditions, ultimately modulating the level of cAMP.
Cells in which the cAMP-PKA pathway is inactivated arrest at the Start point of the cell cycle and do not synthesize cyclins in spite of the presence of a full growth medium (Hubler et al., 1993). Hence, it is clear that one of the direct or indirect targets of PKA must be a factor that is required for cyclin synthesis. The *CDC35* gene encodes the adenylate cyclase enzyme, Cdc35-Cyr1, which is localized in the plasma membrane and catalyses the conversion of ATP to cAMP. Adenylate cyclase in budding yeast is activated by Ras-GTP complexes (Toda et al., 1985) formed by the two proteins Ras1 and Ras2. The very low intrinsic GTPase activity of Ras proteins is increased by Ira1 and Ira2, the yeast homologs of mammalian GAP. Yeast adenylate cyclase activity is not only stimulated by active Ras in the absence of active Ras, basal cAMP synthesis *in vivo* is extremely low and insufficient for viability.
Inactivation of Ras causes arrest at the same point in the cell cycle as nutrient depletion, and the cells permanently enter into the stationary phase G_0. The Cdc25 protein is a guanine nucleotide exchange factor (GEF) acting on Ras proteins to promote the transitions from the GDP- to the GTP-bound form.

Mutations that inactivate this mechanisms (*cdc25, cdc35, rad1* or *ras2* mutations), reduce the ability to increase cAMP levels in the cell and block growth in a starvation-like manner.
On the opposite site, there are mutations that iperactivate the pathway increasing constitutively the cAMP levels, such the activated mutant $RAS2^{Val132}$ (Toda et al., 1985).
The downstream action of activate protein kinase A involves phosphorylation of a variety of substrates, especially transcription factors.

The critical size requirement appears to be modulated by the cAMP pathway since mutants in this pathway show size alteration. Mutants impairing the cAMP pathway have a smaller critical size for budding and mutations that activate the pathway lead to mass (Baroni et al., 1989).
The critical cell size is also remarkably affected directly by the cyclic nucleotide when it is exogenously added to cAMP-permeable cells exponentially growing. It specifically inhibits the G_1-S transition delaying the time of entering the budded phase of small unbudded cells and increasing critical protein content and volume required for budding (Baroni et al., 1992). These findings are not necessarily in contrast with the cAMP mediated increase of Cln3 protein level, since cyclic AMP appears to act differently in the Start area, with a positive induction of cell growth at Start B and inhibitions of Cln1 and Cln2 later.

Cln3 is not inhibited by cAMP and counteracts Cln1 and Cln2 inhibitions by mediating their growth-dependent expression. The inhibitory action of cAMP (and consequently of protein Kinase A in response to rich nutrients) serves to reset the critical size in function of the changing nutritional conditions (Baroni et al., 1994).

GPCRs: the Gpa2-Gpr1 system

Yeast cells growing on a fermentable carbon source, such as glucose, display low levels of the storage carbohydrates trehalose and glycogen, as well as low expression of stress resistance genes. The latter effect, together with the low level of trehalose, which also acts as a stress-protective sugar, results in a general low tolerance to various stress conditions. On the other hand, in the stationary phase or when growing on a nonfermentable carbon source, such as glycerol or ethanol, the cells display the opposite phenotype. This high intrinsic stress tolerance is also a general characteristic of strains with impaired PKA activity, even when they are growing on a fermentable carbon source.

The cAMP-PKA pathway has been implicated in the regulation of these phenotypes as a function of the nutrient conditions. The addition of glucose to glucose-deprived cells activates adenylate cyclase (Cyr1) and causes a rapid increase in cAMP, followed by a concomitant increase in PKA activity (figure 10). For this, a dual glucose-responsive system is required: detection of the extracellular glucose occurs through a GPCR system, whereas intracellularly, the system depends on sugar phosphorylation. How sugar phosphorylation impinges on cAMP signaling is not yet fully understood, but it may occur through regulation of the Ras proteins (Colombo et al., 2004).

The rapid stimulation of cAMP synthesis requires a low level of glucose phosphorylation by any one of the three glucose kinases encoded by *GLK1*, *HXK1* or *HXK2* (Rolland et al., 2000). This means that partial metabolism of the ligand by phosphorylation is required to sustain stimulation of the adenylate cyclase Cyr1. In details the sugar-sensing GPCR system consists of the receptor Gpr1, the Gα protein Gpa2 (Colombo et al., 1998) and its regulator of heterotrimeric G protein-signaling (*RGS*) protein, Rgs2 (Versele et al., 1999).

The structural features that are commonly found in GPCRs are also present in Gpr1: it contains seven transmembrane domains, has an extended N and C-terminus, and a large third intracellular loop. Gpr1 was originally isolated as an interaction partner of Gpa2, a Gα protein previously implicated in glucose-induced activation of the cAMP-PKA pathway (Xue et al., 1998; Kraakman et al.,1999). Gpr1 was also picked up in a separate screen for mutants with an increased stress resistance after initiation of fermentation. In this case, the mutant gene was designated as fil2 (for 'fermentation-induced loss of stress resistance'; Van Dijck et al., 2000). The identification of fil2 as a nonsense mutation in the *GPR1* gene revealed the importance of this receptor protein for rapid adaptation to the presence of glucose (Kraakman et al., 1999).
Among the array of sugars tested for their ability to trigger cAMP-PKA pathway activation via Gpr1, only glucose and sucrose were effective.
The structurally very similar sugars fructose and galactose had no effect, whereas mannose had an antagonistic effect (Lemaire et al., 2004). This illustrates the very high specificity of Gpr1, a typical hallmark of GPCRs. The absence of Gpr1 activation by fructose, a rapidly fermentable sugar, implies that fructose only activates cAMP signaling via the glucose phosphorylation-dependent mechanism (Colombo et al., 2004; Paiardi et al., 2007).

Gpr1 is also essential for glucose induced Ca^{2+} signaling, and the interaction between Gpr1 and the Plc1 phospholipase C might have a role in this pathway (figure 10).

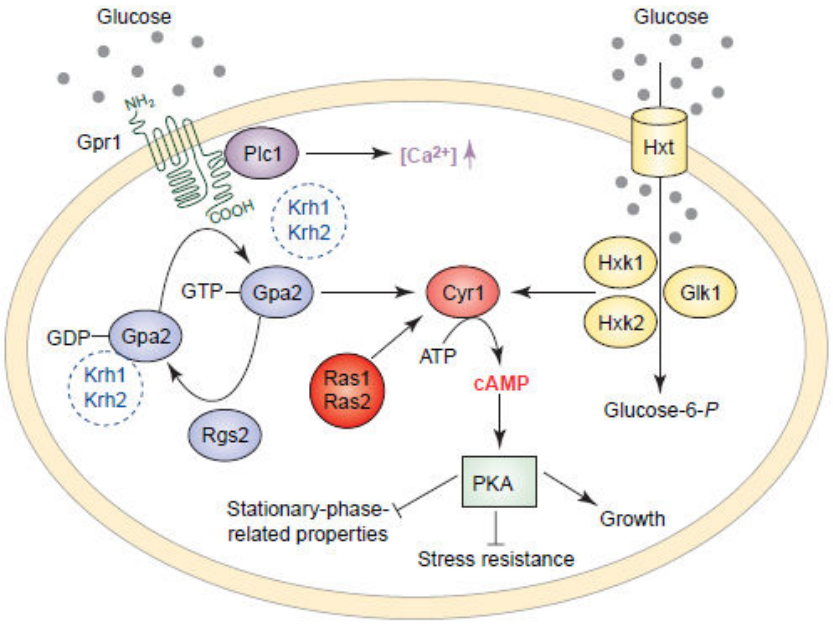

Figure 10. **Current model of glucose sensing in Saccharomyces cerevisiae**.
Rapid stimulation of cyclic AMP (cAMP) synthesis and subsequent activation of protein kinase A (PKA) occurs when glucose is added to cells growing on non-fermentable carbon sources or to derepressed stationary phase cells. Glucose is detected via a dual glucose sensing process and results in activation of the adenylate cyclase Cyr1 (also known as Cdc35). The intracellular sensing system requires any glucose transporter (encoded by the *HXT* genes) and glucose phosphorylation by one of the sugar kinases (Glk1, Hxk1 or Hxk2). The extracellular sensing system involves the Gpr1-Gpa2 G-protein coupled receptor (GPCR) system. Rgs2 has been identified as a regulator of Gpa2. The Gα protein Gpa2 apparently functions without a classical β- or γ-subunit. The kelch repeat proteins, Krh1 and Krh2, might act as alternative β -subunits, although this possibility remains controversial. How glucose phosphorylation supports GPCR signaling remains unclear. The G proteins Ras1 and Ras2, as well as the Plc1 phospholipase C, might be involved in this pathway. The latter is required for a glucose-induced influx of Ca^{2+}.
(From Holsbeeks et al., 2004).

The interdependency between the GPCR system and cAMP signaling

The constitutively active *GPA2^{V132}* allele is able to bypass the inactivation of *GPR1* for glucose-induced activation of cAMP synthesis, but not the request for sugar uptake and phosphorylation (Rolland et al., 2000; Kraakman et al., 1999). Interestingly, the *GPA2^{V132}*allele also increases the fructose-induced cAMP signal to the same intensity as the glucose signal and enables concentrations of glucose as low as 5 mM to fully activate the cAMP-PKA pathway; this is consistent with the fact that the *GPA2^{V132}* strain only needs to fulfill the phosphorylation request in order to activate the cAMP signaling, since the GPCR module is constitutively activated (Rolland et al., 2000; Rolland et al., 2002).
Thus, *GPA2^{V132}* can fully substitute for the requirement of high extracellular glucose, allowing ligands that are phosphorylated but not detected by the Gpr1-Gpa2 system (such as fructose and low glucose) to fully activate the cAMP circuit (Rolland et al., 2000).

The interdependency between the GPCR system and the sugar phosphorylation for glucose-dependent cAMP signaling is rather puzzling: apparently, glucose, which acts as an extracellular ligand for the GPCR system, has to be transported inside the cell and phosphorylated in order to be able to stimulate its effector system (Colombo et al., 2004). Glucose phosphorylation seems to be required in some way to make adenylate cyclase responsive to activation by the GPCR system (Colombo et al., 2004). Interestingly, the glucose-induced Ras-GTP loading is also dependent on sugar uptake and phosphorylation, while it does not require the presence of a functional GPCR system. Furthermore, even low glucose levels (5mM) can trigger the increase in Ras-GTP in a *gpa2Δ gpr1Δ* strain: therefore, it has been suggested that glucose phosphorylation might act through the Ras proteins to activate the cAMP signaling (Colombo et al., 2004). According to the proposed model, a glucose phosphorylation-dependent mechanism would cause inhibition of the Ira proteins, resulting in a rapid increase in Ras2-GTP levels; activated Ras would then prime adenylate cyclase for further stimulation by the GPCR system (Colombo et al., 2004).

RIBOSOME BIOGENESIS

Cell growth requires the synthesis of proteins, the synthesis of proteins requires ribosomes. Thus, the control of growth potential must somehow involve the control of ribosome synthesis (Rudra and Warner, 2004).
The budding yeast ribosome consists of 79 ribosomal proteins, encoded by 138 genes (RP regulon), and four rRNAs (5S, 5.8S, 18S, and 25S) encoded by 150 rDNA repeats existing as a tandem array in the genome.
Another 236 genes (Ribi regulon) encodes proteins involved in ribosome assembly (which takes place in the nucleolus) and activity (RNA polymerases I and III, tRNA synthetases, rRNA processing and modifying enzymes, translation factors). The promoters of these genes contain two motifs, termed RRPE and PAC (Zaman et al., 2008).

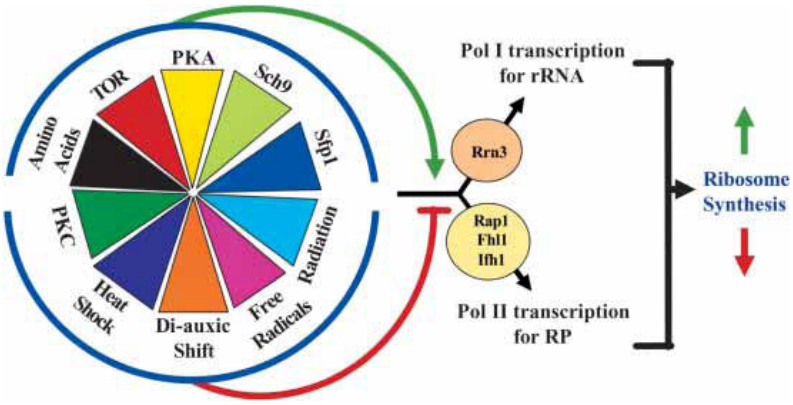

Figure 11. **Regulation of ribosome biosynthesis in *S. cerevisiae*.**
Ribosome biosynthesis requires several elements working in tandem: an active TOR pathway; an active PKA pathway; sufficient amino acids; and the factors Rap1, Fhl1, Ifh1, Sfp1, Sch9, Rrn3 (for rRNA), and perhaps others (see text for details). Repression of ribosome synthesis can come through inactivation of the TOR pathway, reduction of PKA activity, signaling via PKC, deprivation of an amino acid, stress of many kinds including heat shock, free radicals, radiation, and so on.
(From Jorgensen et al., 2004b).

To maintain robust growth in response to favourable conditions, yeast cells synthesize about 2000 ribosomes per minute (Warner, 2001).
Ribosome biogenesis is the predominant biosynthetic activity in yeast cells and is extremely expensive in energetic terms; it is estimated that during exponential growth synthesis of the translation machinery accounts for 50% of total transcription and utilizes about 90% of the cellular energetic resources (Warner et al., 2001). Therefore, it is not surprisingly that yeast cells carefully adjust their ribosome biogenesis rate in response to changes in nutrient availability (Zaman et al., 2008).

Two key nutrient-sensing circuits, the cAMP-PKA and TOR signaling pathways, regulate the transcription of rRNA, RP, and Ribi genes (Neuman-Silberberg et al., 1995).
The effects of the TOR pathway on regulation of ribosome biogenesis are (at least partially) mediated by the Sch9 kinase (Jorgensen et al., 2004; Urban et al., 2007). Sch9 is specifically required for maximal expression of the RP regulon and is regulated in a nutrient-sensitive fashion by both phosphorylation and localization to the vacuolar membrane. The abundance of Sch9 is also regulated by TOR activity: under steady-state proliferation on different carbon sources, Sch9 levels correlate with growth rate, RP/Ribi transcription, and cell size (Jorgensen et al., 2004).

A key role for the transcription factor Sfp1 has also been documented (Jorgensen et al., 2004; Jorgensen et al., 2002). Sfp1 act as a "master regulator" controlling a large cohort of >200 genes of the Ribi regulon and (directly or indirectly) also activates the RP regulon transcription (Jorgensen et al. 2002; Fingerman et al., 2003).
The sub-cellular localization of Sfp1 is highly responsive to nutrient conditions: in glucose medium, Sfp1 resides in the nucleus, but upon nutrient starvation or exposure to stress, Sfp1 rapidly re-localizes to the cytoplasm (Jorgensen et al. 2004). Nutrient-responsive localization of Sfp1 is modulated by both TOR and cAMP-PKA pathway, although the molecular details of this regulation is not entirely known. Sfp1are able to dictate the nuclear localization of Fhl1 and Ifh1, two transcription factors implicated in RP gene expression (Martin et al. 2004; Rudra et al. 2005): nutrient starvation or loss of *SFP1* forces Fhl1 and Ifh1 to localize to nucleolus, concomitant with reduced RP gene transcription. Recent evidences have demonstrated that Sfp1 is a direct substrate of the TORC1 complex, which regulates Sfp1 function via phosphorylation at multiple residues. Sfp1, in turn, negatively regulates TORC1 phosphorylation of Sch9, the other key target of Tor in ribosome biogenesis, revealing a feedback mechanism that regulates RP and Ribi gene transcription.

A genome-wide analysis of size control in yeast has revealed surprising connections between ribosome biogenesis and cell size (Jorgensen et al., 2004; Jorgensen et al., 2002).
Mutations that accelerate cell division relative to cell growth result in a small cell size, referred to as *whi* phenotype. The systematic screens has shown that most of the mutations reducing cell size affect genes involved in respiration or ribosome biosynthesis. Notably, two of the smallest strains identified lack either the Sch9 kinase or the transcription factor Sfp1; the inactivation of these genes also results in reduced expression of RP and Ribi genes and in a slow-growth phenotype, but the effects on size (~40% of wild type strain volume) are disproportionate relative to the changes in doubling time, indicating that growth and cell division are partially uncoupled in these strains. In contrast, ectopic expression of either *SFP1* or *SCH9* leads to large cells (Jorgensen et al., 2004).

Consistent with a possible role of Sch9 and Sfp1 as negative regulators of Start, the activation of the G_1-S transcriptional program and the progress into S phase are accelerated in both *sfp1Δ* and *sch9Δ* null strains: this result suggest that Sch9 and Sfp1 may act upstream of the G_1-S transcriptional network (Jorgensen et al., 2004).
Even more interesting, both *sfp1Δ* and *sch9Δ* null strains are largely defective in carbon source modulation of cell size threshold, in contrast to a *cln3Δ bck2Δ whi5Δ* mutant, which is fully responsive to carbon source despite the loss of all the known regulator of Start (Jorgensen et al., 2004). Introduction of the *sfp1Δ* mutation into a *cln3Δ bck2Δ whi5Δ* background reduces cells size, but not as much as the single *sfp1Δ* mutant: since by criterion of cell size *sfp1Δ* is not fully epistatic neither to the triple *cln3Δ bck2Δ whi5Δ* null strain nor to any of the single mutant, Whi5, Cln3, and Bck2 still play a role in *sfp1Δ* null cells.
Apparently, nutrients operate through Sfp1 and Sch9 to match the critical size threshold required for Start to the rate of ribosome biogenesis: surprisingly, this mechanism seems to be largely independent of known upstream regulators of the G_1-S transition (Jorgensen et al., 2004).

Tyers and colleagues (Jorgensen and Tyers, 2004) have proposed that the cAMP-PKA pathway, the TOR pathway, Sch9 and Sfp1 function in a nonlinear network that dictates both the critical cell size threshold and expression of the Ribi and RP regulons according to nutrients availability and stresses (Jorgensen and Tyers, 2004). Alterations in any component of this quartet has a profound impact on cell size: reduced activity of the cAMP-PKA pathway or loss of Sfp1 and Sch9 renders the cells small and impervious to carbon source regulation of their size (Jorgensen et al., 2004; Belotti et al., 2006).

On the other hand, overproduction of Sfp1 and Sch9 or constitutive activation of the cAMP circuit results in large cells (Jorgensen et al., 2004; Baroni et al., 1989; Baroni et al., 1992). Like cAMP-PKA and TOR networks, Sfp1 and Sch9 are sensitive to nutrient status and to stresses (at the level of localization and abundance, respectively). Interestingly, as noted above, cAMP-PKA, Sfp1, and Sch9 all converge on ribosome biogenesis by regulating the transcription of the RP and Ribi regulons in response to nutrient (and stress) signals (Jorgensen et al., 2002; Jorgensen et al., 2004). In addition, strains deleted for other genes implicated in ribosome synthesis are similarly (although less dramatically) uncoupled for growth and division.
All these evidences have been unified in a model where the rate of ribosome biogenesis, which is proportional to nutrient quality and abundance, negatively regulates Start execution, thereby linking nutrient status to the setting of the critical cell size: the current rate of ribosome biogenesis would modulate the critical cell size according to nutrients availability, whereas the overall translation rate (which depends on the current cellular ribosome content and nutrient status) would steadily report cell size to the cell division machinery (Jorgensen & Tyers, 2004).
Ribosome biogenesis is optimally placed in the cellular network to integrate both upstream nutrient (stress) signaling pathways and feedback signals from downstream events.
Accordingly, the rate of ribosome biogenesis parallels nutrient effects: under nutrient shortage, ribosome biogenesis rate is low and cells are small, whereas in presence of abundant and good quality nutrient supply ribosome biogenesis rate is high and cells are large (Jorgensen et al., 2004). Moreover, just like the critical size itself, the rate of ribosome biogenesis rapidly and dynamically adapts to changes in nutrient status (Kief and Warner, 1981).
By coupling the size threshold directly to ribosome biogenesis the yeast cell may anticipate future changes in its protein synthesis rate (triggered by fluctuations in nutrients availability or stresses) and thus promptly adjust its size long before these changes actually occur (Jorgensen et al., 2002).
Under favorable growth conditions, the cell needs vigorous ribosome biosynthesis to enable rapid growth and at the same time is interested in delaying cell cycle entry in order to grow to an optimal size: according to the proposed model, the PKA and the TOR pathway would relay nutrient (and/or stress) signals to Sfp1 and Sch9, thus promoting the transcription of RP and Ribi regulons and a resulting delay in Start execution through an unknown mechanism.

Then, when environmental conditions deteriorate, as a consequence of stress or nutrient shortage, cells needs more resources to respond to the hostile situation: under these circumstances, Sfp1 rapidly abandons the nucleus and Sch9 abundance/localization are altered, ribosome synthesis slow down and the cell size threshold can be consequently reset to a lower value (accordingly) (Rudra and Warner, 2004; Cook and Tyers, 2007).
The mechanisms connecting ribosome biogenesis to Start execution via Sfp1 and Sch9 are still unknown. As discussed above, it has been hypothesized that these effects may at least partially independent of Cln3 and Whi5, since the critical size threshold can be reset also in strains lacking these upstream regulators of the G_1-S transition.
An interesting hypothesis is that the cell cycle machinery and the ribosome biosynthetic apparatus might have something in common to compete for. Aldea and colleagues have proposed that chaperones availability might be the "missing link" between ribosome biogenesis and regulation of the critical size threshold required for cell cycle entry (Aldea et al., 2007; Verges et al., 2007) as already discussed.
According to the proposed model, in rapidly growing cells high ribosome and protein synthesis rates might reduce the availability of Ydj1 for the ER-release of Cln3, as an inevitable consequence, lead to a delay in cell cycle entry. A simple corollary derived from this hypothesis is that the critical threshold size at Start would be proportional to the growth rate: the faster the cell grows, the larger it must grow to accumulate enough chaperone amounts to overcome constant growth demands and release Cln3 from the ER to trigger Start (Aldea et al., 2007; Verges et al., 2007).
Although interesting, this model fails to explain how a strain lacking *CLN3* can still adjust its size in response to nutrient availability (Jorgensen et al., 2004; deBruin et al., 2004; Costanzo et al., 2004).
Consistent with the model described by Tyers and colleagues, recent studies evaluating the effect of deficiencies in ribosome biosynthesis on cell cycle progression have confirmed that changes in the rate of ribosome biogenesis can affect execution of Start long before any alterations in overall protein synthesis rates occur (Bernstein et. al., 2007). However, the effects on size observed in this case are opposite from those predicted by the model: in fact, upon depletion of an essential ribosomal protein, biogenesis rate slow down, the passage through Start is inhibited through a Whi5 dependent mechanism and cell size increase instead of decreasing (Bernstein et al., 2007).

Abstract

The budding yeast *Saccharomyces cerevisiae* is a model organism for studies on cell cycle. For the survival of these cells a tight coordination of cell growth and division occurs at Start, a regulatory area of the cell cycle positioned immediately before beginning of S phase, at the G_1-S boundary. After Start, a cell is committed to a new round of division. Start execution requires reaching a critical cell size (cellular protein content per at the onset of DNA replication, Ps) to enter into S phase. Ps increases in proportion with ploidy and is modulated by nutrients.
Our laboratory identified Far1, a cyclin kinase dependent inhibitor, and Cln3, a G_1 phase cyclin, as components of a nutritional modulated threshold controlling the entrance into S phase. *FAR1* overexpression induces a nutritionally modulated increase in cell size (Alberghina et al., 2004). By genome-wide transcriptional analysis of *FAR1*-overexpressing and *far1Δ* cells grown in ethanol- or glucose-supplemented minimal media with a range of phenotypic analysis, our group showed that Far1 overexpression originates large transcriptional remodelling that affects pathways involved in controlling cell growth, including sugar sensing (that is known to affect the cell growth rate) and the PKA and TOR pathways that are the major pathways involved in regulating cell growth in yeast.
In *S. cerevisiae*, Sch9 and Sfp1 are two main downstram targets of the Tor pathway involved in controlling cell growth through regulation of the protein synthesis. The first is a zinc finger protein, promoting the transcription of a large cluster of genes involved in ribosome biogenesis, where the latter is a serine/threonine protein kinase involved in stress response and nutrient-sensing signaling pathway. Both *SFP1* and *SCH9* were identified in a genome-wide screen for small size (*whi*) mutants. Therefore it was of interest to see whether the increase in size (RNA and protein) brought about by *FAR1* overexpression was mediated by Sfp1 and Sch9.
The effect of *FAR1* overexpression on cell size parameters in the wild type BY4741 strain (isogenic to the *sch9Δ* and *sfp1Δ* mutants), grown in synthetic complete media supplemented with either ethanol or glucose as a carbon source, was similar to that reported in the W303 background. *sfp1Δ* and *sch9Δ* mutants were much smaller than wild type both in glucose - confirming previous data As observed in wild type cells, in both mutant strains *FAR1* overexpression had only minor effects on cell cycle and cell size related parameters on glucose-grown cells. *FAR1* overexpression did not affect duplication time in ethanol-grown *sch9Δ* cells, while *sfp1Δ* mutants overexpressing the *FAR1* gene product were quite unhealthy with a large increase in duplication time.
Overall increase in cell size was dramatic in ethanol-grown cells: however, while in wild type cells and *sch9Δ* mutants the increase in cell size derived from a balanced increase in RNA and protein content, in the *sfp1Δ* mutant the increase in protein content was not accompanied by an increase in RNA content, as shown by both FACS and chemical analysis, indicating that Sfp1

is required to maintain proper coupling of RNA and protein syntheses when the Far1 protein is overexpressed in ethanol-grown-cells.

S. cerevisiae needs to regulate growth and cell cycle progression according to the frequent changes in the nutrient status, so that proliferation is rapid when large supplies of nutrients are available and ceases when these become exhausted. Nutrients like glucose must therefore generate signals that are received and elaborated by the complex machinery governing growth and cell cycle progression. Accordingly, yeast evolved several mechanisms to monitor glucose level: the cAMP-PKA pathways (with its two branches comprising Ras and the Gpr1-Gpa2 module), the Rgt2/Snf3-Rgt1 pathway and the main repression pathway involving the kinase Snf1.

In order to dissect whether the glucose effect on cell size was due to its function as nutrient, that require metabolism of the sugar, or to sensing of extracellular glucose levels, we analyzed yeast strains in which one or more of the glucose sensing pathway was impaired, due to deletions in one or more genes encoding glucose receptors: *GPR1* encoding a sensor for high glucose, *SNF3* encoding a sensor monitoring the presence of low glucose concentrations, and stimulating the expression of high affinity glucose transporters and *RGT2* encoding a receptor that monitors the presence of high glucose concentration, and therefore leads to expression of low affinity glucose transporters).

The *gpa2Δ gpr1Δ* strain does not show substantial changes in duplication time compared to its isogenic wild type grown in the same conditions, while its protein content is consistently lower. In the *snf3Δ rgt2Δ* and in the *snf3Δ rgt2Δ gpa2Δ gpr1Δ* strains a lower protein content is accompanied by an increase in duplication time, when compared to wild type.

In wild type cells a steep correlation between P and MDT is observed for cell grown in glucose containing media, whereas when glucose is substituted with ethanol a dramatic increase in MDT in accompanied by a minor decrease in average protein content (P). Qualitatively, the same trend can be observed in glucose sensing mutants, that hence retain at least a partial ability to modulate cell size. Although fine details of metabolism may differ between wild type, on one side, and sensing mutants, on the other, the type of metabolism remains unchanged (*i.e.*, all mutants grown in glucose-containing media use a fermentative metabolism). These finding suggest that under conditions of balanced exponential growth cell size is *driven* by metabolism, but *actual fine tuning* of P is set according to sensing of extracellular glucose.

In conclusion, this work highlighted that the elements involved in the cell size determination are multiple and interconnected. A strong alteration in cell size and protein content could originate not only from alteration in the dosage of genes involved in the molecular mechanism of the threshold which controls Ps, but also from environmental conditions. Notably glucose acts not only as a carbon and energy source, but as a modulator molecule as well.

Materials and Methods

Construction of yeast strains

DNA manipulations were performed according to standard techniques. *Saccharomyces cerevisiae* aploid strains used in this study were derivatives of CEN.PK2-1C (MATa*, leu2-3, 112 ura3-52, trp1-289, his3-1, MAL2-8c, SUC2, hxt17*) and from BY4741 (MATa, *his3Δ1, leu2Δ0, met15Δ0, ura3Δ0*). Strains used in this study are listed in Table I. .
Auxotrophic strains were made prototrophic by integration of the appropriated *URA3*, *LEU2*, *HIS3* and *TRP1* cassettes, obtained by digestion with *BamHI* of the YDp plasmids (Berben et al., 1991).
Deletion mutants were generated by the PCR-mediated gene disruption method (short flanking homology *loxP::marker::loxP/Cre* recombinase system: Guldener et al., 1996; Guldener et al., 2002). Cells were transformed by the classic lithium acetate procedure (Schiestl & Gietz 1989).
After growth of transformants on selective media, deletion of the targeted gene sequences was routinely confirmed by colony PCR using the primer sets listed in Table II. When necessary, markers used for disruption were removed by inducing the recombination of the flanking *loxP* sequences through expression of the Cre recombinase (Guldener et al., 1996; Guldener et al., 2002). In Table II primers for generations of multiple disruption cassettes containing different heterologous selectable markers using the pUGXX series of plasmids (Euroscarf) as template are shown.
Primers were designed using the PerlPrimer software and purchased from Primm.

A complete set of isogenic strains expressing C-terminal HA-epitope tagged versions of key cell cycle regulators (Cln3, Cln2, Clb5, Sic1, Far1) were constructed by in-locus 3'in-frame insertion, according to the procedure described by Longtine et al., 1998. The *4HA-KANMX* fragments used for the tag of the various proteins were generated by PCR using the pDHA plasmid (Tripodi et al., 2007). Successful genomic-tag was verified in yeast transformants by PCR colony and subsequent western blot analysis.
To obtain double-tagged strains, the pDHA-hph plasmids was constructed by replacing the *KANMX* marker of pDHA (*BglII-PmeI* fragment) with a *BamHI-EcoRV* segment from pAG26 (Goldstein et al., 1999), containing the *hph* gene (*Klebsiella pneumoniae)* that confers resistance to the antibiotic hygromycin B. Tagged strains were phenotypically indistinguishable from their parent strain in all the tested growth conditions.

Growth conditions

All strains cells were grown in shake flask at 30°C on a rotary shaker (160 r.p.m) in synthetic medium containing 0.67 g/L YNB (Formedium), supplemented with appropriate quantities of "drop-out" mixture (CSM, Formedium). Carbon source were either 5%, 2%, 0.5%,0.2%, 0.1% and 0.05% glucose (w/v) or 2% ethanol (v/v). Growth media also contained 0.2% (v/v) glycerol to improve growth in presence of ethanol. Solid media contained 2% (w/v) agar. Growth of liquid cultures was monitored as increase in cell number using a Coulter Counter model Z2 (Coulter Electronics, Inc.).
The fraction of budded cells was scored by direct microscopic observation on at least 200 cells, fixed in 3.6% formalin and mildly sonicated. For growth plate assay, serially diluted cellular suspensions were spotted on plates and incubated at 30°C.
The length of the budded phase was calculated according to the formula

$$T\mathrm{B} = \log 2\ (1 + F\mathrm{B})\ T$$

where FB is the percentage of the budded cells and T is the population doubling time ($T = \ln 2/\alpha$, where α is the experimentally determined growth rate).
Analysis of the cell size distribution was performed on asynchronous cultures during log-phase growth using a Coulter Z2 Particle Cell Analyzer (Beckman-Coulter). Cell size distribution was analyzed with the Z2 AccuComp software (Beckman-Coulter).

Flow cytometric analysis

Samples of growing cultures (about 2×10^7 cells) were collected and fixed in 70% ethanol before analysis (Coccetti et al., 2004). Cells were washed twice times with PBS (3.3 mM NaH_2PO_4, 6.7 mM Na2HPO4, 127 mM NaCl, 0.2 mM EDTA, pH 7.2), resuspended in RNAse solution (1 mg/ml RNAse (Roche) in PBS) and incubated over night at 30°C.
To obtain protein distribution, cells were washed once with PBS, resuspended in 1mL of freshly prepared FITC staining solution (50 µg/mL fluorescein isothiocianate (Sigma-Aldrich) in 0.5 M $NaHCO_3$) and incubated at 4°C in the dark for 1h. Cells were then washed three times with PBS and resuspended in 1 ml PBS before the analysis.
For DNA staining, cells treated with RNAse were washed once with PBS, resuspended in 1 ml of DNA staining solution (1 M Sytox Green (Molecular Probes) in 50 mM Tris pH 7.5) and incubated in ice and dark for at least 30 min.

All samples were mildly sonicated for 20s before FACS analysis, which was performed on at least 2×10^5 cells with a BD FACStarPlus fluorescence-activated cell sorter equipped with a Coherent Innova 70 Ion-Argon laser with a 488-nm laser emission.
Plot generation and data analysis were performed using the WinMDI 2.9 software. For DNA/Protein biparametric staining, cells were washed once in PBS, resuspended in 1 ml of PBS with RNAse 1 mg/ml for at least 1 h, centrifuged and resuspended in 1 ml of 10 000-fold diluted protein staining solution (FITC 5 ng/ml final concentration in 0.5 M $NaHCO_3$) and incubated for 30 min in ice and dark, washed four times with PBS and resuspended in DNA staining solution in ice and dark for 30 min. All the washing and staining steps were performed in 2 ml Eppendorf tubes and centrifugations at 12000 r.p.m. for 5 min at 4°C. Cell suspensions were transferred in FACS Falcon tubes and sonicated for 10 s before FACS analysis. Analysis were performed with a BD FACStarPlus equipped with a Coherent Innova 70 Ion-Argon laser with a 488-nm laser emission. Average protein content at the beginning of the cell cycle (Po), at the onset of DNA replication (Ps) were determined as average protein content (average channel number) of appropriately gated cells from the density plot derived from FACS analysis of double DNA/protein stained cells. Plot generation, analysis and gating process were performed with WinMDI 2.8 software (downloadable from TSRI Cytometry Software Page at http://facs.scripps.edu/software.html). The validity of gating S phase cells (i.e. good selection of cells actually belonging to S phase among the entire population visualized in the density plot) was assessed by overlapping the DNA histogram of differentially gated cells to the DNA histogram of the entire population.

Determination of RNA and protein content by chemical assay

Exponentially growing cells ($5*10^8$ total cells) were collected by filtration, washed twice with ice-cold 5% Trichloroacetic Acid (TCA) and stored at -20°C for at least 12 hours. Samples were then slowly thawed in ice, resuspended in 5 ml of perchloric acid 0.3 N and heated 30 minutes at 90° C. After centrifugation (10 minutes at 3500 rpm) the supernatant was recovered and used for RNA determination, whereas the pellet was used for protein determination as described below. Samples were appropriately diluted in water, an equal volume of Orcinol solution (0.5 g Orcinol Monohydrate and 0.25 g FeCl-$6H_2O$, dissolved in 50ml of 37% HCl) was added and the mixtures were heated at 90°C for 20 minutes. Absorbance was read at 660 nm. Ribonucleic acid from baker's yeast (MP biochemicals) was used as a standard (Alberghina et al., 1975). For protein determination, pellets were resuspended in 1N NaOH, and incubated overnight at room temperature on a rolling drum.
Samples were then centrifuged (10 minutes at 3500 rpm) and the resulting supernatants were used for protein determination according to the microbiuret method, using bovine serum albumin as a standard (Alberghina et al., 1975).

Protein extraction and Western blot analysis

For preparation of crude extracts, exponentially growing cells (about $4x10^8$) were collected and lysated in cold 20% TCA buffer with glass beads, according to the procedure described in Reid & Schatz, 1982, with minor modifications. Protein concentration was determined by UV dosage at 280nm. Typically 50-100 μg of total extract were used for Western blot analysis. As a loading control, blotted membranes were stained with Anti-Cdc34 monoclonal antibodies (Coccetti's lab) before immunodecoration. Anti-HA monoclonal antibodies (12CA5) were purchased from Roche. Enhanced chemioluminescence system (ECL, Amersham Biosciences) was used for immunoblot detection according to the manufacturer's instructions. Protein levels were quantified by densitometry analysis of raw scanned images using the Scion Image software (Scion Corporation). Images were resized and eventually adjusted for brightness/contrast for figures preparation

Table I. List of strains

Strains	***Relevant genotype***	***Reference***
BY4741 background		
BY4741	MATa, *his3Δ1, leu2Δ0, met15Δ0, ura3Δ0*	Brachmann & Boeke, 1998
BY4741 [pCM189]	MATa, *his3Δ1, leu2Δ0, met15Δ0, ura3Δ0* [pcM189]	This study
BY4741 [pTet-*FAR1*-15myc]	MATa, *his3Δ1, leu2Δ0, met15Δ0, ura3Δ0* [pTet-*FAR1*-15myc]	This study
*sfp1*Δ	MATa, *his3Δ1, leu2Δ0, met15Δ0, ura3Δ0, sfp1*::KAN.MX4	
*sfp1*Δ [pCM189]	MATa, *his3Δ1, leu2Δ0, met15Δ0, ura3Δ0, sfp1*::KAN.MX4 [pcM189]	This study
*sfp1*Δ [pTet-*FAR1*-15myc]	MATa, *his3Δ1, leu2Δ0, met15Δ0, ura3Δ0, sfp1*::KAN.MX4 [pTet-*FAR1*-15myc]	This study
sch9Δ	MATa, *his3Δ1, leu2Δ0, met15Δ0, ura3Δ0, sch9*::HIS3	
sch9 [pCM189]	MATa, *his3Δ1, leu2Δ0, met15Δ0, ura3Δ0, sch9*::HIS3 [pcM189]	This study
*sch9*Δ [pTet-*FAR1*-15myc]	MATa, *his3Δ1, leu2Δ0, met15Δ0, ura3Δ0, sch9*::HIS3 [pTet-*FAR1*-15myc]	This study
CEN.PK background		
CEN.PK2-1C	*MATa leu2-3,112 ura3-52 trp1-289 his3-1 MAL2-8^{c} SUC2 hxt17*	Entian & Koetter, 2007
snf3Δ	*snf3::his5^{Sp}*	This study
rgt2Δ	*rgt2::KANMX*	This study
snf3Δ rgt2Δ	*snf3::his5^{Sp} rgt2::KANMX*	This study
gpa2Δ	*gpa2::LEU2*	This study
gpr1Δ	*gpr1::his5^{Sp}*	This study
gpa2Δ gpr1Δ	*gpa2::LEU2 gpr1::his5^{Sp}*	This study
snf3Δ rgt2Δ gpa2Δ gpr1Δ	*snf3::loxP rgt2::KANMX gpa2::LEU2 gpr1::his5^{Sp}*	This study
Tagged-strains		
snf3Δ rgt2Δ CLB5-4HA SIC1-4HA	*snf3::loxP rgt2::loxP CLB5-4HA::KANMX SIC1-4HA::HPH*	This study
gpa2Δ gpr1Δ CLB5-4HA SIC1-4HA	*gpa2::LEU2 gpr1::his5^{Sp} CLB5-4HA::KANMX SIC1-4HA::HPH*	This study
snf3Δ rgt2Δ gpa2Δ gpr1Δ CLB5-4HA SIC1-4HA	*snf3::loxP rgt2::KANMX gpa2::LEU2 gpr1::his5^{Sp} CLB5-4HA::KANMX SIC1-4HA::HPH*	This study
gpa2Δ CLN2-4HA	*gpa2::LEU2 CLN2-4HA::KANMX*	
gpr1Δ CLN2-4HA	*gpr1::his5^{Sp} CLN2-4HA::KANMX*	This study
snf3Δ rgt2Δ CLB5-4HA	*snf3::loxP rgt2::loxP CLB5-4HA::KANMX*	This study
snf3Δ rgt2Δ CLN2-4HA	*snf3::loxP rgt2::loxP CLN2-4HA::KANMX*	This study
CLB5-4HA SIC1-4HA	CEN.PK2-1C *CLB5-4HA::KANMX SIC1-4HA::HPH*	This study

Table II. List of primers

Name	*Sequence (5'→3')*	*Comments*
5'-CLN3-HA-K	ACTGAAAAAGAGATCAACTTCCTCTGTGGATTGTGATTTTAATGATAG TAGCAACCTCAAGAAAACTCGCcggccgcatggatcctatcc	*CLN3-HA::KANMX*
3'-CLN3-HA-K	ATGTATGTTAACGTATTTGCTTTGCAAATTTTAATTTATTTGTTGTTAA ATGCATTTTTTTTTTGTCGTTggatggcggcgttagtatcg	*CLN3-HA::KANMX*
5'-SIC1-HA-K	AAGGTTAACGGATGAAGAAAAGAGAAGATTCAAGCCAAAGGCATTG TTTCAATCTAGGGATCAAGAGCATcggccgcatggatcctatcc	*SIC1-HA::KANMX* *SIC1-HA::hph*
3'-SIC1-HA-K	TTGCAAATAAATGTAGAATAAGTAAGTAAATAAAATATAATCGTTCC AGAAACTTTTTTTTTTCATTTCTggatggcggcgttagtatcg	*SIC1-HA::KANMX*
3'-SIC1-HA-HPH	TTGCAAATAAATGTAGAATAAGTAAGTAAATAAAATATAATCGTTCC AGAAACTTTTTTTTTTCATTTCTATCGATGAATTCGAGCTC	*SIC1-HA::hph*
5'-FAR1-HA-K	GATAGAAATAGAATATTTTGACCTGGTAAAGCAGCAAAGAATTCATC AGACCCTGGAAGTTCCCAACCTCcggccgcatggatcctatcc	*FAR1-HA::KANMX* *FAR1-HA::hph*
3'-FAR1-HA-K	ATAGACGTGGAGAAACGAAAAAAAAAAAAAGGAAAAGCAAAAGCCTC GAAATACGGGCCTCGATTCCCGAAggatggcggcgttagtatcg	*FAR1-HA::KANMX*
3'-FAR1-HA-HPH	ATAGACGTGGAGAAACGAAAAAAAAAAAAAGGAAAAGCAAAAGCCTC GAAATACGGGCCTCGATTCCCGAAATCGATGAATTCGAGCTC	*FAR1-HA::hph*
CLB5-HA For	TTATTTCCAAACTTTCAAGTGGTGTACATCCGAAATGCATAGCAACTT TCAAAATCTATTTAATCTTAAGcggccgcatggatcctatcc	*CLB5-HA::KANMX*
CLB5-HA Rev	CCTTTTAGTTCAGCAAAAAGAAAAGAAAATGTAAAGAGTATGCGAAT TCATGAGCATTACTAGTACTAATggatggcggcgttagtatcg	*CLB5-HA::KANMX*
5'-CLN2-HA-K	ATAAATAGCGGTAAATCTAGCAGTGCCTCATCTTTAATTTCTTTTGGT ATGGGCAATACCCAAGTAATAcggccgcatggatcctatcc	*CLN2-HA::KANMX*
5'-CLN2-HA-K	CTCTCTTTTCCCGCAGAATATGAAAGCTTTTCTTTTATAAATCTTATAA TATTGGTCTCTTTTTGGTACggatggcggcgttagtatcg	*CLN2-HA::KANMX*
gpr1::loxP-FW	CGACAAACAAGTGATCCGAAGTGTGACGAATAAAGCAAACTCTCCAA CTCcagctgaagcttcgtacgc	*gpr1* deletion
gpr1::loxP-RE	GTCAATTTGTATTACGTTCCTTACTTTCCATTTTCAAACATCGCGATAC gcataggccactagtggatctg	*gpr1* deletion
snf3::HPH-FW	CAGAAGGATATGCCTTTGTTGGCATAGAAAGAAGAATTTATAAcagctga agcttcgtacgc	*snf3* deletion
snf3::HPH-RE	GCACGTCCGCTTAATTAATACATCGAATAACATTAAATTAAgcataggcca ctagtggatctg	*snf3* deletion
rgt2::KAN-FW	CAGAAACCACTATATATATATGGAAATATCTCGAATATTGCTTGTcagct gaagcttcgtacgc	*rgt2* deletion
rgt2::KAN-RE	CGGTTTATAAGACCTCGAACGATCGTAAGATGCTATTGGTTTgcataggcc actagtggatctg	*rgt2* deletion
gpa2α	GCGCATCTTCAGAAAAGAACG	Control *gpa2* deletion
gpa2β	TGATGGCGGCAAATACTAATC	Control *gpa2* deletion
FW-gpr1 (-152 ATG)	TTGTCTACATCCCTTTCTCTACG	Control *gpr1* deletion
RE-gpr1 (+155 STOP)	ACTTATCGAGGAATCACATTGC	Control *gpr1* deletion
FW-SNF3 (-210 ATG)	CTAGACAATAGTCCTATCCTCGGCA	Control *snf3* deletion
RE-SNF3(+245 STOP)	TAATGACTTCCGACGTTGACCG	Control *snf3* deletion
RGT2-CNT::KAN-FW	GAGCAGATCAGGAATAGTATC	Control *rgt2* deletion
3'-CNT-HA-KAN	ATTCTGGGCCTCCATGTCG	Control *KANMX* deletion Control *HA::KANMX* TAG
KAN-CNT-RE	CCTGGAATGCTGTTTTGCCG	Control *KANMX* deletion Control *HA::KANMX* TAG
HPH-CNT-RE	CACTATCGGCGAGTACTTC	Control *hph* deletion Control *HA::hph* TAG
KAN/HIS5Sp-FW	CCTCGACATCATCTGCCC	Control *KANMX* deletion Control *his5*^{Sp} deletion
KAN/HIS5Sp-RE	GGATGTATGGGCTAAATG	Control *KANMX* deletion Control *his5*^{Sp} deletion
HIS5-RE(1126bp)	TTACAACACTCCCTTCGTGC	Control *his5*^{Sp} deletion
LEU2Kl-FW	ATCTCATGGATGATATCC	Control *LEU2*^{Kl} deletion
LEU2Kl-RE	AGTTATCCTTGGATTTGG	Control *LEU2*^{Kl} deletion
URA3Kl-FW	CAGACCGATCTTCTACCC	Control *URA3*^{Kl} deletion
URA3Kl-RE	TTGGCTAATCATGACCCC	Control *URA3*^{Kl} deletion
*FW-SIC1 (-187 STOP)	TGAACTGGTCACTCAGGAAATTAG	Control *SIC1-HA*
RE-SIC1 (+231 STOP)	CTCGCTTTGACGAAATACTACAATG	Control *SIC1-HA*
*FW-FAR1 (-183 STOP)	GATGTAACTCTTCGTCTACCAC	Control *FAR1-HA*
RE-FAR1 (+174 STOP)	CCAATAGGTTCTTTCTTAGGCA	Control *FAR1-HA*

*FW-CLB5 (-306 STOP)	CATTTACCTCCATCTACCGT	Control *CLB5-HA*
RE-CLB5 (+536 STOP)	TTCTCACTAATAACACCACACC	Control *CLB5-HA*
*FW-cln3 (-280 STOP)	TTCAGGTTCGTTCTCTTCTACC	Control *CLN3-HA*
CNT-cln3-RE	TAATGTGACTAGAGGAAGTAAGGAG	Control *CLN3-HA*
*FW-CLN2 (-363 STOP)	CAATCATCACCAATCACTCCA	Control *CLN2-HA*
RE-CLN2 (+362 STOP)	ATATGTCGTCGCTTCTTATCC	Control *CLN2-HA*

Aim of the study

Cell proliferation requires the tight coordination of different processes, such as mass accumulation, DNA replication and cell division. This coordination, which heavily relies on the ability of a cell to integrate environmental and metabolic signals with the activity of key regulators of cell cycle progression, ensures maintenance of cell size homeostasis over multiple generations and faithful partitioning of the genetic material.

An essential requisite for the survival of free living microorganism like the budding yeast *Saccharomyces cerevisiae* is the capacity to regulate growth and cell cycle progression according to the frequent changes in the nutrient status, so that proliferation is rapid when large supplies of nutrients are available and ceases when these becomes exhausted. Nutrients like glucose must therefore generate signals that are somehow received and elaborated by the complex machinery governing growth and cell cycle progression.

The budding yeast *Saccharomyces cerevisiae* is a model organism for studies on cell cycle. For the survival of these cells a tight coordination of cell growth and division occurs at Start, a regulatory area of the cell cycle positioned upstream of the S phase, at the G_1-S boundary and whose execution commits a cell to a new round of cellular division.

To execute Start, a cells needs to achieve a critical cell size (protein content per cell at the onset of DNA replication, Ps) to enter into S phase. Ps increases in proportion with ploidy and is modulated by nutrients. In fact, in bach cultures, the average cell size remains at low levels during growth on non-fermentable substrates and increases in a linear way with the specific growth rate only during growth on fermentable substrates.

Recent work from our laboratory allowed to identify Far1, a cyclin kinase dependent inhibitor, and Cln3, a G_1 phase cyclin, as the component of a nutritional modulated threshold controlling the entrance into S phase.

FAR1 overexpression increases cell size in a nutritionally modulated way, so cells growing in ethanol medium are larger than cells growing in glucose indicating that the function of this important cell cycle regulator is modulated by the nutritional status.

Accordingly, the major aims of this thesis can be described as follows:

- To describe the molecular mechanisms that induce an increase in cell size in *FAR1*-overexpressing cells (based on the transcriptomic analysis by our group) and notably to ask whether such an increase in cell size was accompanied by a coordinated increase in protein and RNA content.
- To determine whether (and possibly, to which extent) the regulatory function of glucose can be separated from its nutrient function in the coordination between cell growth and cell cycle. Accordingly, yeast strains in which glucose sensing is strongly reduced due to the absence of the major glucose sensing protein known until now, (*i.e.*, Gpr1, Snf3 and Rgt2) will be studied.

Results

COORDINATED INCREASE IN CELLULAR RNA AND PROTEIN CONTENT INDUCED BY OVEREXPRESSION OF Far1, A CYCLIN DEPENDENT KINASE INHIBITOR, INVOLVES LARGE TRANSCRIPTIONAL REPROGRAMMING AND REQUIRE THE Sfp1 PROTEIN

Besides its well established role in the response to pheromone, recent evidences suggest that Far1 may also regulate cell cycle progression in mitotic cells (Alberghina et al., 2004; Fu et al., 2003). In particular, it has been proposed that Far1, together with the G_1 cyclin Cln3, may be part of a nutritionally modulated cell sizer plus timer mechanism that controls the entry into S phase (Alberghina et al., 2004; Barberis et al., 2007; Di Talia et al., 2007). Each threshold consists of an activator and an associated inhibitor blocking its function. The first one involves the G_1 cyclin Cln3, the Cdk inhibitor (Cki) Far1 and the cyclin-dependent kinase Cdc28, whereas the second one comprises the S phase cyclin Clb5 (and Clb6), the Cki Sic1 and Cdc28 (Alberghina et al., 2009; Alberghina et al., 2004; Barberis et al., 2007).
Basically, a molecular "threshold" is given by the interplay between an "activator" and an inhibitor blocking its activity: when the number of molecules of the activator exceeds that of the inhibitor, the threshold is overcome. As previously describe, the first threshold regulating the G_1-S transition involves the G_1 cyclin Cln3, Far1 and the Cdc28, whereas the second one comprises the S phase cyclin Clb5 (and Clb6), Sic1 and Cdc28.
According to the model, the Cln3-Far1 threshold is set by the amount of Far1, which is mostly inherited by newborn cells at the end of the previous mitotic cycle and remains roughly constant during the G_1 phase.

Carbon source affects the expression level of the components of both thresholds: for instance, Cln3 and Far1 levels are higher in cells growing on glucose than on ethanol (Alberghina et al., 2004; Hall et al., 1998), whereas Sic1 content is higher in non-fermentable carbon sources (Rossi et al., 2005). The two thresholds cooperate to set the critical cell size according to the available carbon source: consistently with this notion, when both the thresholds are inactivated yeast cells loose the capacity to increase their size in presence of glucose (Alberghina et al., 2004).

Identification of the Far1 interaction network

As we reported above, Far1 overexpression affects cell size. This observation suggests that Far1 may interact, directly or indirectly, with proteins involved in processes leading to increase in cell mass and cell division.
We thus searched in databases for proteins interacting with Far1 either physically or genetically, indentifying a total of 99 proteins.

Of these proteins, 28 have a direct physical interaction with Far1 (figure 12 A, straight lines), mutations within the genes encoding 31 proteins interact genetically with mutations in the *FAR1* gene (figure 12 A, dotted lines) whereas the remaining 36 have been identified in 10 Far1-containing protein complexes. For the latter proteins, no Far1-connecting line is shown in figure 12 A since binary protein-protein interactions within the complex are unknown. The composition of the Far1-containing complexes is reported in figure 12 B.

These proteins are color-coded according to their biological function in figure 12. This figure shows that Far1 interacts either physically or genetically with a relevant number of proteins involved in RNA transcription, processing and transport, protein synthesis, folding, transport and degradation as well as in metabolism, consistently with the notion that Far1 may have unrecognized role in these processes.

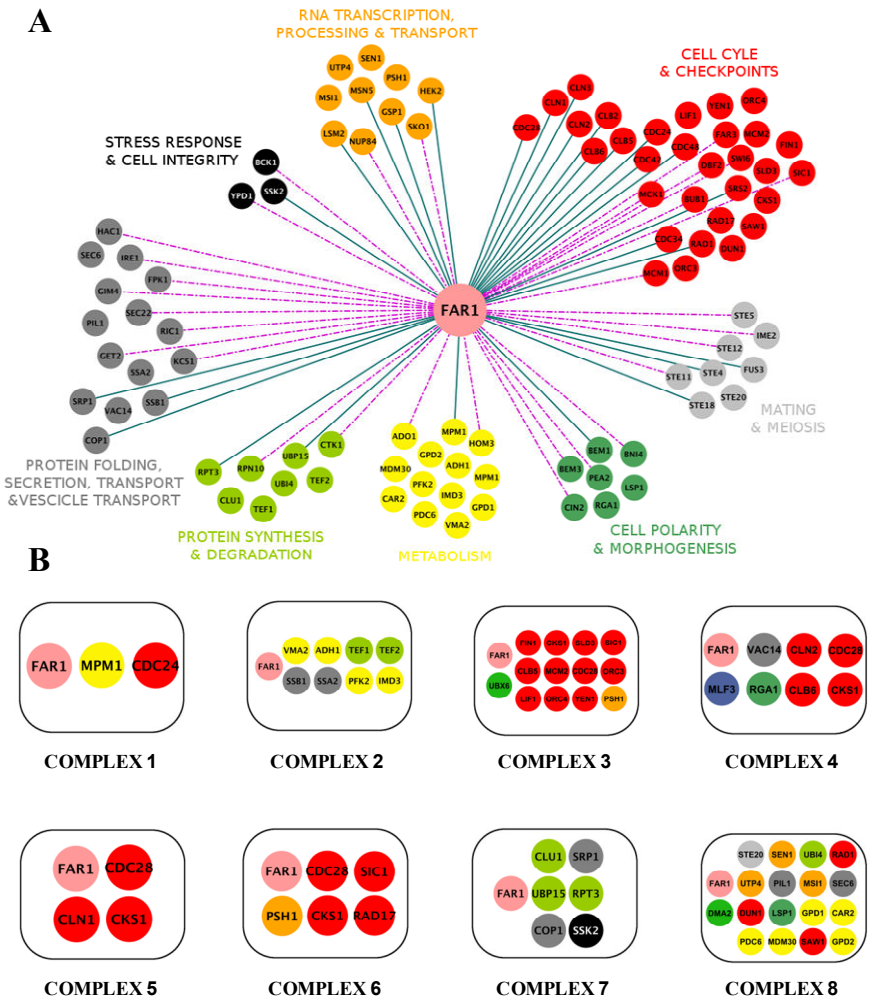

Figure 12. **The Far1 interaction network**.
A) Proteins interacting with Far1 by direct physical interaction (solid lines), genetic interactions (dotted lines) or that are present within Far1-containing complexes (no Far1-connecting lines) are shown. Nodes are color-coded according to function. Four proteins (MLF3, UBX6, DMA2 and YHR033W) are omitted since they are of unknown function or their functional group has no known direct interaction with FAR1.
B) Far1-containing protein complexes are depicted. Two further complexes have been found, but they are not represented in the picture since they are two subsets of the complexes **2** and **8** respectively. Complex **8** also contains the protein encoded by ORF YHR033W. It has been omitted since its function is unknown. Genetic and direct physical connections were obtained from the *Saccharomyces* Genome Database (http://www.yeastgenome.org/), complex composition from the Database of Interacting Proteins (http://dip.doe-mbi.ucla.edu/).

FAR1 overexpression coordinately upregulates RNA and protein content

Cells in exponential balanced growth spend a relevant fraction of their energy in RNA and protein synthesis. The interactome analysis reported above indicate that the large amount of proteins involved in protein synthesis, RNA trasnscription and processing and metabolism directly or indirectly interact with Far1.
Since we know that *FAR1* overexpression induces a nutritionally modulated increase in cell size, we asked whether such an increase in cell size was accompanied by a coordinated increase in protein and RNA content.

The effect of Far1 overexpression on average RNA and protein level (assayed by the orcinol and microbiuret methods, respectively) and on RNA and protein distribution (assayed by flow cytometric analysis of propidium iodide and fluorescein isothiocianate respectively) were assay on W303 cell grown in both ethanol- and glucose-supplemented media (Table I).
As reported (Alberghina et al., 2004) in ethanol-grown cells *FAR1* overexpression largely increases cell volume. Little, if any, effect in any of the above parameters can be observed in glucose-grown W303 cells.
Both chemical and flow cytometric assay indicate that protein and RNA increase coordinately, so that their ratio is not altered by the *FAR1* dosage, indicating that increased cells size results from a coupled increase in both RNA and protein syntheses. The rate of growth was unaffected in glucose and slightly reduce in ethanol, (where both unbudded and budded phase were affected to a similar degree).

Table I. Growth parameters of wild type strain (W303 background)

Carbon source	Strain	MDT (min)	T_B (min)	T_Σ (min)	V (fL)	P^a (ch #)	Ps^b (ch #)	$P_0{}^b$ (ch #)	R^a (ch #)	R/P	Protein[c] (pg/cell)	RNA[c] (pg/cell)	RNA/Protein
Ethanol	W303-1A [pCM189]	239 ± 7	137 ± 5	149 ± 4	38 ± 1	297 ± 13	269 ± 4	190 ± 6	233 ± 13	0.78 ± 0.04	3.27 ± 0.07	0.66 ± 0.06	0.20 ± 0.02
	W303-1A [pFAR1^{OE}]	332 ± 9	190 ± 9	197 ± 7	45 ± 1	435 ± 24 **	353 ± 4	326 ± 4	293 ± 3 **	0.67 ± 0.02	4.94 ± 0.13 **	0.94 ± 0.05 *	0.19 ± 0.01
Glucose	W303-1A [pCM189]	92 ± 2	71 ± 2	74 ± 1	53 ± 1	526 ± 8	448 ± 6	394 ± 7	508 ± 13	0.97 ± 0.02	5.48 ± 0.17	1.73 ± 0.02	0.32 ± 0.01
	W303-1A [pFAR1^{OE}]	98 ± 2	73 ± 3	76 ± 2	53± 1	542 ± 8	470 ± 9	419 ± 11	526 ± 7	0.97 ± 0.01	5.79 ± 0.08	1.79 ± 0.06	0.31 ± 0.01

MDT = mean doubling time; T_B = length of the budded phase; T_Σ = length of combined S+G2+M+G1* phases; P = average protein content of the whole cell population; P_0 = protein content of newborn cells; Ps = protein content at the onset of DNA synthesis; R = average protein content of the whole cell population.

All data are average ± s.e.m. from at least 3 independent experiments. The difference in values for P, R, protein and RNA obtained on mock-transformed and *FAR1*-overexpressing cells were tested for statistical significance using the Student's t test. *, 95% significant; **, 99% significant.

[a] Obtained by monoparametric FACS analysis of total protein (P) or RNA (R) content. Note that R and P values are on arbitrary scales (FACS channel number). Hence P/R and protein/RNA ratios cannot be compared one with the other.

[b] Obtained by biparametric (DNA *vs* protein*)* FACS analysis

[c] Obtained by chemical assay of total protein or RNA content using the microbiuret and orcinol methods, respectively.

FAR1 overexpression fails to up-regulate cellular RNA in the absence of Sfp1 protein but not of the Sch9 protein

To clarify the cellular processes leading to the largely increased cell size in ethanol-grown $FAR1^{OE}$, a genome-scale transcriptional analysis of isogenic wild type, *far1Δ* and $FAR1^{OE}$ strains has been performed in our laboratory on cells grown using either ethanol or glucose as a sole carbon source (Busti, Gotti et al., manuscript in preparation). This analysis indicate that Far1 overexpression originates large transcriptional remodeling that affects pathways involved in controlling cell growth, including sugar sensing (that is known to affect the cell growth rate; Youk and van Oudenaardenan; 2009), PKA and TOR pathways, that are the major pathways involved in controlling cell size and ribosome biogenesis.

Sfp1 and Sch9 are the major downstream targets of the TOR pathway affecting the coordination between cell growth and division (Jorgensen et al., 2004; Urban et al., 2007; Lempiainen and Shore, 2009). Accordingly, *sfp1Δ* and *sch9Δ* mutants are among the smallest "whi" mutants identified in a genome-wide screen for abnormally small or large mutants (Jorgensen et al., 2002). Thus, we tested whether the increase in cell size (RNA and protein) brought about by *FAR1* overexpression was mediated by Sfp1 and Sch9 by assaying the same parameters describe above for wild type in *sfp1Δ* [$FAR1^{OE}$] and *sch9Δ* [$FAR1^{OE}$] mutant cells.

Sfp1 is a split zinc-finger protein that emerged recently as a key transcriptional regulator of ribosome biogenesis and plays a [key role in nutritional and stress-dependent control of cell growth by affecting expression of both the RP and RiBi regulons (Jorgensen et al., 2002; Jorgensen et al., 2004; Lempiainen and Shore, 2009; Lempiainen et al., 2009) [and Sch9, a kinase sharing several properties with mammalian S6K1 kinase (Lempiainen and Shore, 2009; Urban et al., 2007).

The effect of *FAR1* overexpression on cell size parameters in the wild type BY4741 strain (isogenic to the *sch9Δ* and *sfp1Δ* mutants), grown in synthetic complete media supplemented with either ethanol or glucose as a carbon source, was similar to that reported in the W303 background (compare Table I and Table II). *sfp1Δ* and *sch9Δ* mutants were much smaller than wild type both in glucose, confirming previous data (Jorgensen et al., 2002; Jorgensen et al., 2004) and ethanol-supplemented media.

As observed in wild type cells, in both mutant strains *FAR1* overexpression had only minor effects on cell cycle and cell size related parameters on glucose-grown cells. *FAR1* overexpression did not affect duplication time in ethanol-grown *sch9Δ* cells, while *sfp1Δ* mutants overexpressing the *FAR1* gene product were quite unhealthy with a large increase in duplication time.
Overall increase in cell size was dramatic in ethanol-grown cells: however, while in wild type cells and *sch9Δ* mutants the increase in cell size derived from a balanced increase in RNA and protein content, in the *sfp1Δ* mutant the increase in protein content was not accompanied by an increase in RNA content, as shown by both FACS and chemical analysis (Table II and figure 13, note that FACS settings for *sch9Δ* and *sfp1Δ* mutants are different, *sfp1Δ* cells being actually smaller than *sch9Δ* cells), indicating that the Sfp1 is required to maintain proper coupling of RNA and protein syntheses when the Far1 protein is overexpressed in ethanol-grown-cells

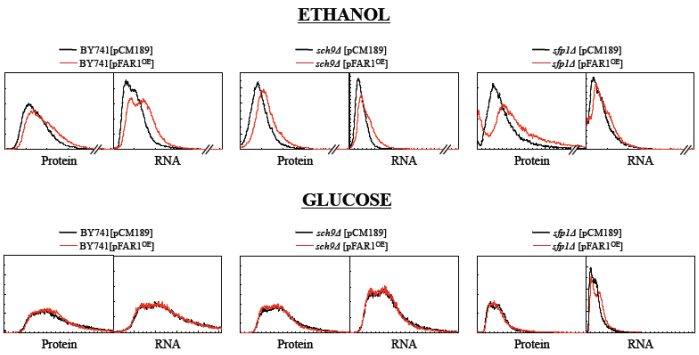

Figure 13. ***FAR1* overexpression fails to upregulate the cellular RNA content in the absence of Sfp1 but not of Sch9.**
Protein and RNA total contents (as determined by cytofluorimetric analysis) for wild type (left panel) *sch9Δ* (center panel) and *sfp1Δ* (right panel) strains cultivated in either ethanol (upper panels) or glucose (lower panels). Protein and RNA scale for the different strains are not directly comparable, since they have been chosen in order to allow differences between mock-transformed and Far1-oberexprrssing strains to be better appreciated

The observation that *FAR1* overexpression has different effects in *sfp1Δ* cells grown in ethanol and glucose media was not entirely unexpected.
First, in untransformed cells, the Far1 level of glucose-grown cells is larger than in ethanol-grown cells, while ectopically expressed Far1 accumulates to a similar level regardless of the carbon source: as a result, Far1 overexpression is more dramatic in ethanol-grown cells than in glucose-grown cells (Alberghina et al., 2004). Accordingly, the effect of Far1 overexpression on cell size are minor on cells grown in glucose-supplemented media and much more dramatic in ethanol-grown cells.

Table II. Growth parameters of wild type *sfp1Δ* and *sch9Δ* strains, (BY4741 background)

Carbon Source	Strain	MDT (min)	T_B (min)	T_Σ (min)	V (fL)	P[a] (ch#)	Ps[b] (ch#)	P_0[b] (ch#)	R[a] (ch#)	R/P	Protein[c] (pg/cell)	RNA[c] (pg/cell)	RNA/Protein
Ethanol	BY474 [pcM189]	264 ± 21	137 ± 2	142 ± 15	28 ± 1	199 ± 9	158 ± 9	113 ± 17	103 ± 16	0.52 ± 0.08	1.89 ± 0.13	0.36 ± 0.03	0.19 ± 0.02
	BY4741 [pFAR1^{OE}]	323 ± 7	153 ± 11	172 ± 10	33 ± 2	250 ± 16 *	208 ± 18	182 ± 19	130 ± 18 *	0.52 ± 0.08	2.65 ± 0.15 **	0.45 ± 0.07 *	0.17 ± 0.03
	sfp1Δ [pcM189]	385 ± 1	153 ± 11	181 ± 4	24 ± 2	104 ± 9	90 ± 9	73 ± 4	51± 11	0.49 ± 0.11	1.38 ± 0.07	0.25 ± 0.02	0.18 ± 0.02
	sfp1Δ [pFAR1^{OE}]	677 ± 16	176 ± 12	244 ± 30	31 ± 2	176 ± 9 **	169 ± 7	135 ± 20	72 ± 1	0.41 ± 0.02	1.78 ± 0.19 *	0.22 ± 0.01	0.12 ± 0.01
Ethanol + Glycerol	BY4741 [pcM189]	345 ± 18	153 ± 4	136 ± 12	30 ± 1	248 ± 5	211 ± 6	154 ± 8	154 ± 5	0.62 ± 0.02	1.91 ± 0.07	0.38 ± 0.01	0.20 ± 0.01
	BY4741 [pFAR1^{OE}]	352 ± 23	157 ± 5	139 ± 8	33 ± 2	298± 2 *	265 ± 11	203 ± 12	185 ± 5 **	0.62 ± 0.02	2.88 ± 0.10 *	0.53 ± 0.01 *	0.18 ± 0.01
	sch9Δ [pcM189]	603 ± 35	190 ± 9	258 ± 6	28 ± 1	185 ± 3	170 ± 7	134 ± 8	71 ± 4	0.38 ± 0.02	1.54 ± 0.11	0.25 ± 0.01	0.16 ± 0.01
	sch9Δ [pFAR1^{OE}]	597 ± 37	171 ± 12	244 ± 10	31 ± 1	210 ± 3 *	197 ± 10	166 ± 5	88 ± 1 **	0.42 ± 0.01	2.31 ± 0.10 *	0.33 ± 0.01 *	0.14 ± 0.01
Glucose	BY4741 [pcM189]	129 ± 2	77 ± 2	89 ± 1	44 ± 2	476 ± 16	430 ± 42	353 ± 39	512 ± 1	1.08 ± 0.04	4.38 ± 0.04	1.10 ± 0.01	0.25 ± 0.01
	BY4741 [pFAR1^{OE}]	120 ± 5	77 ± 3	84 ± 4	46 ± 1	487 ± 11	421 ± 15	356 ± 19	525 ± 1	1.08 ± 0.02	4.41 ± 0.01	1.05 ± 0.04	0.24 ± 0.01
	sfp1Δ [pcM189]	176 ± 2	67 ± 1	86 ± 4	32 ± 1	155 ± 5	141 ± 5	101 ± 1	123 ± 1	0.79 ± 0.03	1.42 ± 0.03	0.25 ± 0.02	0.18 ±0.01
	sfp1Δ [pFAR1^{OE}]	205 ± 12	110 ± 1	103 ± 4	36 ± 1	168 ± 1	154 ± 10	126 ± 15	153 ± 10	0.91 ± 0.03	1.71 ± 0.10	0.32 ± 0.01	0.19 ± 0.01
	sch9Δ [pcM189]	176 ± 4	118 ± 7	117 ± 9	38 ± 1	358 ± 4	330 ± 4	254 ± 7	373 ± 13	1.04 ± 0.04	3.03 ± 0.03	0.69 ± 0.03	0.23 ± 0.01
	sch9Δ [pFAR1^{OE}]	180 ± 7	112 ± 8	118 ± 6	36 ± 1	362 ± 6	326 ± 9	264 ± 8	354 ± 15	0.98 ± 0.04	2.88 ± 0.12	0.63 ± 0.02	0.22 ± 0.01

MDT = mean doubling time; T_B = length of the budded phase; T_Σ = length of combined S+G2+M+G1* phases; P = average protein content of the whole cell population; P_0 = protein content of newborn cells; Ps = protein content at the onset of DNA synthesis; R = average protein content of the whole cell population.

All data are average ± s.e.m. from at least 3 independent experiments. The difference in values for P, R, protein and RNA obtained on mock-transformed and *FAR1*-overexpressing cells were tested for statistical significance using the Student's t test. *, 95% significant; **, 99% significant.

[a] Obtained by monoparametric FACS analysis of total protein (P) or RNA (R) content. Note that R and P values are on arbitrary scales (FACS channel number). Hence P/R and protein/RNA ratios cannot be compared one with the other.

[b] Obtained by biparametric (DNA *vs* protein*)* FACS analysis

[c] Obtained by chemical assay of total protein or RNA content using the microbiuret and orcinol methods, respectively.

We demonstrate that the coordination between RNA and protein syntheses brought about by Far1 overexpression is conserved in the *sch9Δ* mutant, but is relaxed in cells lacking the *SFP1* gene. This is in keeping with the recent proposal that Sch9 is involved in optimal regulation of ribosome biogenesis by the TORC1 complex, but is dispensable for the essential aspects of ribosome biogenesis and cell growth (Wei and Zheng, 2009). Since in ethanol-grown *sfp1Δ* [pFAR1^{OE}] cells an increase in protein, but not RNA, level is observed, the increased protein level is likely due to improved usage of existing ribosomes, that are known to be in excess in ethanol-growing yeast (Waldron et al., 1977), without extensive *de novo* synthesis of ribosomes.

EFFECTS OF GLUCOSE SENSING ON COORDINATION BETWEEN CELL GROWTH AND CELL DIVISION

Glucose dependent modulation of cell size in wild type strain

Glucose is the principal carbon and energy source for most cells, and many organisms have evolved sophisticated means for sensing glucose and utilizing it efficiently. Learning how cells sense and respond to glucose is thus of great interest and major significance.
Glucose is particularly important to the yeast *Saccharomyces cerevisiae*. It is by far the preferred carbon source of this yeast. Yeast cells can sense glucose and utilize it efficiently over a broad range of concentrations.

An essential requisite for the survival of the budding yeast *Saccharomyces cerevisiae* is the capacity to regulate growth and cell cycle progression according to the frequent changes in the nutrient status, so that proliferation is rapid when large supplies of nutrients are available and ceases when these becomes exhausted. Nutrients like glucose must therefore generate signals that are somehow received and elaborated by the complex machinery governing growth and cell cycle progression.
Besides being the favorite carbon and energy source for *S. cerevisia*e, glucose can act as a signaling molecule to regulate multiple aspects of yeast physiology: addition of glucose to quiescent or ethanol growing cells triggers a fast and massive reconfiguration of the transcriptional program, which enables the switch to fermentative metabolism and promotes an outstanding increase of the cell biosynthetic capacity.

Therefore, a central issue in this part of this thesis was to determine whether (and possibly, to which extent) the regulatory function of glucose can be separated from its nutrient function in the coordination between cell growth and cellular division. To this aim, we characterized yeast strains in which glucose sensing is strongly reduced due to a deletion of gene that code for a glucose sensor proteins.

In the first instance, wild type reference CEN.PK strain (that proved to be the best background for chemostat analysis and for studies on glucose transport mutants that complement the results presented in this thesis (Busti PhD thesis)), was employed in our study (Table III) in order to evaluate the effect of carbon source, in particular glucose, on cell size of the budding yeast. In a first set of experiments, several common growth parameters (including doubling time, budding index, length of the budded phase, mean cell volume and average protein content) were evaluated during balanced growth in synthetic complete medium supplemented with either 2% ethanol (SCE) or different glucose concentration as carbon sources.

In the presence of glucose, the wild type strain exhibited the typical distinctive features associated with a fermentative metabolism: the growth rate and the budding index were remarkably high and cells were large.

Table III below summarizes the growth parameters for wild type strain grown at different glucose concentration and in 2% ethanol kept as a reference condition.

Table III. Growth parameters of wild type strain (CEN.PK background)

Carbon source	***Growth parameters of wild type strain***			
	MDT (min)	F_b (%)	T_b (min)	T_Σ
5% glucose	106 ± 4	74.2 ± 0.1	78 ± 3	70 ± 2
2% glucose	97 ± 2	78.7 ± 0.2	78 ± 1	74 ± 3
0.5% glucose	104 ± 5	77.1 ± 0.7	92 ± 3	82 ± 4
0.2% glucose	105 ± 5	76.0 ± 0.1	85 ± 4	77 ± 2
0.1% glucose	107 ± 4	74.8 ± 1.1	92 ± 1	81 ± 3
0.05% glucose	(**) 122 ± 4	74.2 ± 0.4	(*) 97 ± 5	88 ± 5
2% ethanol	(**) 240 ± 2	(**) 60 ± 0.5	(**) 158 ± 3	(**)170 ± 1

MDT = mean doubling time; **Fb** = budding index (%); $\mathbf{T_b}$ = length of the budded phase; $\mathbf{T_\Sigma}$ = length of combined $S+G_2+M+G_1$* phases. Growth parameters were monitored during growth at 30°C in SC/YNB medium supplemented with either 2% ethanol or different glucose concentration. All data are average ± standard error of the mean (SEM) from at least 3 independent experiments. The Student's t test was used to evaluate statistical significant of each parameter, using value of cells grown in 2% glucose as a reference.

In the presence of glucose concentrations from 5% to 0.1%, the doubling times (MDT) and budding index are similar, whereas at the lower glucose concentration tested (0.05%) the duplication time significantly increases (about 20%) compared to the previous conditions, suggesting that only this is a limiting condition for the growth of the yeast cells. This MDT value is however significantly smaller than the value observed in 2% ethanol that only supports a much slower growth.

The average protein content (P) derived from analysis of protein distribution obtained by flow cytometry, was strongly modulated by the carbon source. Figure 14 A reports protein distributions from a typical experiment, while figure 14 B reports average protein contents ± SEM derived from at least three independent experiments. For example the average protein content moves from a value of 503 ± 13 (channel number) in cells grown in synthetic complete (SC) medium supplemented with 5% glucose as sole carbon source to value of 330 ± 9 when we added 0.05% of glucose (ratio of $P_{5\%}$ glucose/ $P_{0.05\%}$ glucose is equal to 1.52). However, in the presence of 2% ethanol the average protein content undergoes a further decrease compared to cells grown in medium with the lowest concentration of glucose tested, ratio of $P_{5\%}$ glucose/ $P_{2\%}$ ethanol being equal to 1.70.

As expected under a condition of balanced exponential growth, the increase in cellular volume (assayed by coulter analysis) parallels the increase observed in average protein content (data not show). In other words, when in the medium there is a high concentration of fermentable carbon source such as 5% glucose, yeast cells accumulate a higher amount of protein content and are also larger compared with cells grown in 2% ethanol.

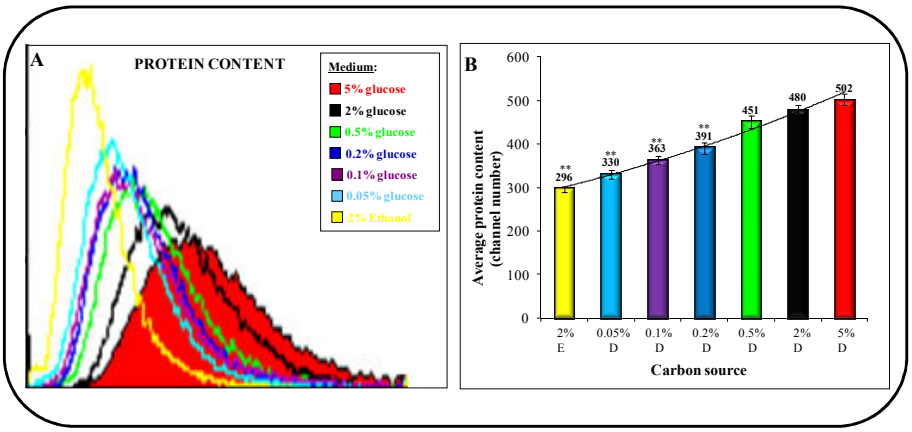

Figure 14. **Different glucose concentrations in the medium culture cause different total protein contents in wild type cells.**
A) Size of wild type cells at different glucose concentration [red=5% glucose, black= 2% glucose, green=0.5% glucose, blue=0.2% glucose, violet=0.1% glucose, sky-blue=0.05% glucose and yellow= 2% EtOH].
B) The value of average of protein content, determined by cytofluorimetric analysis (see materials and methods for details) were determined for wild type at different glucose concentration and 2% ethanol. All data are average ± standard error of the mean (SEM) from at least 3 independent experiments. The Student's t test was used to evaluate statistical significant of P parameter, using value of cells grown in 2% glucose as a reference

Only a 15% increase in MDT was observed when glucose concentration was decreased from 5% to 0.05%. The major increase in MDT was observed when cells were grown in ethanol-containing media (100% increase in MDT from 0.05% glucose to ethanol). Nevertheless, the increase in cell mass that accompanies such a large increase in MDT, although statistically significant, is quite small.

This suggest that setting of cell size is a complex function not only of growth rate and sugar metabolism, but possibly of sugar sensing as well. In fact if no glucose sensing was implied, we would expect that the largest increase in cell size should be observed in parallel with the largest increase in MDT.

Modulation of protein content as a function of glucose concentration: wild type strain versus strains impaired in sugar sensing

As reported above in the wild type cells, the average protein content (P), was strongly modulated by the glucose concentration. In order to investigate whether (and possibly, to which extent) the regulatory function of glucose can be separated from its nutrient function, in the first instance, we characterized yeast strains impaired in glucose uptake (Busti, Gotti et al., manuscript in preparation).
The aim of this thesis was to characterize yeast strains in which glucose sensing is strongly reduced due to deletion of glucose receptors (*GPR1*, *SNF3, RGT2*).

Yeast cells have evolved different mechanism to monitor the levels of extracellular glucose: the cAMP-PKA pathway (involving the Ras protein and Gpa2-Gpr1branches), the Snf3-Rgt2 pathway and the "main repressor pathway" involving the Snf1 kinase (reviewed in Busti et al., 2010). In detail:

1. Snf3 receptor (Sucrose non-fermenting) sensor monitors the presence of low glucose concentrations, and stimulates the expression of high affinity glucose transporters.
2. Rgt2 receptor monitors the presence of high glucose concentration, and therefore leads to expression of low affinity glucose transporters.
3. Gpr1-Gpa2 system: it is a protein complex, in which *GPR1* encodes a sensor for high glucose, whereas *GPA2* encodes its cognate, a G protein. The complex is involved in modulating the levels of cAMP stimulated by the presence of glucose.

We constructed a series of yeast strains in which one or more pathways of glucose sensing are altered as listed below:

1. the *snf3Δ rgt2Δ* strain, which exhibits a moderately reduced glucose uptake capacity as a consequence of the inactivation of the Rgt2-Snf3 pathway required to induce the expression of the *HXT* transporters in the presence of the sugar (Ozcan et al., 1998);
2. inactivation of the Gpr1-Gpa2 branch of the cAMP-PKA glucose sensing system in the wild type strain reduces the average cell size without affecting the cell cycle parameters (doubling time, length of the budded phase (Alberghina et al., 2004; Tamaki et al., 2005);
3. the *snf3Δ rgt2Δ gpa2Δ gpr1Δ* strain in which the inactivation of the Gpr1-Gpa2 branch is in conjunction with Snf3-Rgt2 pathway deletion.

Deletion of components of the Gpr1-Gpa2 pathway results in down-regulation of average protein content in both high and low glucose concentration

Previous data from our laboratory (Albergina et al., 2004) prove that mutants carrying a deletion in either the Gpr1 receptor or the cognate Gpa2, showed significantly altered protein distribution, resulting in a reduction of P.
The first set of experiments planned, was designed to identify whether and which deletion of glucose sensors, induce an alteration in cell size. In that regard, we initially worked in high glucose concentration (precisely 2%) and low glucose (0.05%), chosen based on reported affinity for glucose of the different sensors. Literature data show the importance of *GPA2* for growth in high glucose concentration, while Snf3 is necessary for growth in low glucose concentration.

The following mutant strains were used: *rgt2Δ*, *snf3Δ*, *snf3Δ rgt2Δ, gpr1Δ gpa2Δ*, *gpa2Δ gpr1Δ* and *snf3Δ rgt2Δ gpa2Δ gpr1Δ*

As reported in figure 15, *rgt2Δ, snf3Δ* and *rgt2Δ snf3Δ* mutant strains are indistinguishable from wild type cells in term of average protein content (P), while *gpa2Δ*, *gpa2Δ gpr1Δ* and *snf3Δ rgt2Δ gpa2Δ gpr1Δ* strains showed significantly altered protein distribution, either when grown in media supplemented with high (panel A) or low (panel B) glucose concentration resulting in a reduction of P.
The latter four strains have in common the deletion of at least one gene encoding a component of the Gpa2-Gpr1 pathway indicating that the main contribution in setting the protein accumulations is given by Gpa2-Gpr1 branch of the cAMP-PKA pathway as show by previous data from our laboratory (Alberghina et al., 2004).
Results obtained in low glucose media are of particular interest, supporting the notion that signaling through the Gpr1-Gpa2 pathway specifically modulates P setting not only in 2% glucose, but in low glucose as well whereas the Snf3-Rgt2 pathway seems to have only marginal effects on cell size modulation.
These results represent the first evidence for a phenotypic effect of the Gpa2-Gpr1 pathway in sensing low glucose concentration.

In contrast with other genetic backgrounds, where the inactivation of the Snf3-Rgt2 pathway produces a dramatic growth defect on low glucose concentration (Ozcan et al., 1998), the loss of the two sensors encoded by *SNF3* and *RGT2* in the CEN.PK strain had only marginal effects on growth on low glucose media, as already described (Ramakrishnan et al., 2007).

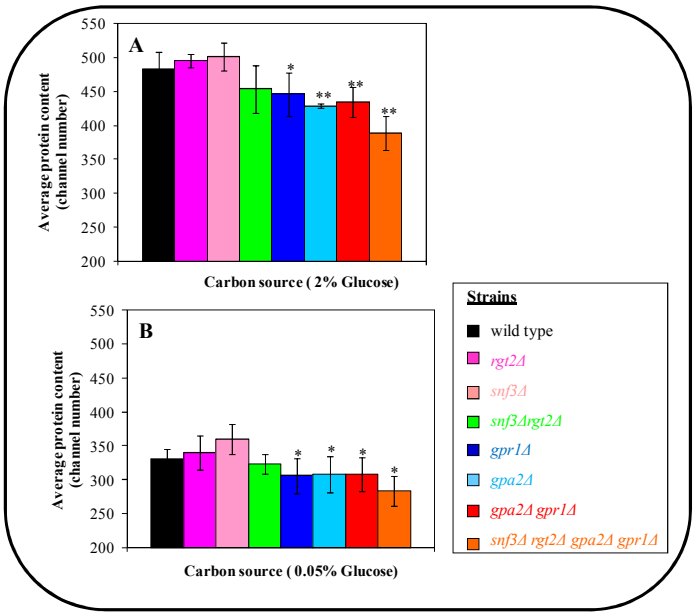

Figure 15. **A functional extracellular glucose sensing system is require to properly set cell size (P) for cells growing in both high (A) and low (B) glucose concentrations.** The value of average of protein content, determined by cytofluorimetric analysis (see materials and methods for details) were determined for wild type cells (black), *rgt2Δ* cells (pink), *snf3Δ* cells (light pink), *snf3Δ rgt2Δ* cells (green), *gpr1Δ* cells (blue), *gpa2Δ* cells (azure), *gpr1Δ gpa2Δ* cells (red) and *snf3Δ rgt2Δ gpa2Δ gpr1Δ* cells (orange). Value reported are mean ± standard error of the mean (SEM), of at least three independent experiments.
The Student's t test was used to evaluate statistical significant of P amount, using value of cells grown in 2% glucose as a reference

Modulation of protein content dependent of glucose concentration in strains impaired for sugar sensing

Concurrent deletion of all three glucose sensors for extracellular glucose only partially abolishes glucose dependent modulation of cell size

Since we have observed that there is a strong decrease in average protein content in the *snf3Δ rgt2Δ gpa2Δ gpr1Δ* strain in both high and low growth glucose conditions (2% and 0.05% glucose), we extended the analysis made in wild type strain (table III and figure 14) to this mutant in which all the glucose sensors known until now were deleted with the aim to investigate whether glucose dependent size modulation was retained in this strains.
As reported for wild type strain (compare table III and IV) in the presence of glucose, this strain exhibited the typical distinctive features associated with a fermentative metabolism: the growth rate and the budding index were remarkably high and cells were large.

Table IV below summarizes the growth parameters for *snf3Δ rgt2Δ gpa2Δ gpr1Δ* strain grown at different glucose concentration and in 2% ethanol kept as a reference condition.

Table IV. Growth parameters of *snf3Δ rgt2Δ gpa2Δ gpr1Δ* strain (CEN.PK background)

Carbon source	***Growth parameters of snf3Δ rgt2Δ gpa2Δ gpr1Δ strain***			
	MDT (min)	F_b (%)	T_b (min)	T_Σ
5% glucose	111 ± 5	68.5 ± 0.7	82 ± 3	77 ± 5
2% glucose	115 ± 2	67.2 ± 0.5	86 ± 1	85 ± 1
0.5% glucose	121 ± 1	67.2 ± 1.0	98 ± 8	87 ± 4
0.2% glucose	(*) 124 ± 3	67.1 ± 2.2	99 ± 7	(*) 87 ± 1
0.1% glucose	(**) 137 ± 2	65.5 ± 1.4	(**) 100 ± 1	(**) 98 ± 4
0.05% glucose	(*) 137 ± 7	64.6 ± 0.8	(*) 107 ± 6	(*) 101 ± 7
2% ethanol	(**) 224 ± 4	(**) 59.4 ± 1.0	(**) 150 ± 1	(**) 154 ± 3

MDT = mean doubling time; **Fb** = budding index (%); $\mathbf{T_b}$ = length of the budded phase; $\mathbf{T_\Sigma}$ = length of combined $S+G_2+M+G_1$* phases. Growth parameters were monitored during growth at 30°C in SC/YNB medium supplemented with either 2% ethanol or different glucose concentration. All data are average ± standard error of the mean (SEM) from at least 3 independent experiments. The Student's t test was used to evaluate statistical significant of each parameter, using value of cells grown in 2% glucose as a reference

As reported for wild type strains in the presence of glucose concentrations from 5% to 0.1%, the doubling times (MDT) and budding index are similar, whereas at the lower glucose concentration tested (0.05%) the duplication time significantly increases (about 20%) compared to the previous conditions, suggesting that only this is a limiting condition for the growth of the yeast cells. This MDT value is however significantly smaller than the value observed in 2% ethanol that only supports a much slower growth.

Flow cytometric analysi by FACS for determination of average protein content using cells grow in medium containing either glucose concentration from 5% to 0.05% or 2% ethanol indicate that average protein content (P) was strongly modulated by the carbon source.
Figure 15 A reports protein distributions from a typical experiment, while figure 14 B reports average protein contents ± SEM derived from at least three independent experiments. For example the average protein content moves from a value of 418 ± 11 (channel number) in cells grown in synthetic complete (SC) medium supplemented with 5% glucose as sole carbon source to value of 284 ± 11 when we added 0.05% of glucose (ratio of $P_{5\%}$ glucose/ $P_{0.05\%}$ glucose is equal to 1.47). However, in the presence of 2% ethanol the average protein content undergoes a further decrease compared to cells grown in medium with the lowest concentration of glucose tested, ratio of $P_{5\%}$ glucose/ $P_{2\%}$ ethanol being equal to 1.68.

As expected under a condition of balanced exponential growth, the increase in cellular volume (assayed by coulter analysis) parallels the increase observed in average protein content (data not show). In other words, when in the medium there is a high concentration of fermentable carbon source such as 5% glucose, yeast cells accumulate a higher amount of protein content and are also larger compared with cells grown in 2% ethanol.

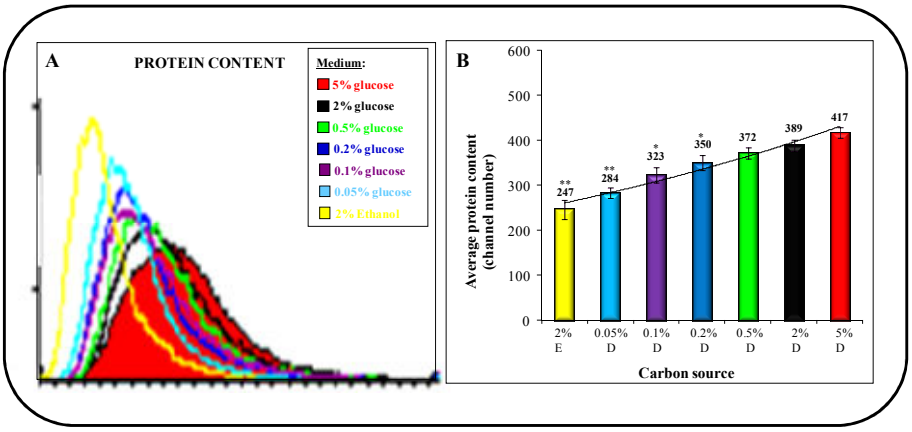

Figure 16. **Different glucose concentrations in the medium culture cause different total proteins content in *snf3Δ rgt2Δ gpa2Δ gpr1Δ* cells.**
A) Size of *snf3Δ rgt2Δ gpa2Δ gpr1Δ* cells at different glucose concentration [red=5% glucose, black= 2% glucose, green=0.5% glucose, blue=0.2% glucose, violet=0.1% glucose, sky-blue=0.05% glucose and yellow= 2% EtOH].
B) The value of average of protein content, determined by cytofluorimetric analysis (see materials and methods for details) were determined for *snf3Δ rgt2Δ gpa2Δ gpr1Δ* cells at different glucose concentration. All data are average ± ± standard error of the mean (SEM) from at least 3 independent experiments. The Student's t test was used to evaluate statistical significant of P amount, using value of cells grown in 2% glucose as a reference

As reported for wild type cells also in the *snf3Δ rgt2Δ gpa2Δ gpr1Δ* strain there was only a 15% increase in MDT observable when glucose concentration was decreased from 5% to 0.05%. The major increase in MDT was observed when cells were grown in ethanol-containing media (100% increase in MDT from 0.05% glucose to effect). Nevertheless the increase in cell mass, that accompanies the large increase in MDT, although statistically significant, is quite small.
Results obtained above show that strain null in glucose receptor maintained, at least a partial ability to modulate cell size.

Contribution of individual receptors to glucose-dependent size modulation: the different role of the Snf3-Rgt2 and the Gpa2-Gpr1 pathways

As we showed above, the *snf3Δ rgt2Δ gpa2Δ gpr1Δ* strain have a longer MDT than wild type cells (compare table III and table IV) in all the glucose concentration tested and display lower level of average protein content than the isogenic strain kept as a reference strain (figures 15 and 16, table III).
The strains null in glucose receptor maintained, at least a partial ability to modulate cell size

To dissected the contribution of each glucose sensing pathway to the setting of size, we analysed *snf3Δ rgt2Δ* and *gpa2Δ gpr1Δ* mutants that are the two pathways involved in glucose sensing.
As before described for wild type and the *snf3Δ rgt2Δ gpa2Δ gpr1Δ* cells, several common growth parameters (including doubling time, budding index, length of the budded phase, mean cell volume and average protein content) were evaluated both in *snf3Δ rgt2Δ* and *gpa2Δ gpr1Δ* strains.

Tables V and VI below summarize the growth parameters relative to *snf3Δ rgt2Δ* and *gpa2Δ gpr1Δ* strains respectively grown at different glucose concentration and in 2% ethanol kept as a reference condition.

Table V. Growth parameters of *snf3Δ rgt2Δ* strain (CEN.PK background)

Carbon source	***Growth parameters of snf3Δ rgt2Δ strain***			
	MDT (min)	F_b (%)	T_b (min)	T_Σ
5% glucose	119 ± 2	69.7 ± 1.1	91 ± 1	86 ± 1
2% glucose	125 ± 4	69.8 ± 0.8	93 ± 4	88 ± 5
0.5% glucose	131 ± 13	69.9 ± 0.5	99 ± 10	95 ± 9
0.2% glucose	133 ± 0	68.7± 0.2	101 ± 0	97 ± 0
0.1% glucose	127 ± 1	68.8 ± 0.9	97 ± 5	92 ± 1
0.05% glucose	(**) 148 ± 2	66.1 ± 1.0	(**) 110 ± 1	(**) 124 ± 2
2% ethanol	(**) 235 ± 4	(**) 61.7 ± 0.3	(**) 162 ± 4	(**) 170 ± 3

Table VI. Growth parameters of *gpa2Δ gpr1Δ* strain (CEN.PK background)

Carbon source	***Growth parameters of gpa2Δ gpr1Δ strain***			
	MDT (min)	F_b (%)	T_b (min)	T_Σ
5% glucose	94 ± 4	72.8 ± 0.9	70 ± 1	66 ± 1
2% glucose	91 ± 1	74.0 ± 0.8	71 ± 1	65 ± 1
0.5% glucose	95 ± 1	73.7 ± 0.2	69 ± 4	67 ± 2
0.2% glucose	99 ± 4	73.7 ± 1.2	80 ± 9	72 ± 6
0.1% glucose	94 ± 4	74.2 ± 1.7	72 ± 1	64 ± 1
0.05% glucose	(*) 111 ± 6	72.0 ± 0.9	(**) 83 ± 1	(**) 76 ± 2
2% ethanol	(**) 217 ± 1	(**) 59.0 ± 1	(**) 144 ± 3	(**) 156 ± 3

MDT = mean doubling time; **Fb** = budding index (%); **T_b** = length of the budded phase; **T_Σ** = length of combined S+G_2+M+G_1* phases. Growth parameters were monitored during growth at 30°C in SC/YNB medium supplemented with either 2% ethanol or different glucose concentration. All data are average ± standard error of the mean (SEM) from at least

The *snf3Δ rgt2Δ* displayed longer MDT than wild type in all tested glucose concentrations possibly to an even greater extent than the *snf3Δ rgt2Δ gpa2Δ gpr1Δ* mutant. On the contrary the *gpa2Δ gpr1Δ* strain grew possibly a bit faster than wild type.
In detail, in the presence of glucose concentrations from 5% to 0.1%, the doubling times (MDT) and budding index are similar, whereas at the lower glucose concentration tested (0.05%) the duplication time significantly increases (about 20%) compared to the previous conditions. This MDT value is however significantly higher than the value observed in 2% ethanol that only supports a much slower growth.

The average protein content (P) derived from analysis of protein distribution obtained by flow cytometry, was strongly modulated by the carbon source. Figure 17 A reports protein distributions from a typical experiment, while figure 17 B reports average protein contents ± SEM derived from at least three independent experiments.

For example in the case of *snf3Δ rgt2Δ* cells, the average protein content moves from a value of 486 ±5 (channel number) in cells grown in synthetic complete (SC) medium supplemented with 5% glucose as sole carbon source to value of 323 ± 5 when we added 0.05% of glucose (ratio of $P_{5\%}$ glucose/ $P_{0.05\%}$ glucose is equal to 1.5).
However, in the presence of 2% ethanol the average protein content undergoes a further decrease compared to cells grown in medium with the lowest concentration of glucose tested, ratio of $P_{5\%}$ glucose/ $P_{2\%}$ ethanol being equal to 1.68

For the *gpa2Δ gpr1Δ* cells however, the average protein content moved from a value of 446 ± 5 (channel number) in cells grown in complete medium supplemented with 5% of glucose to the value of 308 ± 10 in the presence of 0.05% glucose in the growth medium glucose (ratio of $P_{5\%}$ glucose/ $P_{0.05\%}$ glucose is equal to 1.44).
However, in the presence of 2% ethanol the average protein content undergoes a further decrease compared to cells grown in medium with the lowest concentration of glucose tested, ratio of $P_{5\%}$ glucose/ $P_{2\%}$ ethanol being equal to 1.62

For both strains, as expected under a condition of balanced exponential growth, the increase in cellular volume (assayed by coulter analysis) parallels the increase observed in average protein content (data not show). In other words, when in the medium there is a high concentration of fermentable carbon source such as 5% glucose, yeast cells accumulate a higher amount of protein content and are also larger compared with cells grown in 2% ethanol.

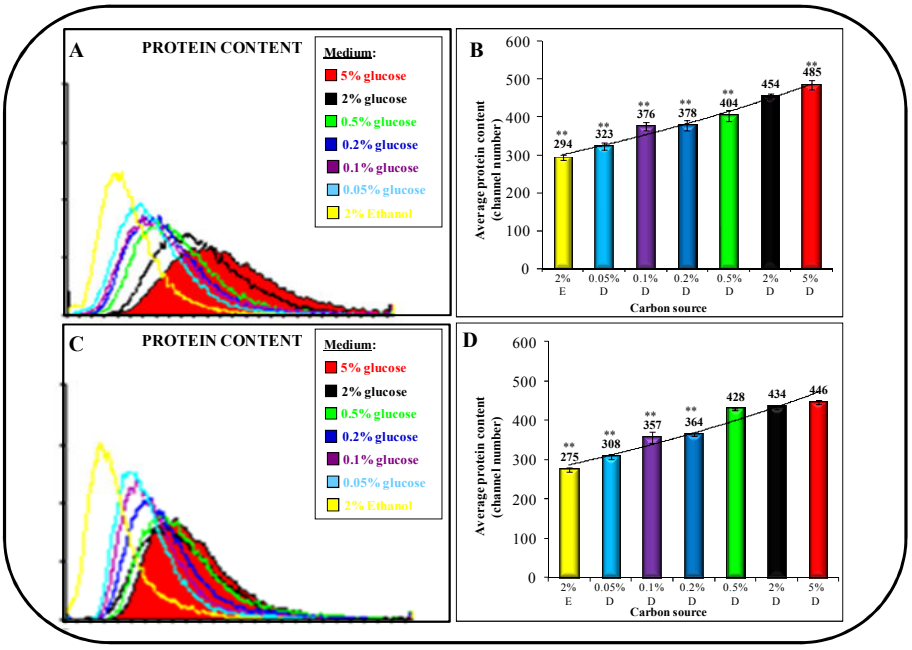

Figure 17. **Different glucose concentration in the medium culture cause different total proteins content both in *snf3Δ rgt2Δ* and *gpa2Δ gpr1Δ* cells.**
A) Size of *snf3Δ rgt2Δ* cells at different glucose concentration [red=5% glucose, black= 2% glucose, green=0.5% glucose, blue=0.2% glucose, violet=0.1% glucose, sky-blue=0.05% glucose and yellow= 2% EtOH].
B) The value of average of protein content, determined by cytofluorimetric analysis (see materials and methods for details) were determined for *snf3Δ rgt2Δ* cells at different glucose concentration. The Student's t test was used to evaluate statistical significant of P amount, using value of cells grown in 2% glucose as a reference
C) Size of *gpa2Δ gpr1Δ* cells at different glucose concentration [red=5% glucose, black= 2% glucose, green=0.5% glucose, blue=0.2% glucose, violet=0.1% glucose, sky-blue=0.05% glucose and yellow= 2% EtOH
D) The value of average of protein content, determined by cytofluorimetric analysis were determined for *gpa2Δ gpr1Δ* cells at different glucose concentration. The Student's t test was used to evaluate statistical significant of P amount, using value of cells grown in 2% glucose as a reference.

Data present here showed that both strains maintained the ability to modulate cell size as a function of glucose concentration.
Since the presence of *snf3Δ rgt2Δ* deletions affect not only cell size, but the MDT as well (figure 5 and table V) possibly because reduction in *HXT* expression, data on strains carrying these deletions do not allow to draw unambiguous results on the role played by Snf3 and Rgt2 protein in the setting of cell size.

Expression levels of cell cycle regulators in strains impaired for glucose sensing: a preliminary analysis

Results presented in the above paragraphs indicate that glucose sensing plays a role in setting the coordination between cell growth and division. Since such coordination takes place mostly at G_1-S transition, we sought to investigate if altered levels of some of the major players of the G_1-S transition namely Far1, Sic1 (cyclin kinase dependent inhibitor), Cln3, a G_1 phase cyclin, Clb5, and Cln2 may be observed in strains devoid of glucose receptors. Obtainment of "tagged" strains suitable for protein quantification proved to be more difficult than expected, possibly because of low expression level of cell cycle proteins. Strains harbouring concurrently both Cln3 and Far1 fusions with a detectable tag were difficult to obtain and will not be examined.
The amounts of the various cell cycle regulators (quantified by Western blot analysis) were monitored during balanced growth in synthetic complete media supplemented with either 2% glucose or 2% ethanol.
A preliminary analysis of strains is presented below.

Clb5 and Sic1 proteins

Deletion of *SIC1* gene affects the coordination between cell growth and cell cycle thereby hampering the yeast's ability to modulate cell size and the size required to enter S-phase as a function of the carbon source (Alberghina et al., 2004). It has been show in our laboratory that the carbon source affects the expression of Sic1 (Rossi et al., 2005) in fact we show that Sic1 level was higher in ethanol-growing cells.
Cells expressing HA C-terminal tagged version of Sic1 and Clb5 proteins were grown in complete synthetic mixture media (SC) containing either 2% glucose (SCD) or 2% ethanol (SCE) as a carbon source.
Cells were collected in mid exponential phase, total protein extracted and Sic1 and Clb5 detected by Western blot analysis, the internal loading control has been made by checking the level of Cdc34 protein.

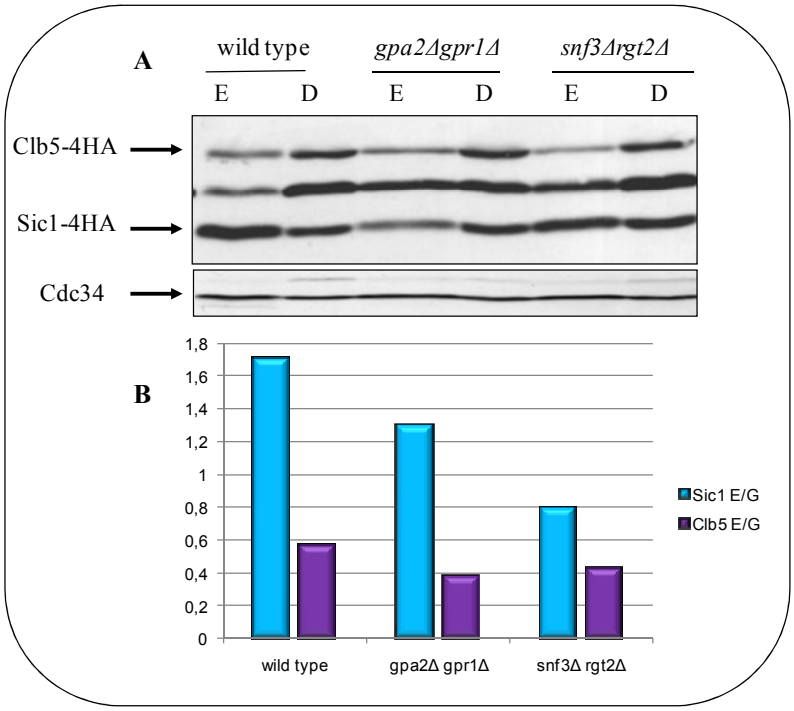

Figure 18. **Expression levels of Sic1 and Clb5 in wild type and mutants impaired for glucose sensing during growth either in ethanol or glucose medium.**
A) Wild type and the mutant strains cells were grown either in ethanol (SCE) or glucose (SCD) medium. 50µg µg of total extract were used for Western blot analysis. As a loading control, blotted membranes were stained with Cdc34 antibodies. Blot shown is representative of experiments repeated twice with similar results.
B)Ethanol/Glucose ratio of Sic1 (blue) and Clb5 (violet) content quantified by densitometric analysis in cells during growth on ethanol and glucose medium.

Consistent with previous findings, the Sic1 content in wild type cells cultivated in glucose containing medium was about 1.5/2-fold lower than the one of ethanol growing cells (Rossi et al., 2005). No difference were observed in the Clb5 level.
Deletion of glucose receptors appears to modulate the ratio between the two proteins that may crucial for proper timing of s phase initiation. Because of intrinsic noise of the methods more experiment are needed to derive unambiguous conclusions.

Cln2 protein

As expected from previous studies, the expression levels of the Cln2 cyclins in the wild type strain were significantly higher when cells were grown in presence of glucose than in medium containing ethanol as sole carbon source. The same results were obtained in the case of *gpa2Δ gpr1Δ* mutants cells. (figure 19; Hall et al., 1998; Schneider et al., 2004; Alberghina et al., 2004).

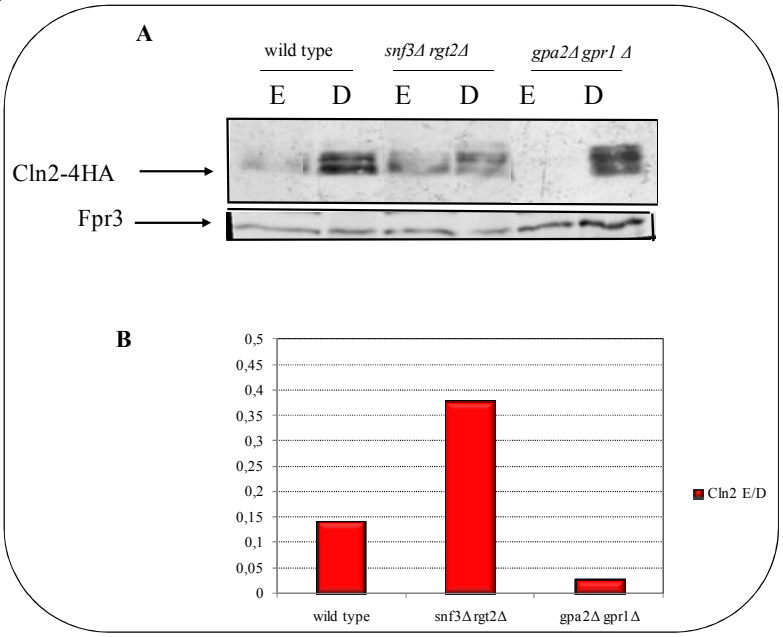

Figure 19. **Expression levels of Cln2 in the wild type *snf3Δ rgt2Δ*, *gpa2Δ* and *gpr1Δ* strains during growth in ethanol or glucose media.**
A) Wild type and the mutant cells were grown in ethanol (SCE) or glucose medium (SCD). As a loading control, blotted membranes were stained with Cdc34 antibodies after immunodecoration with anti-HA antibodies. As a loading control, blotted membranes were stained with Cdc34 antibodies Blot shown (upper panel) is representative of experiments repeated twice with similar results.
B) E/D ratio in cells growing either in 2% ethanol or 2% glucose

Reported results on the expression ratio in etanol versus glucose suggest that two receptors play antagonist roles in the control of Cln2 expression.
Anyway more experiment are needed to derive unambiguous conclusions.

Conclusions

Cell proliferation requires careful coordination of different processes, such as mass accumulation, DNA replication and cell division. This coordination is based on the cell's ability to integrate the environmental and metabolic signals with the activity of the key elements involved in the cell cycle progression.

This mechanism is based on achieving of a critical cell size (protein content per cell at the onset of DNA replication, Ps) to enter into S phase. Ps increases in proportion with ploidy and is modulated by nutrients. In fact, in bach cultures, the average cell size remains at low levels during growth on non-fermentable substrates, while the average size of cells increases in a linear way with the specific growth rate only during growth on fermentable substrates.

Recently Barberis et al. developed a mathematical model that describes the molecular events that occurring at the G_1-S transition (Barberis et al., 2007).

A simulation analysis performed with the model described above has provided a novel, intriguing conclusion: the critical cell size required for entry into S phase (as defined by the parameter Ps, the protein content at the onset of DNA replication) is an emergent property of the G_1-S network and is strongly influenced by growth rate (Barberis et al. 2007; Alberghina et al., 2009). In other words, Ps is a property that individual components of the G_1-S network do not possess but that emerges from their interaction. The setting of the critical cells size (Ps) is carried out by a mechanism consisting of a "sizer "plus a "timer".

The Far1/Cln3 threshold acts essentially as a growth-sensitive sizer, which is activated at similar cell size both in cells growing in rich or poor media: in fact, the Cln3/Far1 ratio remains almost equimolecular in the various growth conditions, since both Cln3 and Far1 levels increase or decrease accordingly to the growth rate (Hall et al., 1998; Alberghina et al., 2004; Alberghina et al., 2009; Barberis et al., 2007). The first Cln3/Far1 threshold and the second one involving Clb5,6 and Sic1 are temporally spaced ("timer") (Barberis et al., 2007): therefore, the actual value of Ps depends not only on the Cln3/Far1 "sizer", but also on the length of the "timer", which is the period elapsing between the passage through the first threshold and the overcoming of the second one (Barberis et al., 2007).

When one or both components of each threshold are inactivated, cells largely retain their ability to modulate their size according to carbon source availability. In contrast, concurrent loss of either *CLN3* or *FAR1* (first threshold) and *SIC1* (second threshold), abolishes glucose modulation of cell size (Alberghina et al., 2004). Consistently, nutrient status (and in particular the quantity and quality of available carbon source) influences the components of the two thresholds at the level protein abundance and sub-cellular localization.

For instance, Cln3 and Far1 levels are higher in cells growing on glucose than in cell cultivated on ethanol (Hall et al., 1998; Alberghina et al., 2004). On the contrary, Sic1 content is higher in ethanol growing cells; the sub-cellular localization of Sic1 is also carbon source-modulated: the inhibitor is mostly nuclear in cells grown in glucose- media, whereas a sizeable amount of Sic1 is detected also in the cytoplasm during growth on ethanol (Rossi et al., 2005).

It has been reported that *FAR1* overexpression induces a nutritionally modulated increase in cell size (Alberghina et al., 2004) in wild type cells. Here we show that the larger size of *FAR1*-overexpressing cells results from coordinated increased accumulation of both RNA and protein. Regulation of cell growth, or increase in cell mass, requires extensive coordination of several processes including transcription, ribosome biogenesis, translation, and nutrient metabolism. Being energetically highly demanding, these process are strictly regulated. In *S. cerevisiae*, the TOR and PKA pathways are the main regulators connecting the above processes with the nutritional status of the cell. By genome-wide transcriptional analysis of *FAR1*-overexpressing and *far1Δ* cells grown in ethanol- or glucose-supplemented minimal media with a range of phenotypic analysis, we could show that Far1 overexpression originates large transcriptional remodelling that affects pathways involved in controlling cell growth, including sugar sensing (that is known to affect the cell growth rate (Youk and van Oudenaarden, 2009) and the PKA and TOR pathways that are the major pathways involved in regulating cell growth in yeast (Busti, Gotti et al., manuscript in preparation).

In *S. cerevisiae*, Sch9 and Sfp1 are two main downstram targets of the Tor pathway involved in controlling cell growth through regulation of the protein synthesis machinery (reviewed in Lempainen and Shore, 2009). Sfp1 is a key transcriptional regulator of ribosome biogenesis (Jorgensen and Tyers, 2004; Lempiainen and Shore, 2009)). It binds directly to a subset of promoters of genes encoding ribosomal proteins (Fingerman et al., 2003; Jorgensen et al., 2002; Jorgensen et al., 2004; Lempiainen et al., 2009; Marion et al., 2004), as well as activating a large set of genes involved in ribosome biogenesis (Ribi genes; (Cipollina et al., 2008a; Jorgensen et al., 2002; Jorgensen et al., 2004; Marion et al., 2004). Sfp1 interacts directly with - and is phosphorylated by - the Tor1-containing TORC1 complex (Lempiainen et al., 2009). Sch9 is a protein kinase that shares several properties with the S6K1 kinase in mammals (Urban et al., 2007). A feedback mechanism controlling the activity of these proteins - likely acting as a homeostatic buffer to regulate the intricate balance of ribosome factor transcription - is operative, since Sfp1, negatively regulates TORC1 phosphorylation of Sch9.

The coordination between RNA and protein syntheses brought about by Far1 overexpression is conserved in the *sch9Δ* mutant, but is relaxed in cells lacking the *SFP1* gene. This is in keeping with the recent proposal that Sch9 is involved in optimal regulation of ribosome biogenesis by the TORC1 complex, but is dispensable for the essential aspects of ribosome biogenesis and cell growth (Wei and Zheng, 2009). Since in ethanol-grown *sfp1Δ* [pFAR1^{OE}] cells an increase in protein - but not RNA - level is observed, the increased protein level is likely due to improved usage of existing ribosomes, that are known to be in excess in ethanol-growing yeast (Waldron et al., 1977), without extensive *de no*vo synthesis of ribosomes.

It has been proposed that Sfp1 is a putative yeast functional analog of c-Myc (Jorgensen et al., 2004), a ubiquitous transcription factor from multicellular eukaryotes, which has been implicated in regulatory mechanisms coordinating all three RNA polymerases, since not only it is as a direct activator of RP and translation-related genes (RNA Polymerase II targets) but also as an activator of RNA Polymerase I and RNA Polymerase III (reviewed in (Eilers and Eisenman, 2008; Gomez-Roman et al., 2006)). Significantly, c-Myc, Sfp1, S6K1, and Sch9 all have dramatic effects on cell size regulation (Jorgensen et al., 2002; Jorgensen et al., 2004), which likely results from their role in coupling cell growth and cell division. Different studies in yeast showed that some aspect of ribosome biogenesis influences the cell-cycle commitment step (Start) through Whi5, an Rb-like protein (Bernstein et al., 2007). When ribosome biogenesis is blocked (but before ribosome levels are actually altered) a Whi5-dependent mechanism inhibits Start.

In summary, results obtained in the first part of this thesis suggest that the molecular mechanism that couples cell growth and cell cycle (i.e. the Far1/Cln3 sizer) contributes to regulate cell cell growth either directly or indirectly by affecting nutrient sensing and/or utilization, protein synthesis and pathways known to modulate ribosome biogenesis. A crucial role in mediating the effect of Far1 is played by the Sfp1 protein, whose presence is mandatory to allow coordinated increase in both RNA and protein in ethanol-grown cells, but not in glucose-grown cells.

The budding yeast *Saccharomyces cerevisiae* is able to regulate growth and cell cycle progression according to the frequent changes in the nutrient status. In fact, proliferation is rapid when large supplies of nutrients are available and ceases when these become exhausted. Glucose, the preferred energy source for this microorganism, must therefore generate signals that are somehow received and elaborated by the complex machinery governing growth and cell cycle progression: addition of glucose to quiescent or ethanol growing cells triggers a fast and massive reconfiguration of the transcriptional program, which enables the switch to fermentative metabolism and promotes an outstanding increase of the cell biosynthetic capacity.

Glucose signaling in *S. cerevisiae* requires in most cases at least partial metabolism of the sugar (Gancedo, 2008; Zaman et al., 2008; Santangelo, 2006): as a result, the roles of glucose as nutrient and signaling molecule are closely intertwined and it is difficult to separate the two functions.
In order to dissect whether the glucose effect on cell size was due to its function as nutrient, that require metabolism of the sugar, or to sensing of extracellular glucose levels, we analyzed yeast strains in which one or more of the glucose sensing pathway was impaired, due to deletions in one or more genes encoding glucose receptors: *GPR1* encoding a sensor for high glucose, *SNF3* encoding a sensor monitoring the presence of low glucose concentrations, and stimulating the expression of high affinity glucose transporters and *RGT2* encoding a receptor that monitors the presence of high glucose concentration, and therefore leads to expression of low affinity glucose transporters).
The *gpa2Δ gpr1Δ* strain does not show substantial changes in duplication time compared to its isogenic wild type grown in the same conditions, while its protein content is consistently lower. In the *snf3Δ rgt2Δ* and in the *snf3Δ rgt2Δ gpa2Δ gpr1Δ* strains a lower protein content (in any give growth condition) is accompanied by an increase in duplication time, when compared to wild type strain.
These correlations are highlighted in figure 20 that repots data presented in the results section.

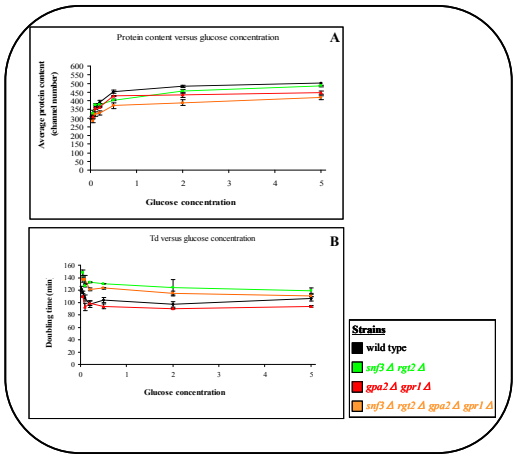

Figure 20. **Correlation between glucose concentration in medium culture and total protein content (A) and between glucose concentration in medium culture and duplication time (B) in all strains tested.**
The value of average of protein content, determined by cytofluorimetric analysis (see materials and methods for details) were determined for each strains either at different glucose concentration or 2% ethanol (SCE). Each point represents mean ± standard error of the mean (SEM), represented by error bars of at least three independent experiments
A) Correlation between protein content and the glucose concentration in the culture medium in all strains tested.
B) Plotting values of duplication time versus glucose concentration in the medium.

The relationship between growth and cell size can be better appreciated in figure 21 where the average protein content is plotted a function of MDT for wild type (panel A), *snf3Δ rgt2Δ gpa2Δ gpr1Δ* (panel B), *gpa2Δ gpr1Δ* (panel C), *snf3Δ rgt2Δ* (panel D).

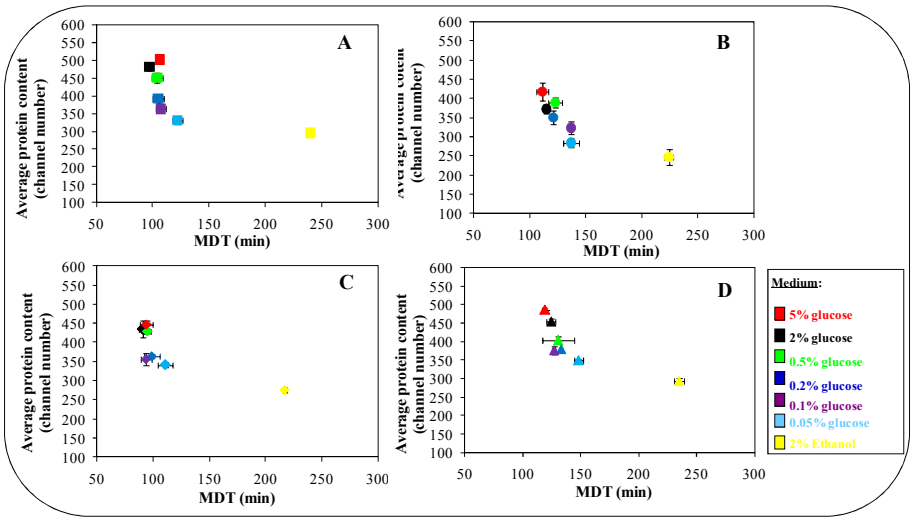

Figure 21. **Correlation between the average protein content (Ch.#) and the doubling time (min) in wild type, *snf3Δ rgt2Δ gpa2Δ gpr1Δ*, *gpa2Δ gpr1Δ* and *snf3Δ rgt2Δ* strains.** The value of average of protein content, determined by cytofluorimetric analysis (see materials and methods for details) were determined for each strains either at different glucose concentration or 2% ethanol (SCE). Each point represents mean ± standard error of the mean (SEM), represented by error bars of at least three independent experiments. **A)** The wild type strain **B)** *snf3Δ rgt2Δ gpa2Δ gpr1Δ* **C)** *gpa2Δ gpr1Δ* **D)** *snf3Δ rgt2Δ* strain trend either to various concentration of glucose or 2% ethanol (SCE)

In wild type cells a steep correlation between P and MDT is observed for cell grown in glucose containing media, whereas when glucose is substituted with ethanol a dramatic increase in MDT in accompanied by a minor decrease in average protein content (P).
Qualitatively, the a same trend can be observed in glucose sensing mutants. Although fine details of metabolism may differ between wild type, on one side, and sensing mutants, on the other, the type of metabolism remains unchanged (*i.e.*, all mutants grown in glucose-containing media use a fermentative metabolism). These finding suggest that under conditions of balanced exponential growth cell size is *driven* by metabolism, but *actual fine tuning* of P is set according to sensing of extracellular glucose.

A contributions of sensing in setting specific growth rate of yeast has been recently reported by Youk and van Oudenaarden, (Nature, 2009). They could in fact show that it is the interaction between glucose sensing and transport (that in turn is the major determinant of the glycolitic flux in S.cerevisiae (Teusink et al, 2000) that defines the growth rate according to the following equation:

$$\mu\ (r,g) = P\ (g)\ X\ \ln(r/rc) + \mu_c$$

in which r_c and μ_c are constants, while P(g) quantifies the effect that extracellular glucose has on the growth rate independently of its transport, but because of its perception. Key determinants of P(g) are Snf3 and Rgt2 glucose sensors.

Glucose sensing may be particularly important during transient, non steadaìy state conditions, as suggested by Levy and colleagues who propose that yeast cells use a feed-forward mechanism to couple nutrient availability with the actual growth rate (Levy et al., 2007). Results recently obtained by our group also point in this direction (Busti, Gotti et al, in preparation). We could in fact show that glucose induces a transient increase of cell size even in strains where sugar metabolism is dramatically reduced or completely abolished, due to the absence of a functional uptake system (*hxt*-null strains) or to the loss of the three kinases catalyzing the first step in glycolysis (*hxk2Δ hxk1Δ glk1Δ* strain): in fact, during an ethanol/glucose nutritional shift-up, both the *hxt*-null mutant and the triple *hxk2Δ hxk1Δ glk1Δ* null mutant initially respond to glucose addition by increasing their cellular volumes and their average protein content, analogously to wild type cells. However, the time frame and the kinetic of the "adaptation phase" to glucose in the two mutants are quite different from those of the wild type strain.

Furthermore, in the absence of sugar metabolism, glucose-dependent modulation of cell size is only transient: the effect of sugar addition on both cell volumes and protein content runs out within few generations, when the triple *hxk2Δ hxk1Δ glk1Δ* mutant strain again adopt the usual small size typical of the growth on ethanol medium, whereas the *hxt*-null strain undergoes a permanent G_1-arrest of the cell cycle progression. A reasonable explanation for our results may be that the initial effect of glucose on cell size mainly relies on sugar sensing and is partially independent of sugar metabolism; in contrast, long term maintenance of "large size phenotype" requires glucose uptake and metabolism.

In conclusion, this work highlighted that the elements involved in the cell size determination are multiple and interconnected. A strong alteration in cell size and protein content could originate not only from alteration in the dosage of genes involved in the molecular mechanism of the threshold which controls Ps, but also from environmental conditions. Notably glucose acts not only as a carbon and energy source, but as a modulator molecule as well.

References

Alberghina L, Rossi RL, Querin L,Wanke V, Vanoni M.
A cell sizer network involving Cln3 and Far1 controls entrance into S phase in the mitotic cycle of budding yeast. J Cell Biol 2004;167:433–43.

Aldea M, Garí E, Colomina N.
Control of cell cycle and cell growth by molecular chaperones.
Cell Cycle. 2007 Nov 1;6(21):2599-603. Epub 2007 Aug 19. Review

Amon, A., Tyers, M., Futcher, B. & Nasmyth, K.
Mechanisms that help the yeast cell cycle clock tick: G2 cyclins transcriptionally activate G2 cyclins and repress G1 cyclins.
Cell 1993; 74, 993–1007

Barberis, M., De Gioia, L., Ruzzene, M., Sarno, S., Coccetti, P., Fantucci, P., et al.
The yeast cyclin-dependent kinase inhibitor Sic1 and mammalian p27Kip1 are functional homologues with a structurally conserved inhibitory domain. Biochem J 2005;387:639–647.

Barberis M, Klipp E, Vanoni M, Alberghina L.
Cell size at S phase initiation: an emergent property of the G1/S network.
PLoS Comput Biol 2007;3:e64.

Barbet, N.C., Schneider, U., Helliwell, S.B., Stansfield, I., Tuite, M.F.,and Hall, M.N.
TOR controls translation initiation and early G1progression in yeast.
Mol. Biol. Cell 1996; 7, 25–42.

Baroni, M. D., Martegani, E. Monti, P.and Alberghina L.
Cell size modulation by CDC25 and RAS2 genes in Saccharomyces cerevisiae.
Mol. Cell. Biol. 1989; 9:2715–2723.

Baroni MD, Monti P, Marconi G, Alberghina L.
cAMP-mediated increase in the critical cell size required for the G1 to S transition in Saccharomyces cerevisiae. Exp Cell Res. 1992 Aug;201(2):299-306.

Baroni M.D., Monti P, Alberghina L.
Repression of growth-regulated G1 cyclin expression by cyclic AMP in budding yeast.
Nature. 1994 Sep 22;371(6495):339-42.

Belotti F, Tisi R, Martegani E.
The N-terminal region of the Saccharomyces cerevisiae RasGEF Cdc25 is required for nutrient dependent cell-size regulation Microbiology 2006;152:1231–1242.
Bernstein KA, Bleichert F, Bean JM, Cross FR, Baserga SJ.
Ribosome biogenesis is sensed at the Start cell cycle checkpoint.
Mol Biol Cell. 2007 Mar;18(3):953-64. Epub 2006 Dec 27.

Berry, L.D. and Gould, K.L.
Regulation of Cdc2 activity by phosphorylation at T14/Y15
Prog Cell Cycle Res 1996;2: 99-105

Brauer MJ, Huttenhower C, Airoldi EM, Rosenstein R, Matese JC, Gresham D, Boer VM, Troyanskaya OG, Botstein D.
Coordination of growth rate, cell cycle, stress response, and metabolic activity in yeast.
Mol Biol Cell. 2008 Jan;19(1):352-67. Epub 2007 Oct 24.

Bisson, L. F., and D. G. Fraenkel..
Involvement of kinases in glucose and fructose uptake by *Saccharomyces cerevisiae*.
Proc. Natl. Acad. Sci.USA 1983; 80:1730–1734

Bisson, L. F., and D. G. Fraenkel.
Expression of kinase-dependent glucose uptake in *Saccharomyces cerevisiae*.
J. Bacteriol. 1984; 159:1013–1017.

Bloom J, Cross FR.
Multiple levels of cyclin specificity in cell-cycle control.
Nat Rev Mol Cell Biol. 2007 Feb;8(2):149-60. Review.

Boles E, Hollenberg CP.
The molecular genetics of hexose transport in yeasts.
FEMS Microbiol Rev. 1997 Aug;21(1):85-111. Review.

Carlson M.
Glucose repression in yeast.
Curr Opin Microbiol. 1999 Apr;2(2):202-7. Review.

Celenza, J. L., L. Marshall-Carlson, and M. Carlson.
The yeast *SNF3* gene encodes a glucose transporter homologous to the mammalian protein.
Proc. Natl. Acad. Sci. USA 1988; 85:2130–2134.

Chang F, Herskowitz I.
Identification of a gene necessary for cell cycle arrest by a negative growth factor of yeast: FAR1 is an inhibitor of a G1 cyclin, CLN2. Cell 1990; 63:999-1011.

Chen KC, Calzone L, Csikasz-Nagy A, Cross FR, Novak B, Tyson JJ.
Integrative analysis of cell cycle control in budding yeast.
Mol Biol Cell 2004;15:3841–62.

Cismowski, M.J., Laff, G.M., Solomon, M.J., and Reed, S.I
KIN28 encodes a C-terminal domain kinase that controls mRNA transcription in Saccharomyces cerevisiae but lacks cyclin-dependent kinase-activating (CAK) activity.
Mol Cell Biol .1995; 15: 2983-2992

Cherkasova, V.A., and Hinnebusch, A.G.
Translational control by TOR and TAP42 through dephosphorylation of eIF2alpha kinase GCN2. Genes Dev. (2003). 17, 859–872**.**

Coccetti P, Rossi RL, Sternieri F, Porro D, Russo GL, di Fonzo A, Magni F, Vanoni M, Alberghina L.
Mutations of the CK2 phosphorylation site of Sic1 affect cell size and S-Cdk kinase activity in Saccharomyces cerevisiae. Mol Microbiol. 2004 Jan;51(2):447-60.

Coccetti P, Zinzalla V, Tedeschi G, Russo GL, Fantinato S, Marin O, Pinna LA, Vanoni M, Alberghina L.
Sic1 is phosphorylated by CK2 on Ser201 in budding yeast cells.
Biochem Biophys Res Commun. 2006 Aug 4;346(3):786-93. Epub 2006 Jun 6.

Colombo S, Ma P, Cauwenberg L Winderickx J,Crauwels M, Teunissen A, Nauwelaers D, de Winde JH, Gorwa MF, Colavizza D, Thevelein JM.
Involvement of distinct G-proteins, Gpa2 and Ras, in glucose- and intracellular acidification induced cAMP signalling in the yeast Saccharomyces cerevisiae.
EMBO J 1998; 17: 3326–3341.

Colombo S, Ronchetti D, Thevelein JM, Winderickx J, Martegani E.
Activation state of the Ras2 protein and glucose-induced signaling in Saccharomyces cerevisiae. J Biol Chem. 2004 Nov 5;279(45):46715-22. Epub 2004 Aug 31.

Cook M, Tyers M.
Size control goes global.
Curr Opin Biotechnol. 2007 Aug;18(4):341-50. Epub 2007 Sep 4. Review.

Coons, D. M., R. B. Boulton, and L. F. Bisson..
Computer-assisted nonlinear regression analysis of the multicomponent glucose uptake kinetics of *Saccharomyces cerevisiae*. J. Bacteriol. 1995; 177:3251–3258.

Coons DM, Vagnoli P, Bisson LF.
The C-terminal domain of Snf3p is sufficient to complement the growth defect of snf3 null mutations in Saccharomyces cerevisiae: SNF3 functions in glucose recognition.
Yeast. 1997 Jan;13(1):9-20.

Costanzo, M., Nishikawa, J.L., Tang, X., Millman, J.S., Shub, O.,Breitkreuz, K., Dewar, D., Rupes, I., Andrews, B., and Tyers, M.
CDK activity antagonizes Whi5, an inhibitor of G1/S transcription in yeast.
Cell. 2004; 117, 899–913.

Cross, F. R., Archambault, V., Miller, M. & Klovstad, M.
Testing a mathematical model of the yeast cell cycle.
Mol. Biol. Cell 2002;13, 52–70

Cross FR.
DAF1, a mutant gene affecting size control, pheromone arrest, and cell cycle kinetics of Saccharomyces cerevisiae. Mol Cell Biol. 1988 Nov;8(11):4675-84.

Crabtree, H.
Observations on the carbohydrate metabolism of tumours.
Biochem. J. 1929; 23, 536–545

Csikasz-Nagy A, Battogtokh D, Chen KC, Novak B, Tyson JJ.
Analysis of a generic model of eukaryotic cell-cycle regulation.
Biophys J. 2006;90:4361–79.

Darieva, Z. Pic-Taylor A, Boros J, Spanos A, Geymonat M, Reece RJ, Sedgwick SG, Sharrocks AD, Morgan BA.
Cell cycle-regulated transcription through the FHA domain of Fkh2p and the coactivator Ndd1p. Curr. Biol. (2003); 13, 1740–1745

de Bondt, H.L., Rosenblatt, J., Jancarik, J., Jones, H.D., Morgan, D.O., and Kim, S.-H
Crystal structure of cyclin-dependent kinase 2. Nature 1993; 363: 595-602

de Bruin RA, McDonald WH, Kalashnikova TI, Yates J 3rd, Wittenberg C.
Cln3 activates G1-specific transcription via phosphorylation of the SBF bound repressor Whi5. Cell. 2004 Jun 25;117(7):887-98.

Elliott, S.G., and McLaughlin, C.S.
Rate of macromolecular synthesis through the cell cycle of the yeast *Saccharomyces cerevisiae.* Proc. Natl. Acad. Sci. USA 1978; 75, 4384–4388

Deshaies, R.J., and Ferrell, J.E., Jr
Multisite phosphorylation and the countdown to S phase.
Cell 2001;107:819–822.

DeVit, M.J. and Johnston, M.
The nuclear exportin Msn5 is required for nuclear export of the Mig1 glucose repressor of Saccharomyces cerevisiae. Curr. Biol. 1999; 9, 1231–1241

Dirick, L.and Nasmyth, K.
Positive feedback in the activation of G1 cyclins in yeast.
Nature 1991; **351**,754–757

Dirick L, Böhm T, Nasmyth K.
Roles and regulation of Cln-Cdc28 kinases at the start of the cell cycle of Saccharomyces cerevisiae.EMBO J. 1995 Oct 2;14(19):4803-13.

Di Talia S, Skotheim JM, Bean JM, Siggia ED, Cross FR.
The effects of molecular noise and size control on variability in the budding yeast cell cycle.
Nature. 2007 Aug 23;448(7156):947-51. Erratum in: Nature. 2007 Dec 20;450(7173):1272.

Donovan, J. D., J. H. Toyn, A. L. Johnson, and L. H. Johnston.
$p40^{SDB25}$, a putative CDK inhibitor, has a role in the M/G1 transition in Saccharomyces cerevisiae. Genes Dev. 1994;8:1640–1653.

Edgington NP, Futcher B.
Relationship between the function and the location of G1 cyclins in S. cerevisiae.
J Cell Sci. 2001 Dec;114 (Pt 24):4599-611.

Epstein CB, Cross FR.
Genes that can bypass the *CLN* requirement for Saccharomyces cerevisiae cell cycle START.
Mol Cell Biol. 1994 Mar;14(3):2041-7.

Fangman, W.L. and Brewer, B.J.
A question of time: replication origins of eukaryotic chromosomes. Cell. 1992; 71, 363-366.

Fantes, P., and Nurse, P.
Control of cell size at division in fission yeast by a growth-modulated size control over nuclear division. Exp. Cell Res. 1977; 107, 377–386.

Fingerman I, Nagaraj V, Norris D, Vershon AK.
Sfp1 plays a key role in yeast ribosome biogenesis. Eukaryot Cell. 2003 Oct;2(5):1061-8.

Friedman, K.L., Raghuraman, M.K., Fangman, W.L., Brewer, B.J.
Analysis of the temporal program of replication initiation in yeast chromosomes.
J Cell Sci Suppl. 1995; 19, 51-58.

Fu X, Ng C, Feng D, Liang C.
Cdc48p is required for the cell cycle commitment point at Start via degradation of the G1-CDK inhibitor Far1p. J Cell Biol 2003;163: 21–26.

Futcher B.
Cyclins and the wiring of the yeast cell cycle.
Yeast. 1996 Dec;12(16):1635-46. Review.

Futcher, B.
Transcriptional regulatory networks and the yeast cell cycle.
Curr. Opin. Cell Biol. 2002; 14, 676–683..

Garí E, Volpe T, Wang H, Gallego C, Futcher B, Aldea M.
Whi3 binds the mRNA of the G1 cyclin CLN3 to modulate cell fate in budding yeast.

Gelade, R., Van de Velde, S., Van Dijck, P. and Thevelein, J.M
Multi-level response of the yeast genome to glucose
Genome Biol.2003;4, 233

Genes Dev. 2001 Nov 1;15(21):2803-8.

Gartner, A., Jovanovic, A., Jeoung, D.I., Bourlat, S., Cross, F.R., and Ammerer, G. Pheromone-dependent G1 cell cycle arrest requires Far1 phosphorylation, but may not involve inhibition of Cdc28-Cln2 kinase, in vivo *Mol Cell Biol* 1998;18(7): 3681-3691

Gancedo JM.
The early steps of glucose signalling in yeast.
FEMS Microbiol Rev. 2008 Jul;32(4):673-704. Review.

Gasser, S.M.
Visualizing chromatin dynamics in interphase nuclei.
Science 2002; 296, 1412–1416.

Hadwiger, J. A., C. Wittenberg, H. E. Richardson, M. de Barros Lopes, and S. I. Reed.
A family of cyclin homologs that control the G1 phase in yeast.
Proc. Natl. Acad. Sci. USA 1989;.86:6255–6259.

Hall, D.D., Markwardt, D.D., Parviz, F., and Heideman, W.
Regulation of the Cln3-Cdc28 kinase by cAMP in Saccharomyces cerevisiae
Embo J.1998; 17(15): 4370-4378 .

Hartwell LH, Culotti J, Pringle JR, Reid BJ.
Genetic control of the cell division cycle in yeast.
Science. 1974 Jan 11;183(4120):46-51. No abstract available.

Hartwell LH, Unger MW.
Unequal division in *Saccharomyces cerevisiae* and its implications for the control of cell division. J Cell Biol 1977; 1:422‑35

Henchoz S, Chi Y, Catarin B, Herskowitz I, Deshaies RJ, Peter M.
Phosphorylation- and ubiquitin-dependent degradation of the cyclindependent kinase inhibitor Far1p in budding yeast. Genes Dev 1997;11:3046–3060.

Ho, Y., Costanzo, M., Moore, L., Kobayashi, R., and Andrews, B.J.
Regulation of transcription at the *Saccharomyces cerevisiae* start transition by Stb1, a Swi6-binding protein. Mol. Cell. Biol. 1999; 19,5267–5278.

Hubler, L., Bradshaw-Rouse, J., and Heideman, W.
Connections between the Ras-cyclic AMP pathway and G1 cyclin expression in the budding yeast Saccharomyces cerevisiae Mol Cell Biol 1993; 13(10): 6274-6282

Johnston, G.C., Pringle, J.R., and Hartwell, L.H.
Coordination of growth with cell division in the yeast Saccharomyces cerevisiae.
Exp. Cell Res. 1977;105:79–98.

Johnston M.
Feasting, fasting and fermenting. Glucose sensing in yeast and other cells.
Trends Genet. 1999 Jan;15(1):29-33. Review.

Jorgensen P, Nishikawa JL, Breitkreutz BJ, Tyers M.
Systematic identification of pathways that couple cell growth and division in yeast.
Science. 2002 Jul 19;297(5580):395-400. Epub 2002 Jun 27.

Jorgensen P, Rupes I, Sharom JR, Schneper L, Broach JR, Tyers M.
A dynamic transcriptional network communicates growth potential to ribosome synthesis and critical cell size. Genes Dev. 2004 Oct 15;18(20):2491-505. Epub 2004 Oct 1.

Jorgensen P, Tyers M.
How cells coordinate growth and division.
Curr Biol. 2004 Dec 14;14(23):R1014-27. Review.

Kaldis, P., Sutton, A., and Solomon, M.J.
The Cdk-activating kinase (CAK) from budding yeast. Cell 1996; 86: 553-564

Kappeli, O.
Regulation of carbon metabolism in Saccharomyces cerevisiae and related yeasts.
Adv. Microb. Physiol. 1986; 28, 181–209

Kief, D.R., and Warner, J.R.
Coordinate control of syntheses of ribosomal ribonucleic acid and ribosomal proteins during nutritional shift-up in *Saccharomyces cerevisiae.* Mol. Cell. Biol. 1981; 1, 1007–1015.

Klein, C., and Struhl, K.
Protein kinase A mediates growthregulated expression of yeast ribosomal protein genes by modulating Rap1 transcriptional activity. Mol. Cell. Biol. 1994; 14, 1920–1928.

Ko, C. H., H. Liang, and R. F. Gaber.
Roles of multiple glucose transporters in *Saccharomyces cerevisiae*.
Mol. Cell. Biol. 1993; 13:638–648.

Kraakman L, Lemaire K, Ma P, Teunissen AW, Donaton MC, Van Dijck P, Winderickx J, de Winde JH , Thevelein JM
A Saccharomyces cerevisiae G protein-coupled receptor, Gpr1, is specifically required for glucose activation of the cAMP pathway during the transition to growth on glucose.
Mol Microbiol 1999; 32: 1002–1012

Kruckeberg, A. L., and L. F. Bisson.
The *HXT2* gene of *Saccharomyces cerevisiae* is required for high-affinity transport.
Mol. Cell. Biol. 1990; 10:5903–5913.

Kruckeberg, A. L.
The hexose transporter family of *Saccharomyces cerevisiae*.
Arch. Microbiol. 1996; 166:283–292.

Laabs TL, Markwardt DD, Slattery MG, Newcomb LL, Stillman DJ, Heideman W.
ACE2 is required for daughter cell-specific G1 delay in Saccharomyces cerevisiae.
Proc Natl Acad Sci U S A. 2003 Sep 2;100(18):10275-80. Epub 2003 Aug 22.

Lagunas, R.
Energetic irrelevance of aerobiosis for S. cerevisiae growing on sugars
Mol. Cell. Biochem. 1979; **27**, 139–146

Lagunas, R.
Misconceptions about the energy metabolism of Saccharomyces cerevisiae
Yeast ,1986; **2**, 221–2

Lee, J.M., and Greenleaf, A.L.
CTD kinase large subunit is encoded by CTK1, a gene required for normal growth of Saccharomyces cerevisiae. *Gene Exp* 1991; 1: 149-167

Lengronne, A. and Schwob, E.
The yeast CDK inhibitor Sic1 prevents genomic instability by promoting replication origin licensing in late G(1). Mol. Cell 2002;9:1067–1078

Lemaire K, Van de Velde S, Van Dijck P, Thevelein JM
Glucose and sucrose act as agonist and mannose as antagonist ligands of the G protein-coupled receptor Gpr1 in the yeast Saccharomyces cerevisiae. Mol Cell. 2004;16: 293–299.

Lew, D.J., N.J. Marini, and S.I. Reed.
Different G1 cyclins control the timing of cell cycle commitment in mother and daughter cells in the budding yeast Saccharomyces cerevisiae. Cell 1992;69:317-327.

Liang, H., and R. F. Gaber.
A novel signal transduction pathway in *Saccharomyces cerevisiae* defined by Snf3-regulated expression of *HXT6*. Mol. Biol. Cell 1996; 7:1953–1966

Lim, H.H., Loy, C.J., Zaman, S., and Surana, U.
Dephosphorylation of threonine 169 of Cdc28 is not required for exit from mitosis but may be necessary for Start in Saccharomyces cerevisiae.
Molecular and Cellular Biology. 1996; 16: 4573-4583

Lorincz, A., and Carter, B.L.A.
Control of cell size at bud initiationin *Saccharomyces cerevisiae.*
J. Gen. Microbiol. 1979; 113, 287–295.

Maeda, T., S. M. Wurgler-Murphy, and H. Saito.
A two-component system that regulates an osmosensing MAP kinase cascade in yeast.
Nature 1994; 369:242–245.

MacKay VL, Mai B, Waters L, Breeden LL.
Early cell cycle box-mediated transcription of CLN3 and SWI4 contributes to the proper timing of the G(1)-to-S transition in budding yeast.
Mol Cell Biol. 2001 Jul;21(13):4140-8.

Mai B, Miles S, Breeden LL.
Characterization of the ECB binding complex responsible for the M/G(1)-specific transcription of CLN3 and SWI4.Mol Cell Biol. 2002 Jan;22(2):430-41.

Marion, R.M., Regev, A., Segal, E., Barash, Y., Koller, D., Friedman, N., and O'Shea, E.K.
Sfp1 is a stress- and nutrient-sensitive regulator of ribosomal protein gene expression. Proc. Natl. Acad. Sci. USA 2004; 101, 14315–14322.

Marshall-Carlson, L., J. L. Celenza, B. C. Laurent, and M. Carlson.
Mutational analysis of the SNF3 glucose transporter of Saccharomyces cerevisiae.
Mol. Cell. Biol. 1990; 10:1105–1115.

Marshall-Carlson, L., L. Neigeborn, D. Coons, L. Bisson, and M. Carlson.
Dominant and recessive suppressors that restore glucose transport in a yeast *snf3* mutant. Genetics 1991; 128:505–512.

Martin DE, Soulard A, Hall MN.
TOR regulates ribosomal protein gene expression via PKA and the Forkhead transcription factor FHL1. Cell. 2004 Dec 29;119(7):969-79.

McInerny CJ, Partridge JF, Mikesell GE, Creemer DP, Breeden LL.
A novel Mcm1-dependent element in the SWI4, CLN3, CDC6, and CDC47 promoters activates M/G1-specific transcription. Genes Dev. 1997 May 15;11(10):1277-88.

Measday, V., Moore, L., Retnakaran, R., Lee, J., Donoviel, M., Neiman, A.M., and Andrews, B.A.
A family of cyclin-like proteins that interact with the Pho85 cyclin-dependent kinase.
Mol Cell Biol 1997; 17: 1212-1223

Mendenhall MD, Hodge AE.
Regulation of Cdc28 cyclin-dependent protein kinase activity during the cell cycle of the yeast Saccharomyces cerevisiae. Microbiol Mol Biol Rev. 1998 Dec;62(4):1191-243. Review

Miller, M. E. & Cross, F. R.
Distinct subcellular localization patterns contribute to functional specificity of the Cln2 and Cln3 cyclins of Saccharomyces cerevisiae. Mol. Cell. Biol.2000; **20**:542–555.

Miller ME, Cross FR.
Mechanisms controlling subcellular localization of the G(1) cyclins Cln2p and Cln3p in budding yeast.Mol Cell Biol. 2001 Sep;21(18):6292-311.

Moffat J, Andrews B.
Late-G1 cyclin-CDK activity is essential for control of cell morphogenesis in budding yeast. Nat Cell Biol 2004; 6:59–66.

Mortimer RK.
Radiobiological and genetic studies on a polyploid series haploid to hexaploid of *Saccharomyces cerevisiae*.
Rad Research 1958; 9:312‑26.

Nash R, Tokiwa G, Anand S, Erickson K, Futcher AB.
The WHI1+ gene of Saccharomyces cerevisiae tethers cell division to cell size and is a cyclin homolog. EMBO J. 1988 Dec 20;7(13):4335-46.

Nash RS, Volpe T, Futcher B.
Isolation and characterization of WHI3, a size-control gene of Saccharomyces cerevisiae.
Genetics. 2001 Apr;157(4):1469-80.

Nash, P., X. Tang, S. Orlicky, Q. Chen, F. B. Gertler Mendenhall MD, Sicheri F, Pawson T, Tyers M.
Multisite phosphorylation of a CDK inhibitor sets a threshold for the onset of DNA replication. Nature 2001b;414:514–521.

Nasmyth, K.
At the heart of the budding yeast cell cycle. Trends Genet. 1996; 12, 405–412.

Neigeborn, L., P. Schwartzberg, R. Reid, and M. Carlson.
Null mutations in the SNF3 gene of Saccharomyces cerevisiae cause a different phenotype than do previously isolated missense mutations. Mol. Cell. Biol. 1986;6:3569–3574.

Newcomb LL, Diderich JA, Slattery MG, Heideman W.
Glucose regulation of Saccharomyces cerevisiae cell cycle genes.
Eukaryot Cell. 2003 Feb;2(1):143-9.

Nishizawa M, Kawasumi M, Fujino M, Toh-e A.
Phosphorylation of sic1, a cyclin-dependent kinase (Cdk) inhibitor, by Cdk including Pho85 kinase is required for its prompt degradation. Mol Biol Cell. 1998 Sep;9(9):2393-405.

Neigeborn, L., and M. Carlson..
Genes affecting the regulation of *SUC2* gene expression by glucose repression in *Saccharomyces cerevisiae*. Genetics 1984; 108:845–858.

Neuman-Silberberg FS, Bhattacharya S, Broach JR.
Nutrient availability and the RAS/cyclic AMP pathway both induce expression of ribosomal protein genes in Saccharomyces cerevisiae but by different mechanisms.
Mol. Cell Biol. 1995;15:3187–96.

Nugroho, T. T., and M. D. Mendenhall.
An inhibitor of yeast cyclindependent protein kinase plays an important role in ensuring the genomic integrity of daughter cells. Mol. Cell. Biol. 1994;14:3320–3328.

Oehlen, L.J., McKinney, J.D., and Cross, F.R.
Ste12 and Mcm1 regulate cell cycle-dependent transcription of FAR1
Mol Cell Biol. 1996; 16(6): 2830-2837

Ozcan, S., and M. Johnston..
Three different regulatory mechanisms enable yeast hexose transporter (*HXT*) genes to be induced by different levels of glucose. Mol. Cell. Biol. 1995; 15:1564–1572.

Ozcan S, Dover J, Rosenwald AG, Wölfl S, Johnston M.
Two glucose transporters in Saccharomyces cerevisiae are glucose sensors that generate a signal for induction of gene expression.
Proc Natl Acad Sci U S A. 1996b Oct 29;93(22):12428-32.

Ozcan S, Dover J, Johnston M.
Glucose sensing and signaling by two glucose receptors in the yeast Saccharomyces cerevisiae. EMBO J. 1998 May 1;17(9):2566-73.

Paiardi C, Belotti F, Colombo S, Tisi R & Martegani E
The large N-terminal domain of Cdc25 protein of the yeast Saccharomyces cerevisiae is required for glucose-induced Ras activation. FEMS Yeast Res.2007; 7: 1270–1275.

Parviz F, Hall DD, Markwardt DD, Heideman W.
Transcriptional regulation of CLN3 expression by glucose in Saccharomyces cerevisiae.
J Bacteriol. 1998 Sep;180(17):4508-15.

Parviz F, Heideman W.
Growth-independent regulation of CLN3 mRNA levels by nutrients in Saccharomyces cerevisiae. J Bacteriol. 1998 Jan;180(2):225-30.

Pasteur, L.
Bulletin de la Societe Chimique de Paris 79; 1861

Pavletich, N.P. and Pabo, C.O
Zinc finger-DNA-Recognition: crystal structure of a Zif268-DNA complex at 2.1 Å.
Science 1991; **252**, 809-817.

Peter M, Gartner A, Horecka J, Ammerer G, Herskowitz I.
FAR1 links the signal transduction pathway to the cell cycle machinery in yeast.
Cell 1993; 73:747-60.

Peter, M. and Herskowitz, I.
Direct inhibition of the yeast cyclin-dependent kinase Cdc28-Cln by Far1
Science 1994; 265(5176): 1228-1231

Petroski MD, Deshaies RJ.
Redundant degrons ensure the rapid destruction of Sic1 at the G1/S transition of the budding yeast cell cycle. Cell Cycle 2003;2:410-1.

Pfeiffer, T., Schuster, S. and Bonhoeffer, S
Cooperation and competition in the evolution of ATP-producing pathways.
Science. 2001; 292, 504–507

Polakis, E.S., Bartley, W. and Meek, G.A.
Changes in the structure and enzyme activity of Saccharomyces cerevisiae in response to changes in the environment. Biochem. J. 1964; 90, 369–374

Polymenis M, Schmidt EV.
Coordination of cell growth with cell division.
Curr Opin Genet Dev. 1999 Feb;9(1):76-80. Review.

Ramakrishnan V., Theodoris G. & Bisson LF.
Loss of IRA2 suppresses the growth defect on low glucose caused by the snf3 mutation in Saccharomyces cerevisiae
FEMS Yeast Res 2007;7:67–77.

Reynolds, D.
Recruitment of Thr319-phosphorylated Ndd1p to the FHA domain of Fkh2p requires Clb kinase activity: a mechanism for CLB cluster gene activation.

Genes Dev. 2003; 17, 1789–1802

Rolland F, De Winde JH, Lemaire K, Boles E, Thevelein JM, Winderickx J.
Glucose-induced cAMP signalling in yeast requires both a G-protein coupled receptor system for extracellular glucose detection and a separable hexose kinase-dependent sensing process.
Mol Microbiol. 2000 Oct;38(2):348-58.

Rolland F, Winderickx J, Thevelein JM.
Glucose-sensing mechanisms in eukaryotic cells.
Trends Biochem Sci. 2001 May;26(5):310-7. Review.

Rolland F, Winderickx J, Thevelein JM.
Glucose-sensing and -signalling mechanisms in yeast.
FEMS Yeast Res. 2002 May;2(2):183-201. Review.

Rossi RL, Zinzalla V, Mastriani A, Vanoni M, Alberghina L.
Subcellular localization of the cyclin dependent kinase inhibitor Sic1 is modulated by the carbon source in budding yeast.Cell Cycle 2005;4:1798–1807.

Rudra D, Warner JR.
What better measure than ribosome synthesis?
Genes Dev. 2004 Oct 15;18(20):2431-6.

Rudra D, Zhao Y, Warner JR.
Central role of Ifh1p-Fhl1p interaction in the synthesis of yeast ribosomal proteins.
Embo J 2005;24:533–542

Rupes I.
Checking cell size in yeast.
Trends Genet. 2002 Sep;18(9):479-85. Review.

Santangelo GM.
Glucose signaling in Saccharomyces cerevisiae.
Microbiol Mol Biol Rev. 2006 Mar;70(1):253-82. Review.

Schleiden, M.J. (1838) Beitraege sur phytogenesis, Muller's Archiv

Schneider BL, Yang QH, Futcher AB.
Linkage of replication to start by the Cdk inhibitor Sic1.
Science. 1996 Apr 26;272(5261):560-2.

Schneider, B.L., Zhang, J., Markwardt, J., Tokiwa, G., Volpe, T., Honey, S., and Futcher, B
Growth rate and cell size modulate the synthesis of, and requirement for, G1-phase cyclins at Start. Mol.Cell. Biol. 2004; 24, 10802–10813.

Schwab, M., A. S. Lutum and W. Seufert.
Yeast Hct1 is a regulator of Clb2 cyclin proteolysis. Cell 1997;90:683–693.

Schwann, T.(1839) Mikroscopische untersuchungen ueber die Uebereinstimmung in der struktur und dem wachsthum der theire und planzen (Berlin).

Schwob, E., and K. Nasmyth.
CLB5 and CLB6, a new pair of B cyclins involved in DNA replication in Saccharomyces cerevisiae. Genes Dev. 1993;7:1160–1175.

Schwob, E., T. Bohm, M. D. Mendenhall and K. Nasmyth.
The B-type cyclin kinase inhibitor p40SIC1 controls the G1 to S transition in S. cerevisiae.
Cell 1994;79: 233–244.

Schwob, E.
Flexibility and governance in eukaryotic DNA replication.
Curr Opin Microbiol. 2004 Dec;7(6):680-90. Review.

Sherlock, G. and Rosamond, J.
Starting to cycle: G1 control regulating cell division in budding yeast.
Journal of General Microbiology 1993 139: 2531-2541

Shuster, J.R.
"Start" mutants of *Saccharomyces cerevisiae* are suppressed in carbon catabolite-derepressing medium. J. Bacteriol. 1982; 151, 1059–1061.

Skotheim JM, Di Talia S, Siggia ED, Cross FR.
Positive feedback of G1 cyclins ensures coherent cell cycle entry.
Nature. 2008 Jul 17;454(7202):291-6.

Stuart, D., and Wittenberg, C.
CLN3, not positive feedback, determines the timing of *CLN2* transcription in cycling cells. Genes Dev. 1995; 9, 2780–2794.

Sudbery, P.E., Goodey, A.R., and Carter, B.L.
Genes which control cell proliferation in the yeast Saccharomyces cerevisiae.
Nature. 1980; 288:401–404.

Sudbery, P.
Cell biology. When wee meets whi.
Science. 2002; 297,351–352.

Toda, T., Uno, I., Ishikawa, T., Powers, S., Kataoka, T., Broek, D., Cameron, S., Broach, J., Matsumoto, K., and Wigler, M.
In yeast, RAS proteins are controlling elements of adenylate cyclase Cell 1985; 40(1): 27-36

Tokiwa, G.
Cell cycle control in *Saccharomyces cerevisiae*: G1 cyclin regulation and a connection with the Ras/cAMP signaling pathway. (State University of New York, Stony Brook); 1995

Toyn JH, Johnson AL, Donovan JD, Toone WM, Johnston LH.
The Swi5 transcription factor of Saccharomyces cerevisiae has a role in exit from mitosis through induction of the cdk-inhibitor Sic1 in telophase.Genetics. 1997 Jan;145(1):85-96.

Tripodi F, Zinzalla V, Vanoni M, Alberghina L, Coccetti P.
In CK2 inactivated cells the cyclin dependent kinase inhibitor Sic1 is involved in cell-cycle arrest before the onset of S phase.
Biochem Biophys Res Commun. 2007 Aug 10;359(4):921-7. Epub 2007 Jun 4.

Tyers, M., Tokiwa, G., Nash, R., and Futcher, B.
The Cln3- Cdc28 kinase complex of *S. cerevisiae* is regulated by proteolysis and phosphorylation. EMBO J. 1992; 11, 1773–1784.

Tyers M, Tokiwa G, Futcher B.
Comparison of the Saccharomyces cerevisiae G1 cyclins: Cln3 may be an upstream activator of Cln1, Cln2 and other cyclins EMBO J. 1993 May;12(5):1955-68.

Tyers, M., and B. Futcher.
Far1 and Fus3 link the mating pheromone signal transduction pathway to three G1-phase Cdc28 kinase complexes. Mol. Cell. Biol. 1993b;13:5659–5669.

Tyers, M., Tokiwa, G., and Futcher, B.
Comparison of the *Saccharomyces cerevisiae* G1 cyclins: Cln3 may be an upstream activator of Cln1, Cln2 and other cyclins. EMBO J. 1993; 12, 1955–1968

Tyers, M.
The cyclin-dependent kinase inhibitor p40SIC1 imposes the requirement for Cln G1 cyclin function at Start. Proc. Natl. Acad. Sci. USA 1996;93:7772–7776.

Toone WM, Aerne BL, Morgan BA, Johnston LH.
GETTING STARTED: Regulating the Initiation of DNA Replication in Yeast
Annu. Rev. Microbiol. 1997;51:125-49.

Urban J, Soulard A, Huber A, Lippman S, Mukhopadhyay D, Deloche O, Wanke V, Anrather D, Ammerer G, Riezman H, Broach JR, De Virgilio C, Hall MN, Loewith R.
Sch9 is a major target of TORC1 in Saccharomyces cerevisiae.
Mol Cell. 2007 Jun 8;26(5):663-74

Unger, M.W., and Hartwell, L.H.
Control of cell division in *Saccharomyces cerevisiae* by methionyl-tRNA.
Proc. Natl. Acad. Sci. USA 1976;73, 1664–1668.

Vagnoli P, Coons DM, Bisson LF.
The C-terminal domain of Snf3p mediates glucose-responsive signal transduction in Saccharomyces cerevisiae. FEMS Microbiol Lett. 1998 Mar 1;160(1):31-6.

Van Dijck P, Gorwa MF, Lemaire K et al
Characterization of a new set of mutants deficient in fermentation-induced loss of stress resistance for use in frozen dough applications. Int J Food Microbiol. 2000, 55: 187–192.

Vanoni M, Rossi RL, Querin L, Zinzalla V, Alberghina L.
Glucose modulation of cell size in yeast.
Biochem Soc Trans. 2005 Feb;33(Pt 1):294-6. Review.

Vergés E, Colomina N, Garí E, Gallego C, Aldea M.
Cyclin Cln3 is retained at the ER and released by the J chaperone Ydj1 in late G1 to trigger cell cycle entry. Mol Cell. 2007 Jun 8;26(5):649-62.

Verma R, Annan RS, Huddleston MJ, Carr SA, Reynard G, Deshaies RJ.
Phosphorylation of Sic1p by G1 Cdk required for its degradation and entry into S phase.
Science 1997; 278:455–460.

Versele M, deWinde JH, Thevelein JM
A novel regulator of G protein signalling in yeast, Rgs2, downregulates glucoseactivation of the cAMP pathway through direct inhibition of Gpa2. EMBO J. 1999; 18: 5577–5591.

Visintin, R., S. Prinz and A. Amon.
CDC20 and CDH1: a family of substrate-specific activators of APC-dependent proteolysis.
Science 1997;278:460–463.

Warner JR, Vilardell J, Sohn JH.
Economics of ribosome biosynthesis.
Cold Spring Harbor Symp.Quant. Biol.2001;66:567–74.

Wang H, Garí E, Vergés E, Gallego C, Aldea M.
Recruitment of Cdc28 by Whi3 restricts nuclear accumulation of the G1 cyclin-Cdk complex to late G1. EMBO J. 2004b Jan 14;23(1):180-90. Epub 2003 Dec 18.

Warner, J.R.
The economics of ribosome biosynthesis in yeast.
Trends Biochem. Sci. 1999; 24, 437–440.

Wehr, C.T., Parks, L.W.
Macromolecular synthesis in *Saccharomyces cerevisiae* in different growth media.
J. Bacteriol. 1969;98, 458–466.

Wijnen, H., Futcher, B.
Genetic analysis of the shared role of *CLN3* and *BCK2* at the G1-S transition in *Saccharomyces cerevisiae.* Genetics. 1999; 153, 1131–1143.

Xue Y, Batlle M, Hirsch JP.
GPR1 encodes a putative G protein-coupled receptor that associates with the Gpa2p Galpha subunit and functions in a Ras-independent pathway. EMBO J. 1998 Apr 1;17(7):1996-2007.

Zachariae,W., M. Schwab, K.Nasmyth and W. Seufert.
Control of cyclin ubiquitination by CDK-regulated binding of Hct1 to the anaphase promoting complex. Science 1998;282:1721–1724.

Zaman S, Lippman SI, Zhao X, Broach JR.
How Saccharomyces responds to nutrients.
Annu Rev Genet. 2008;42:27-81. Review.

Zhang J, Schneider C, Ottmers L, Rodriguez R, Day A, Markwardt J, Schneider BL.
Genomic scale mutant hunt identifies cell size homeostasis genes in *S. cerevisiae*.
Curr Biol. 2002; 12:1992‑2001

Zinzalla V, Graziola M, Mastriani A, Vanoni M, Alberghina L.
Rapamycin-mediated G1 arrest involves regulation of the Cdk inhibitor Sic1 in Saccharomyces cerevisiae. Mol Microbiol 2007;63:1482–94.

Acknowledgements

This Report would not have been possible without the essential and gracious help of many individuals. I thank Professor Lilia Alberghina for her continuous support. I wish to thank Prof. MarcoVanoni for their support and encouragement and for critical discussion of the experimental data.
I am really grateful to Dr.ssa Elena Sacco, Dr.ssa Paola Coccetti and Dr.ssa Renata Tisi, for essential suggestions. I am grateful to a lot of friends in particular I would like to tanks Teo for his precious friendship, thanks to Farida for our long travel to came back home, thanks to Lory for technical and human supports. Sincere thanks to all my workmates
Special thanks to Alessandro and all my family for their patience.

Appendix

Coordinated increase in cellular RNA and protein content induced by overexpression of Far1, a cyclin dependent kinase inhibitor, involves large transcriptional reprogramming and requires the Sfp1 protein

Stefano Busti[1], Laura Gotti[1], Chiara Balestrieri[1], Lorenzo Querin [1], Guido Drovandi[2], Giovanni Felici [2], Gabriella Mavelli[2], Paola Bertolazzi[2], Lilia Alberghina [1] and Marco Vanoni [1*]

[1]Dipartimento di Biotecnologie e Bioscienze, Università di Milano-Bicocca, Piazza della Scienza 2, 20126 Milano, Italy
[2]Istituto di Analisi dei Sistemi ed Informatica ‘‘Antonio Ruberti”, Consiglio Nazionale delle Ricerche, Viale Manzoni 30, 00185 Roma, Italy

* **Corresponding author**: Marco Vanoni, Dipartimento di Biotecnologie e Bioscienze, Università di Milano-Bicocca, Piazza della Scienza 2, 20126 Milano, Italy. **e-mail**: marco.vanoni@unimib.it; **tel**:+039-0264483525

Abstract

The *FAR1* gene encodes an 830 residue bifunctional protein, whose major function is inibtion of cyclin-dependent kinase complexes involved in the G1/S transition. *FAR1* transcription is maximal between mitosis and early G1 phase. Enhanced *FAR1* transcription is necessary but not sufficient for the pheromone-induced G1 arrest, since *FAR1* overexpression itself does not trigger cell cycle arrest.
Besides its well established role in the response to pheromone, recent evidences suggest that Far1 may also regulate the mitotic cell cycle progression: in particular, it has been proposed that Far1, together with the G1 cyclin Cln3, may be part of a cell sizer mechanism that controls the entry into S phase. Far1 is an unstable protein throughout the cell cycle except during G1 phase. Far1 levels peak in newborn cells as a consequence of a burst of synthetic activity at the end of the previous cycle, and the amounts per cell remains roughly constant during the G1 phase. Phosphorylation (at serine 87) by Cdk1-Cln complexes primes Far1 for ubiquitin-mediated proteolysis.
By coupling a genome-wide transcriptional analysis of *FAR1*-overexpressing and *far1Δ* cells grown in ethanol- or glucose-supplemented minimal media with a range of phenotypic analysis, we show that *FAR1* overexpression not only coordinately increases RNA and protein accumulation, but induces strong transcriptional remodelling, metabolism being the most affected cellular property, suggesting that the Far1/Cln3 sizer regulates cell growth either directly or indirectly by affecting metabolism and pathways known to modulate ribosome biogenesis. Consistently *FAR1* overexpression affects sensitivity of yeast cells to the Tor-inhibiting drug rapamycin.

1. Introduction

The *FAR1* gene has been originally identified in a screen for mutants defective in the response to mating factors (Chang and Herskowitz, 1990). It encodes an 830 residue bifunctional protein with two distinct roles in yeast mating (Bardwell, 2005). The major function of the Far1 protein is that of cyclin dependent kinase inhibitor (CKI) (Chang and Herskowitz, 1990; Peter and Herskowitz, 1994). Pheromone signaling enables the MAPK Fus3 to phosphorylate Far1, which inactivates Cdk1/Cln complexes by a still undefined mechanism, leading to G1 arrest at Start: in this way, haploid cells of opposite mating type synchronize their cell cycles, so that they can conjugate and form a diploid (Breitkreutz et al., 2001; Chang and Herskowitz, 1990; Gartner et al., 1998; Jeoung et al., 1998; Peter and Herskowitz, 1994). In the absence of pheromone, Cln/Cdks phosphorylate Far1, targeting it for degradation to allow passage through Start (Blondel et al., 2000; Henchoz et al., 1997; McKinney et al., 1993).
A Far1 fragment including residues 1-393 has been reported to be necessary and sufficient for the G1 arrest function (McKinney and Cross, 1995; Peter et al., 1993), whereas the carboxy-terminus encompassing residues 546-830 interacts with and activates Cdc24 (Wiget et al., 2004). The amino terminal region also contains a H2-RING finger motif (aa 202-252), which during mating is required for the recruitment of Far1 to the site of polarized growth via interaction with the G protein βγ dimer (Butty et al., 1998), and a PH-like domain (residues 418-545), which stabilizes Far1 at the plasma membrane (Wiget et al., 2004). During yeast mating, Far1 is also involved in the establishment of cell polarity (orientation of the growth axis toward the pheromone source) by serving as a scaffold/adapter that links the activated G protein βγ dimer to the guanine-nucleotide exchange factor (GEF) Cdc24, which activates the Rho-type GTPase Cdc42 (Butty et al., 1998; Nern and Arkowitz, 1999).
FAR1 transcription is maximal between mitosis and early G1 phase and is regulated by the Mcm1 (during G2/M phase) and Ste12 transcription factors (G1 phase) (McKinney et al., 1993; Oehlen et al., 1996). *FAR1* expression is further induced by pheromone in a Ste12 -dependent manner (McKinney et al., 1993; McKinney and Cross, 1995; Oehlen et al., 1996): this enhanced *FAR1* transcription is necessary but not sufficient for the pheromone-induced

G1 arrest, since *FAR1* overexpression itself does not trigger cell cycle arrest (Chang and Herskowitz, 1992).
Far1 is an unstable protein throughout the cell cycle except during G1 phase (Henchoz et al., 1997). Far1 level peaks in newborn cells as a consequence of a burst of synthetic activity at the end of the previous cycle, and its amount per cell remains roughly constant during the G_1 phase (McKinney et al., 1993). Its level is controlled by ubiquitin-mediated proteolysis primed by phosphorylation at serine 87 opearated by Cdk1-Cln complexes (Blondel et al., 2000; Henchoz et al., 1997).
Besides its well established role in the response to pheromone, recent evidences suggest that Far1 may also regulate cell cycle progression in mitotic cells (Alberghina et al., 2004; Fu et al., 2003). In particular, it has been proposed that Far1, together with the G1 cyclin Cln3, may be part of a nutritionally modulated cell sizer plus timer mechanism that controls the entry into S phase (Alberghina et al., 2004; Barberis et al., 2007; Di Talia et al., 2007). Each threshold consists of an activator and an associated inhibitor blocking its function). The first one involves the G1 cyclin Cln3, the Cdk inhibitor (Cki) Far1 and the cyclin-dependent kinase Cdk1 (Cdc28), whereas the second one comprises the S phase cyclin Clb5 (and Clb6), the Cki Sic1 and Cdk1 (Alberghina et al., 2009; Alberghina et al., 2004; Barberis et al., 2007). In the first threshold, that is as the actual cell sizer, Cln3 has to overcome Far1 in order to trigger Cln–Cdk1 activation, which is in turn required for SBF- and MBF-dependent transcription.
Carbon source affects the expression level of the components of both thresholds: for instance, Cln3 and Far1 levels are higher in cells growing on glucose than on ethanol (Alberghina et al., 2004; Hall et al., 1998), whereas Sic1 content is higher in non-fermentable carbon sources (Rossi et al., 2005). The two thresholds cooperate to set the critical cell size according to the available carbon source: consistently with this notion, when both the thresholds are inactivated yeast cells loose the capacity to increase their size in presence of glucose (Alberghina et al., 2004).
It has been reported that *FAR1* overexpression increases cell size (Alberghina et al., 2004). In this report we show that *FAR1* overexpression coordinately increases RNA and protein accumulation. Transcriptional analysis and a variety of biochemical and cell-based assays indicate that signal transduction pathways involved in nutrient utilization and in the control of cell growth are affected by *FAR1* overexpression. The absence of Sfp1, a major downstream element of the Target OF Rapamycin (TOR) pathway largely decouples the increase in protein and RNA syntheses observed in wild type cells.
These results suggest that a cell cycle regulatory protein involved in the molecular mechanism that couples cell growth and cell cycle (*i.e.,* the Far1/Cln3 sizer) contributes to regulate cell growth either directly or indirectly by affecting nutrient sensing and/or utilization, protein synthesis and pathways known to modulate ribosome biogenesis.

2. Materials and Methods

2.1. Strains, plasmids and growth conditions
Strains used in this work were W303-1A (*MATa ade2-1 his3-11 leu2-3,112 trp1-1 ura3-1 can1-100*), *far1Δ* (*MATa ade2-1 his3-11 leu2-3 112 trp1-1 ura3-1 can1-100 far1::HIS3*) (Alberghina et al., 2004), BY4741 (*MATa his3Δ1 leu2Δ met15Δ ura3Δ*), *sfp1Δ* (*MATa his3Δ1 leu2Δ met15Δ ura3Δ sfp*1::*KanMX4*) (Cipollina et al., 2005), *sch9Δ* (*MATa his3Δ1 leu2Δ met15Δ ura3Δ sch9*::*LEU2*^{KI}) (a kind gift from M. Vai). The plasmid pTet-*FAR1*-15Myc was used to obtain *FAR1* overexpression (Alberghina et al., 2004). We will refer to transformed cells as W303-1A[pFAR1^{OE}], *sch9Δ*[pFAR1^{OE}] and so forth. Unless otherwise stated, yeast cells were grown at 30°C in Synthetic Complete (SC) Medium (Formedium) containing 6.7 g/L Yeast Nitrogen Base w/o aminoacids (Difco), supplemented with either 2% glucose or 2% ethanol as a carbon source and omitting amino acids as necessary for selection.

Cell growth was monitored by a Coulter counter model Z2 instrument (Beckman Coulter), whereas the budding index was scored by direct microscopic observation on at least 300 cells, fixed in 3.6% formalin and mildly sonicated. DNA manipulations and yeast transformations were carried out according to standard techniques.

2.2. Determination of RNA and protein content by chemical assay and flow cytometry

Samples of growing cultures (at least $2*10^7$ cells) were collected and fixed in 70% ethanol before the cytofluorimetric analysis. For RNA staining, cells were washed once with cold PBS (3.3mM NaH_2PO_4, 6.7mM Na_2HPO_4, 127mM NaCl. 0.2mM EDTA, pH 7.2), resuspended in 1 ml of Propidium Iodide stainining solution (0.046mM propidium iodide in 0.05M Tris-HCl, pH=7.7; 15mM $MgCl_2$) and incubated for 30 minute in ice and dark. Cell suspensions were sonicated for 30 seconds before the analysis. To obtain protein distribution, cells were stained with fluorescein isothyocyanate solution (50 µg /ml FITC in 0.5M $NaHCO_3$) for at least 30min in ice and dark; cells were then washed three times in PBS and sonicated before the analysis. For DNA/Protein biparametric staining, cells were washed once in PBS and resuspended in 1ml of PBS containing 1mg/ml RNAse. After at least 1h at 37°C, cells were resuspended in 1 ml of a 10000-fold diluted FITC staining solution (5ng/ml FITC in 0.5 M $NaHCO_3$) and incubated for 30 min in ice and dark; cells were then washed three times with PBS and resuspended in DNA staining solution (Coccetti et al., 2004). The analysis was performed with a FACScan (Becton Dickinson) instrument equipped with a Ion-Argon laser at 488 nm laser emission. The sample flow rate during analysis did not exceed 500-600 cells/s. Typically, 30000 cells were analysed for each sample.

*For chemical assays, e*xponentially growing cells ($5*10^8$ total cells) were collected by filtration, washed twice with ice-cold 5% Trichloroacetic Acid (TCA) and stored at -20°C for at least 12 hours. Samples were then slowly thawed in ice, resuspended in 5 ml of perchloric acid 0.3 N and heated 30 minutes at 90° C. After centrifugation (10 minutes at 3500 rpm) the supernatant was recovered and used for RNA determination, whereas the pellet was used for protein determination as described below.

Samples were appropriately diluted in water, an equal volume of Orcinol solution (0.5 g Orcinol Monohydrate and 0.25 g FeCl-$6H_2O$, dissolved in 50ml of 37% HCl) was added and the mixtures were heated at 90°C for 20 minutes. Absorbance was read at 660 nm. Ribonucleic acid from baker's yeast (MP biochemicals) was used as a standard (Alberghina et al., 1975). For protein determination, pellets were resuspended in 1N NaOH, and incubated overnight at room temperature on a rolling drum. Samples were then centrifuged (10 minutes at 3500 rpm) and the resulting supernatants were used for protein determination according to the microbiuret method, using bovine serum albumin as a standard (Alberghina et al., 1975)

.

2.3. Measurement of stress resistance-related parameters

Aliquots of exponentially growing cells were either heated at 51°C (heat-shock) or treated with hydrogen peroxide (oxidative stress), lithium chloride (ionic stress) or sorbitol (osmotic stress) at the concentrations and for the time periods indicated in Fig. 6. Treated and untreated cells were then serially diluted, spotted on YPD plates and incubated for 48h at 30°C for the evaluation of the stress resistance.
The strain W-GUS (W303-1A *HSP12::GUS*) used for the **β**-glucoronidase assay was obtained by transforming W303-1A with a modified version of the integrative plasmid pKV3-d2 containing the *HSP12* promoter region fused to the *GUS* reporter gene (Varela et al., 1995). Exponentially growing cells were harvested by centrifugation, washed with ice-cold water and resuspended in GUS-extraction buffer (50mM NaPO4, pH 7.0; 10mM β-

mercaptoethanol; 10mM Na2EDTA; 0.1% sodium lauryl sarcosine; 0.1% Triton X-100; 1mM PMSF). Cells were disrupted with glass beads and protein extracts were clarified by centrifugation at 13,000 rpm for 2min. β-glucoronidase activity was measured by a spectrophotometric assay using p-nitrophenyl β-d-glucuronide (PNPG) as substrate. The assay was performed at room temperature and the reaction was stopped by the addiction of one volume of K_2CO_3. Absorbance was measured at 415nm against a stopped, blank reaction to which identical amounts of extracts and substrate had been added. Protein content was measured using the Bio-Rad protein assay reagent (Bio-Rad).
For the quantification of glutathione levels, $5*10^8$ exponentially growing cells were collected by centrifugation, washed twice with cold PBS, resuspended in 500uL of cold lysis buffer (10mM HCl, 1.3% sulfosalycilic acid) and lysed with glass beads. After centrifugation at 13000rpm, the cleared supernatant was used for the determination of the glutathione content, whereas the pellet was resuspended in 500uL of 1N NaOH and incubated overnight at room temperature on a rolling drum before the protein dosage (biuret method). The total glutathione content was determined with an enzymatic recycling assay based on glutathione reductase using DTNB (5, 5'-Dithiobis(2-nitro-benzoic acid) as a substrate, essentially as previously described (Grant et al., 1998).
For the selective measure of the oxidized glutathione (GSSG) content, samples were treated for 1h with 2-vinyplyridine before the analysis.
Cell wall structure was probed by measuring its resistance to digestion by lytic enzymes. Exponentially growing cells were collected by centrifugation, washed once with PBS and resuspended ($1*10^8$ cells/mL) in zymolase digestion buffer (50 mM Tris-Cl, pH 7.5, 10 mM MgCl2, 1 M sorbitol, 30 mM dithiothreitol, 15 mM β-mercaptoethanol) containing 20 μg/mL T100 zymolase. Cellular suspensions were incubated at 37°C and samples (100uL) were collected at regular intervals. Samples were diluted 1:10 in deionised water in order to promote the lysis of the spheroplasts and the turbidity of the cellular suspensions was measured at 600nM.
The strains Neph8 (*MAT***α** *leu2::hisG ura3-52 trp1::hisG*) and Nephtlys886 (*MAT***a**/**α** *leu2::hisG/leu2::hisG ura3-52/ura3-52 trp1::hisG/trp1::hisG*) used to assay invasive and pseudohyphal growth are congenic to the Sigma1278b genetic background (Magherini et al., 2006). Low ammonium medium (SLAD: 2% glucose, 0.17% YNB w/o ammonium sulphate (Difco), 50μM ammonium sulphate, 2% agar) for induction of pseudohyphal growth has been described (Gimeno et al., 1992). Cells were grown over-night on selective SD medium, streaked on SLAD plates and incubated at 30°C for 3-7 days. Representative microcolonies were photographed directly on agar plates with a Cool snap camera (RS photometries) mounted on a Nikon microscope at 25× magnification. For the invasive growth assay, cells were spotted on YPD plates, incubated at 30°C for 3 days and for an additional 2 days at 24 C. Plates were photographed, washed with a gentle stream of deionized water to remove cells which had not invaded the agar surface and immediately photographed again (Roberts and Fink, 1994).

2.4. Assays of glucose consumption, ethanol production and invertase activity

In order to evaluate glucose consumption and ethanol production, exponentially growing cells were collected by filtration, washed twice with 2 volumes of medium without carbon source and resuspended in fresh medium containing 50mM glucose at a final cellular density of $4*10^6$ cells/mL. Cultures were incubated at 30°C on a rotary shaker and samples were taken at regular intervals to evaluate the glucose consumption and the ethanol production by standard enzymatic assays (Sigma-Aldrich; Megazyme).
For the assay of invertase activity, cells growing in ethanol medium were harvested by filtration, washed once and resuspended in either 2% ethanol medium (basal condition), 2% glucose (repressing condition) or 0.05% glucose (inducing conditions) at a final cellular density of $3\text{-}4*10^6$ cells/mL. After 5 hours at 30°C, $2*10^8$ cells were harvested by filtration, washed once with ice cold 10mM sodium azide and resuspended in 1mL sodium azide/acetate

buffer (10mM NaN_3, 50mM Na-acetate). 1 mL of 200mM saccharose was added and the cellular suspensions were incubated at 37°C for 30 min. The reaction was stopped by addition of 250 µl Tris 1M pH 8.8 and by heating at 90°C for 3 minutes. Samples were centrifugated and the glucose concentration in the surnatant was measured by the glucose oxidase-peroxidase method (Sigma-Aldrich). Invertase activity was calculated as (µmol of glucose released from saccharose min^{-1})/10^8cells.

2.5. RNA preparation and hybridization.

Total RNA was extracted from biological triplicate samples and analyzed using Affymetrix Genechip, Yeast Genome S98 oligonucleotide arrays (YG_S98), containing 9335 probe sets which represent approximately 7000 genes and open reading frames from *S. cerevisiae* Genome database. Messenger RNA was amplified and hybridized onto GeneChip according to the protocols recommended by Affymetrix (Santa Clara, CA).

2.6. Normalization and Filtering

Microarray data were normalized using the software GeneSpring GX 7.1 (Silicon Genetics, http://www.chem.agilent.com/), by means of total intensity approach that make use of a *per chip* normalization to 50th percentile and a *per gene* normalization to median. Each probe set was averaged across biological replicates using the expression intensity to obtain the replicates-combined probe set intensity. Normalized data were then submitted to three consecutive filtering steps, so that only probes that passed the following three filters were retained: 1) Flag (presence call in at least one sample) ; 2) Standard Deviation value between 0 and 1 in at least 4 out of 6 conditions; 3) Probe sets with gene information associated. After this procedure, 5905 probe sets (representing 5503 unique genes) were retained and used for statistical analysis as described below.

2.7. Statistical Analysis and functional investigations

Two independent statistical analyses were applied on data filtered as above: Analysis of variance (ANOVA) that partitions the total variance into parts corresponding to various sources in the model and Principal Component Analysis (PCA) that transforms a number of possibly correlated variables into a smaller number of uncorrelated variables called principal components. The first principal component accounts for as much of the variability in the data as possible, and each succeeding component accounts for as much of the remaining variability as possible. Further details of analysis can be found in Supplementary Materials. Cluster analysis was applied to all genes selected by both PCA and ANOVA analysis. For hierarchical clustering, a Pearson correlation was used to compute similarities and cluster merging was performed using average linkage (as implemented in the GeneSpring software).

In order to identify key proteins involved in the cellular response to *FAR1* deletion and over-expression, we used functional categorization based on Munich Information Center for Protein Sequences (MIPS, http://mips.gsf.de/genre/proj/yeast). Further classification based on bio-molecular interaction networks used the *Report* software that makes use of three different interaction networks, i.e.,. metabolic network (Oliveira et al., 2008), regulators/Transcription Factors (TFs)-'regulated genes' network, and 'Gene Ontology' (GO)-'associated genes network' (Forster et al., 2003). The software for calculating such enrichment scores is freely available at http://www.cmb.dtu.dk/reporters.

Pathway identification was performed using GeneSpring software that provides statistical methods for discovering enriched biological themes within gene lists by overlapping probability; a p-value ≤ 0.05 was used as a cut-off.

The search was performed by using some categories identified in KEGG database (Aoki-Kinoshita and Kanehisa, 2007) and in particular for metabolism, genetic information, environmental information and cellular process pathway.

2.8. Mapping gene expression data on the yeast interactome

Proteins encoded by genes identified above were mapped to the yeast interactome. These proteins were then loaded into Gene-Spring GX 10 using the Yeast database. The protein-protein interaction (PPI) network was assessed using a variety of databases that include: published literature abstracts using a proprietary Natural Language Processing (NLP) algorithm, the experimentally reported physical interactions data was parsed from IntAct (www.ebi.ac.uk/intact), (http://www.ebi.ac.uk/intact) that includes data from other databases like BIND and MINT, and also interactions found in the SGD. The PPI network was then visualized using Cytoscape 2.6.3 software (Cline et al., 2007). Sub-networks were identified using the graph clustering algorithm, "Molecular Complex Detection" (MCODE) (Bader and Hogue, 2003) that detects densely connected regions in large protein-protein interaction networks that may represent molecular complexes.

3. **Results and Discussion**

3.1. Identification of the Far1 interaction network

Data reported in the introduction indicate that Far1 overexpression affects cell size. This observation suggests that Far1 may interact, directly or indirectly, with proteins involved in processes leading to increase in cell mass and cell division. We thus searched in databases for proteins interacting with Far1 either physically or genetically, indentifying a total of 99 proteins. Of these proteins, 95 proteins are color-coded according to their biological function in Figure 1. This Figure shows that Far1 interacts either physically or genetically with a relevant number of proteins involved in RNA transcription, processing and transport, protein synthesis, folding, transport and degradation as well as in metabolism, consistently with the notion that Far1 may have unrecognized role in these processes. Of these proteins, 28 have a direct physical interaction with Far1 (Figure 1A, straight lines), mutations within the genes encoding 31 proteins interact genetically with mutations in the FAR1 gene (Figure 1A, dotted lines) whereas the remaining 36 have been identified in 10 Far1-containing protein complexes. For the latter proteins, no Far1-connecting line is shown in Figure 1a since binary protein-protein interactions within the complex are unknown. The composition of the Far1-containing complexes is reported in Figure 1B. The list of the proteins, reference to the appropriate data-base, and the description of the proteins are reported in Table S1.

3.2. FAR1 overexpression coordinately upregulates cellular RNA and protein content

Results reported in 3.1. suggest that Far1 may affect both RNA and protein synthesis. We previously reported that *FAR1* overexpression increases cell size in exponentially growing cells, the effect being larger in ethanol-growing cells (Alberghina et al., 2004). Hence, unless otherwise stated, in all following experiments the effect of Far1 overexpression was tested on cells grown in both ethanol-and glucose-supplemented media. In order to evaluate if this increased cell size was accompanied by a coordinate increase in macromolecular (i.e. RNA and protein) biosyntheses, chemical determination of RNA and protein content was carried out in the W303 strain (Table 1). As reported in ethanol-grown cells, *FAR1* overexpression largely increases cell volume. Little, if any, effect in any of the above parameters can be observed in glucose-grown W303 cells. Chemical determination of RNA and protein content/cell indicate that protein and RNA increase coordinately, so that their ratio is not altered by the *FAR1* dosage, indicating that increased cells size results from a coupled increase in both RNA and protein syntheses.

3.3. Transcriptional response to FAR1 *dosage in glucose- and ethanol-supplemented media*

To clarify the cellular processes leading to the largely increased cell size in ethanol-grown $FAR1^{OE}$, a genome-scale transcriptional analysis of isogenic wild type, *far1Δ* and $FAR1^{OE}$ strains was performed on cells grown using either ethanol or glucose as a sole carbon source.

After applying the filtering procedure described in Methods, 5905 probes set (corresponding to 5503 unique genes) were retained. To identify differentially expressed genes, we performed ANOVA analysis (p-value ≤ 0.05), adjusted by applying Benjamini and Hochberg False Discovery Rate multiple testing correction, across conditions for each probe. Then, 265 genes with fold change ≥ 1.5 or ≤ -1.5 were selected and deemed as significantly changed.

Transcriptome analysis was extended using Principal Component Analysis on the same initial probe set list used for ANOVA analysis. When samples derived from glucose-grown and ethanol-grown cells were analyzed concurrently in the factorial plane obtained by PCA, the contribution of *FAR1* gene dosage to transcriptional remodelling was masked by the larger

contribution due to the change in carbon source. Data from glucose and ethanol-grown cells were thus analyzed separately. In both cases, the first two Principal Components (PC1 and PC2, respectively) explain a large fraction of variability in our data sets: over 90% for ethanol-grown cells and over 70% for glucose-grown cells. The PC1 axis of the plane does not distinguish wild type (blue diamonds) and *far1Δ* mutant cells (red squares), grown in media supplemented with either ethanol (Fig. 2A) or glucose (Fig. 2B). *far1Δ* mutants are better separated from wild type on the PC1-PC2 plane in glucose-grown cells. Samples from $FAR1^{OE}$ cells (green triangles) are readily distinguishable from wild type and *far1Δ* samples, the more so for RNA prepared from ethanol-grown cells. The more striking transcriptional effect brought about by Far1 overexpression in ethanol-grown cells is in keeping with the reported finding (Alberghina et al., 2004) that Far1 overexpression originates more distinctive phenotypic effects in cells grown in media supplemented with ethanol than in cells growing in media supplemented with glucose.

Genes mostly contributing to PC1 or PC2 (using a correlation cut-off of 0.85) were compared with genes identified on the basis of fold change selection in expression separately for ethanol and glucose-grown cells. The PCA analysis yielded 227 non-redundant genes non-present in the ANOVA analysis: 120 uniquely regulated by *FAR1* dosage in glucose-grown cells, 60 uniquely regulated by *FAR1* dosage in ethanol-grown cells and 47 whose regulation by *FAR1* dosage was observed regardless of the carbon source. The complete list of 487 differentially expressed genes (DEGs) obtained by the union of genes identified through ANOVA and PCA is reported in Table S2, lines 2-488.Unsupervisioned hierarchical clustering shows that a large group of genes, delimited by a blue box, show complementary behaviour in cells prepared from glucose and ethanol media (Fig. 2C and the complete list is highlighted in blue on Table S2). The same list has been used in subsequent analyses, except for mapping on protein-protein interaction network, where the fold-change filtration step was omitted (Table S2, lines 2-789).

The list of 4887 DEGs was used to search for enriched functional categories as defined by the MIPS database (http://mips.gsf.de/genre/proj/yeast/) that provides a global view of the transcriptional response (Fig. 3A and Table S3).

The most represented functional category was metabolism with 173 genes, despite the fact our approach filtered out genes whose change in expression was only dependent on the carbon source, which is known to have a large effect on metabolism. Two other categories were also significantly enriched in MIPS classification: cell rescue, defense and virulence, and interaction with environment.

We further investigated whether there are GO term and Transcriptional Factor network that responded more significantly than the rest using the integrative Reporter tool developed by J. Nielsen's group (Cimini et al., 2009). The Reporter's algorithm has been reported to be able to identify weak but biologically significant changes and hence to highlight the key biological processes/functions/cellular components that collectively respond significantly to the applied perturbation (for the complete list of reporter GOs, see additional File 2 in Cimini et al., 2009). Reporter-GO terms, with a reporter p-value ≤ 0.05 for strains with altered *FAR1* dosage are shown in Fig. 3B**.** The complete list, without p-value filter, is reported in Table S3). The identified group with the largest number of genes was nucleus, indicating that many genes encoding proteins with nuclear location respond to changes in *FAR1* dosage. Another important GO term was related to metabolism. Moreover, the analysis using the KEGG database (Fig. 3C and Table S3) also confirmed that genes encoding metabolic proteins were among the most affected by *FAR1* dosage.

Using Reporter Regulators, we could identify the most representative elements that regulate the expression of genes, in the different conditions. Transcriptional factors collected by Reporter algorithm are shown in Fig. 3D and Table S3 (for the complete list of reporter TFs see additional file 2 in Cimini et al., 2009). Reporter TFs highlight the regulatory pathways affected following a perturbation, and thus uncover the functional links between the perturbation and the regulatory mechanisms invoked in the cell. The most marked reporter-

TFs emerging from this analysis are Ste12 (12 associated genes), Gln3 (8 associated genes), Dal80 (6 associated genes), Swi6 (5 associated genes) and Fks1 (5 associated genes).
Ste12 activates genes involved in mating or pseudohyphal/invasive growth pathways and cooperates with Tec1 transcription factor to regulate genes specific for invasive growth. Notably, two of the genes selected with analysis of GO term, *FAR1* and *FUS3*, are regulated at the transcriptional level by Ste12. Gln3 and Dal80 are involved in the nitrogen pathway. Gnl3 is a transcriptional activator of genes regulated by nitrogen catabolite repression (NCR), whose localization and activity is regulated by the type of nitrogen source, while Dal80 is a negative regulator of genes in multiple nitrogen degradation pathways and whose expression is regulated by nitrogen levels and by Gln3. *SWI6* encodes a transcription cofactor that forms complexes with the DNA-binding proteins Swi4 and Mbp1 to regulate transcription of genes involved in the G1/S transition. *FKS1* encodes the catalytic subunit of 1,3-beta-D-glucan synthase (functionally redundant with the alternate catalytic subunit Gsc) and moreover it binds to regulatory subunit Rho1, that is involved in cell wall synthesis and maintenance and localizes to sites of cell wall remodeling.
Taken together, the findings reported above indicate that Far1 overexpression has a pleiotropic effect on transcriptional regulation.

3.4. Mapping gene expression data on the yeast interactome

Starting from the complete list of 788 selected genes, we constructed an interaction graph where nodes represent proteins encoded by genes and the edges correspond to potential protein-protein interactions (PPIs) extracted from GeneSpring database, which was built integrating different sources (see Methods). From the originated network (genes are listed in Table S4) that includes 559 proteins and 1309 PPIs, we extracted densely interconnected neighborhoods (or clusters) that correspond to functional modules, using the MCODE algorithm (Bader and Hogue, 2003) hosted as a plug-in within Cytoscape.(http://www.cytoscape.org/) This analysis identified 5 sub-network with a score value ≥ 1 (Fig. 4A). Sub-network **1** (13 nodes, 19 PPIs) is enriched in proteasome components (Rpn9, Rpn10 and Rpt6), and proteins involved in nucleosome formation and remodelling (Hta1, Htb2, Htz1, Nap1 and Spt16, subunit of the FACT complex). Sub-network **2** (41 nodes, 70 PPIs) contains Far1 and includes two important cyclins (Cln2 and Clb2), proteasome components or associated proteins (Pre7, Cic1, Pre4), proteins involved in ribosome biogenesis (Tif6, Dbp6, Nop15, Ssb2, Utp15), sub-units or interactors of RNA polymerase II subunits (Srb2, Rpo21, Med7, Sua7). Sub-network **3** (7 nodes, 9 PPIs) includes Srb6, a a subunit of the RNA pol II mediator complex, Rcs56 a component of chromatin remodelling complex, as well as Hta2 and Med7 described above. Sub-network **4** (11 nodes, 13 PPIs) includes the Swi5 and Snf5 subunits of the Swi/Snf cromatin remodelling complex and Gic1/2 involved in budding initiation. Sub-network **5** (6 nodes, 7 PPIs) includes Nrg1,2 transcriptional repressors mediating glucose repression and negatively regulating filamentous growth and Snz2,3, members of a stationary phase induced family. Fig. 4B is a graphical representation of the fold change behaviour of *far1Δ vs* wild type or $FAR1^{OE}$ *vs* wild type comparison pair in ethanol and glucose as carbon source.

3.5. Effect of FAR1 *gene dosage on pathways controlling ribosome biogenesis and metabolism*

In the budding yeast *Saccharomyces cerevisiae*, the TOR (Target of Rapamycin) and the Ras/cAMP-PKA signaling cascades respond to nutrients and coordinately regulate the expression of genes required for cell growth, including ribosomal protein genes, and affect cell size (Busti et al., 2010; Zaman et al., 2008). The Tor, Ras/cAMP-PKA and glucose-sensing pathways are outlined in Fig. 5A and B, where proteins encoded by genes differentially expressed in the $FAR1^{OE}$ strain are shaded in grey. These include *GPR1*,

encoding a glucose receptor whose deletion has been reported to decrease cell size at the beginning of S phase (Ps) (Alberghina et al., 2004; Tamaki et al., 2005), *ASC1*, encoding a substitute Gβ subunit for the Gα protein Gpa2 which regulates glucose signaling (Zeller et al., 2007), *TPK1*, encoding one of the three catalytic subunit of PKA (Toda et al., 1987), *TFS1* (Robinson and Tatchell, 1991) originally identified as a multicopy suppressor of a mutation in *CDC25*, a gene encoding an upstream activator of the Ras/PKA pathway (Jones et al., 1991), *YAK1* encoding a protein kinase that has been proposed to act as bridge between PKA and the Msn2/4 transcription factors (Lee et al., 2008), *RIM15* encoding a protein kinase whose activity is regulated by the interplay of at least four intercepting nutrient-responsive pathways, including the PKA and TOR pathway (reviewed in (Swinnen et al., 2006)) and the small heat shock protein-encoding genes *HSP12* and *HSP26*.

Expression of both *TOR1* and *TOR2* was marginally affected by *FAR1* dosage. Tor1, part of the TORC1 complex, is more directly involved in nutritional control of ribosome biogenesis by binding the 35S rDNA open transcription complex. Other components of the complex affected by the *FAR1* dosage are Rpa190 (a Pol I subunit) and Hmo1, the latter a component also of complexes affecting transcription of RP genes, as is Sfp1, a major factor controlling ribosome biogenesis and cell size. Expression of *MEP1* and *GLN3*, encoding an ammonium permease and trascription factor, respectively, involved in nitrogen catabolite repression and that contribute to rely nitrogen sensing to the TOR pathway was also affected by the *FAR1* dosage. Notably, Gln3 was identified in TF-reporter analysis (see above). In $FAR1^{OE}$ cells exponentially growing in glucose, we observed transcriptional regulation of many genes encoding enzymes involved in two pathways that are normally induced by rapamycin, - *i.e.,* repressed by TOR - namely the Oxydative Phosphorylation and Nitrogen Discrimination pathway (Table 2).

Strikingly, *FAR1* gene dosage seems to affect expression of genes involved in the main pathway of carbohydrate metabolism too: in fact, the $FAR1^{OE}$ mutant showed transcriptional down-regulation of many glycolysis/gluconeogenesis genes when grown in ethanol-supplemented media (Fig. S1A) and, conversely, transcriptional up-regulation of several TCA cycle/oxydative phosphorylation genes and of phosphoenolpyruvate to acetyl-CoA pathway genes when grown in glucose-supplemented media (Fig. S1B).

3.6. Phenotyopic validation of transcriptional data

To evaluate the physiological significance of alterations in expression of genes encoding protein involved in the PKA pathway, several PKA-dependent phenotypes, namely resistance to heat shock, oxidative, ionic and osmotic stress, were tested on both glucose and ethanol-grown cells. None of the stress-related parameters was significantly affected in glucose-grown cell overexpressing *FAR1*. On the contrary, ethanol-grown *FAR1*-overexpressing cells display a significant increase in oxidative stress resistance (Fig. 6A and 6B) that is accompanied by a small increase in cellular glutathione content (Fig. 6C). The ratio between reduced and oxidized glutathione was unaffected by *FAR1* overexpression under basal condition, but was significantly increased in ethanol-grown (but not glucose-grown) *FAR1*-overexpressing strain treated for 1h with sub-lethal doses of H_2O_2 (1mM for glucose grown-cells and 10mM for ethanol grown cells) before the analysis (Fig. 6D). A statistically significant induction of the *HSP12*::*GUS* reporter gene, whose expression is often used as read-out of PKA pathway activation (Amoros and Estruch, 2001; Ferguson et al., 2005; Varela et al., 1995), was also observed in ethanol-grown (95% confidence) and glucose-grown (90% confidence) cells (Fig. 6E). These results indicate that *FAR1* overexpression increases resistance to oxidative stress through a pathway that is at least partially dependent on the PKA pathway.

Under nutrient shortage (*i.e.*, nitrogen starvation in diploids and glucose shortage in haploids), *S. cerevisiae* can undergo a dimorphic switch known as pseudohyphal growth in diploids and invasive growth in haploids, which alters the cell morphology and generates chains of elongated cells that invade the growth substrate (Gimeno et al., 1992; Jin et al., 2008; Palecek et al., 2002; Roberts and Fink, 1994). Nrg1, a zinc finger protein that fine-tunes the regulation

of various glucose and stress-responsive genes (Lamb and Mitchell, 2003; Park et al., 1999; Vyas et al., 2005; Vyas et al., 2001; Zhou and Winston, 2001) and negatively regulates expression of *FLO11* - which encodes a cell surface glycoprotein required for filamentous growth (Kuchin et al., 2002) and biofilm formation (Zara et al., 2009) - is strongly up-regulated in *FAR1* overexpressing strains regardless of the carbon source (Fig. 5, Table S2). Furthermore, our analysis revealed that the transcriptional patterns of *TEC1* (encoding a transcription factor required for filamentous growth (Madhani and Fink, 1997)) and *FUS3* (encoding a MAPK involved in mating, which inhibits invasive growth during the mating process by phosphorylating Tec1, thus promoting its degradation (Chou et al., 2008)) are altered in the *FAR1* overespressing strain (Table S2). Results reported in Figure 6F indicate that *FAR1* overespression attenuates both pseudohyphae formation in diploids and agar invasion in haploid cells. Since the dimorphic transition is regulated by a complex interplay of several signaling pathways, including cAMP-PKA, MAPK, Snf1 and TOR which converge to transcriptionally regulate *FLO11* (Palecek et al., 2002; Vinod et al., 2008) but that individually also affect other targets involved in the process (Palecek et al., 2002; Vinod and Venkatesh, 2007), understanding of the molecular mechanisms underlying the cross-talk between Far1 and the dimorphic transition will require further investigations that go beyond the scope of this paper.

Finally, since our transcriptional analysis identified both Fks1 (Table S3) and Gsc2 (Table S2) (encoding alternative catalytic subunits of the glucan synthase complex, which synthesizes the major structural polymer of the yeast cell wall) as important elements in the cellular response to an increased *FAR1* dosage, we checked whether *FAR1* overespression could alter the cell wall structure by evaluating the cell sensitivity to zymolase treatment. As shown in Fig. 6G, *FAR1* overespressing cells exhibited a significantly decreased sensitivity to zymolase digestion when grown in ethanol medium, thus suggesting the existence of alterations in cell wall under this growth condition.

Since *FAR1* gene dosage affects expression of genes involved in the main pathway of carbohydrate metabolism (see 3.5), we investigated whether the wild type and $FAR1^{OE}$ strain presented differential utilization of carbon source by assaying glucose consumption and ethanol production (in glucose-supplemented media, Fig. 7A) or ethanol utilization (in ethanol-supplemented media, Fig. 7B). No difference in the assayed parameters was detected in either growth condition. This observation does not rule out that minor rearranging of energy and sugar-related metabolism are taking place in *FAR1*-overepressing cells. Indeed, a statistically significant (95% confidence) increase in invertase activity was observed in ethanol-grown cells (whose levels are routinely used as a reporter for glucose repression and derepression). Invertase activity was also reproducibly higher in cells growing in 2% glucose, although difference with wild type was significant only at 90% confidence (Fig. **7C**)

.

3.7. FAR1 overexpression fails to upregulate cellular RNA in the absence of the Sfp1 protein but not of the Sch9 protein

Data presented above indicate that the increase in cell size observed in ethanol-grown $FAR1^{OE}$ cells is accompanied by increase in RNA and protein content and that elements of PKA and Tor pathway - that play a major role in controlling cell size and ribosome biogenesis - are affected by *FAR1* overexpression. Two parallel pathways downstream from the TORC1 complex regulate expression of genes encoding ribosomal proteins (RP) and the so-called RiBi regulon, composed by genes involved in ribosome biogenesis. The two pathways involve Sfp1, a split zinc-finger protein that emerged recently as a key transcriptional regulator of ribosome biogenesis and plays a key role in nutritional and stress-dependent control of cell growth by affecting expression of both the RP and RiBi regulons (Jorgensen et al., 2002; Jorgensen et al., 2004; Lempiainen and Shore, 2009; Lempiainen et al., 2009) and Sch9, a kinase sharing several properties with mammalian S6K1 kinase (Lempiainen and Shore, 2009; Urban et al., 2007). Therefore it was of interest to see whether the increase in

size (RNA and protein) brought about by *FAR1* overexpression was mediated by Sfp1 and Sch9.

The effect of *FAR1* overexpression on cell size parameters in the wild type BY4741 strain (isogenic to the *sch9Δ* and *sfp1Δ* mutants), grown in synthetic complete media supplemented with either ethanol or glucose as a carbon source, was similar to that reported in the W303 background (compare Table 1 and Table 3). *sfp1Δ* and *sch9Δ* mutants were much smaller than wild type both in glucose - confirming previous data (Jorgensen et al., 2002; Jorgensen et al., 2004) - and ethanol-supplemented media.

As observed in wild type cells, in both mutant strains *FAR1* overexpression had only minor effects on cell cycle and cell size related parameters on glucose-grown cells. *FAR1* overexpression did not affect duplication time in ethanol-grown *sch9Δ* cells, while *sfp1Δ* mutants overexpressing the *FAR1* gene product were quite unhealthy with a large increase in duplication time. Overall increase in cell size was dramatic in ethanol-grown cells: however, while in wild type cells and *sch9Δ* mutants the increase in cell size derived from a balanced increase in RNA and protein content, in the *sfp1Δ* mutant the increase in protein content was not accompanied by an increase in RNA content, as shown by both FACS and chemical analysis (Table 3 and Fig. 8, note that FACS settings for *sch9Δ* and *sfp1Δ* mutants are different, *sfp1Δ* cells being actually smaller than *sch9Δ* cells), indicating that the Sfp1 is required to maintain proper coupling of RNA and protein syntheses when the Far1 protein is overexpressed in ethanolo-grown-cells. The observation that *FAR1* overexpression has different effects in *sfp1Δ* cells grown in ethanol and glucose media was not entirely unexpected. First, in untrasformed cells, the Far1 level of glucose-grown cells is larger that in ethanol-grown cells, while ectopically expressed Far1 accumulates to a similar level regardless of the carbon source: as a result, Far1 overexpression is more dramatic in ethanol-grown cells than in glucose-grown cells (Alberghina et al., 2004). Accordingly, the effect of Far1 overexpression on cell size are minor on cells grown in glucose-supplemented media and much more dramatic in ethanol-grown cells. Moreover, nutrients differentially affect the role of Sfp1 in cell size modulation and in transcriptional control. In batch cultures, the role of Sfp1 in sustaining the increase of both rRNA and protein content appears to be modulated by carbon source and/or metabolism (Cipollina et al., 2005). While Sfp1 is necessary for efficient glucose-dependent regulation of ribosome biogenesis genes, it is not required for the proper induction of ribosomal protein genes in response to glucose excess. Sfp1 may also be involved in the regulation of glycolysis, further underlining its involvement in the network that links ribosome biogenesis and cell metabolism (Cipollina et al., 2008a). During glucose-limited growth, major differences in genome-wide transcriptional profiles of *sfp1Δ* were observed compared to growth at the same dilution rate in ethanol-grown chemostat. Sfp1 appeared to be involved in the control of ribosome biogenesis but not of ribosomal protein gene expression, while size defects were present under both growth conditions, suggesting that Sfp1 plays a role in transcriptional and cell size control, operating at two different levels of the regulatory network linking growth, metabolism and cell size (Cipollina et al., 2008b).

4. Conclusions

Proliferating somatic cells are continuously increasing in their mass throughout the cell cycle. As pointed out as early as 1971 by Mitchinson (Mitchison, 1971), the "continuous events of the growth cycle" (*i.e.*, increase in cell mass) and the "discontinuous events of the DNA division cycle" (i.e., DNA replication, mitosis, and cell division) need to be tightly coordinated in order to maintain cell size homeostasis. Hence, according to this view, the growth cycle controls the DNA division cycle that is staret when a cell has reached a critical cell size. In *Saccharomyces cerevisiae*, coordination between growth and cell division takes place primarily at Start, a regulatory area in G1 phase and requires that a yeast cell reaches a critical size before entering into S phase. The critical size at which cell initiates a new round of mitotic division is regulated by the nutrient status, in particular by the available carbon source, cells growing on glucose being larger than cells growing on ethanol (Johnston, 1977; Johnston et al., 1979; Lorincz and Carter, 1979; Tyson et al., 1979).

Recently, through systematic overexpresion, Kitano and coworkers showed that overexpression of cell cycle proteins may become toxic, first slowing down and eventually stopping completely cell proliferation (Moriya et al., 2006). Similarly, we could show that overexpression of Far1, that is involved in the nutritionally modulated cell sizer plus timer mechanism that sets the entrance into S phase in *S. cerevisiae* (Alberghina et al., 2009; Barberis et al., 2007) results in increased cell size (Alberghina et al., 2004).

Here we show that the larger size of *FAR1*-overexpressing cells results from coordinated increased accumulation of both RNA and protein. Regulation of cell growth, or increase in cell mass, requires extensive coordination of several processes including transcription, ribosome biogenesis, translation, and nutrient metabolism. Being energetically highly demanding, these process are strictly regulated. In *S. cerevisiae*, the TOR and PKA pathways are the main regulators connecting the above processes with the nutritional status of the cell. By genome-wide transcriptional analysis of *FAR1*-overexpressing and *far1Δ* cells grown in ethanol- or glucose-supplemented minimal media with a range of phenotypic analysis, we show that Far1 overexpression originates large transcriptional remodelling that affects pathways involved in controlling cell growth, including sugar sensing (that is know to affect the cell growth rate (articolo Nature 2009) and the PKA and TOR pathways that are the major pathways involved in regulating cell growth in yeast.

In *S. cerevisiae*, Sch9 and Sfp1 are two main downstram targets of the Tor pathway involved in controlling cell growth through regulation of the protein synthesis machinery (reviewed in Lempainen and Shore, 2009). Sfp1 is a key transcriptional regulator of ribosome biogenesis (Jorgensen and Tyers, 2004; Lempiainen and Shore, 2009)). It binds directly to a subset of promoters of genes encoding ribosomal proteins (Fingerman et al., 2003; Jorgensen et al., 2002; Jorgensen et al., 2004; Lempiainen et al., 2009; Marion et al., 2004), as well as activating a large set of genes involved in ribosome biogenesis (Ribi genes; (Cipollina et al., 2008a; Jorgensen et al., 2002; Jorgensen et al., 2004; Marion et al., 2004). Sfp1 interacts directly with - and is phosphorylated by – the Tor1-containing TORC1 complex (Lempiainen et al., 2009).

Sch9 is a protein kinase that shares several properties with the S6K1 kinase in mammals (Urban et al., 2007). A feedback mechanism controlling the activity of these proteins - likely acting as a homeostatic buffer to regulate the intricate balance of ribosome factor transcription - is operative, since Sfp1, negatively regulates TORC1 phosphorylation of Sch9.

The coordination between RNA and protein syntheses brought about by Far1 overexpression is conserved in the *sch9Δ* mutant, but is relaxed in cells lacking the *SFP1* gene. This is in keeping with the recent proposal that Sch9 is involved in optimal regulation of ribosome biogenesis by the TORC1 complex, but is dispensable for the essential aspects of ribosome biogenesis and cell growth (Wei and Zheng, 2009). Since in ethanol-grown *sfp1Δ*[pFAR1^{OE}] cells an increase in protein - but not RNA - level is observed, the increased protein level is likely due to improved usage of existing ribosomes, that are known to be in excess in ethanol-growing yeast (Waldron et al., 1977), without extensive *de no*vo synthesis of ribosomes.

It has been proposed that Sfp1 is a putative yeast functional analog of c-Myc (Jorgensen et al., 2004), a ubiquitous transcription factor from multicellular eukaryotes, which has been implicated in regulatory mechanisms coordinating all three RNA polymerases, since not only it is as a direct activator of RP and translation-related genes (RNA Polymerase II targets) but also as an activator of RNA Polymerase I and RNA Polymerase III (reviewed in (Eilers and Eisenman, 2008; Gomez-Roman et al., 2006)). Significantly, c-Myc, Sfp1, S6K1, and Sch9 all have dramatic effects on cell size regulation (Jorgensen et al., 2002; Jorgensen et al., 2004), which likely results from their role in coupling cell growth and cell division. Different studies in yeast showed that some aspect of ribosome biogenesis influences the cell-cycle commitment step (START) through Whi5, an Rb-like protein (Bernstein et al., 2007). When ribosome biogenesis is blocked (but before ribosome levels are actually altered) a Whi5-dependent mechanism inhibits START.

In summary, our results suggest that the molecular mechanism that couples cell growth and cell cycle (i.e. the Far1/Cln3 sizer) contributes to regulate cell cell growth either directly or indirectly by affecting nutrient sensing and/or utilization, protein synthesis and pathways known to modulate ribosome biogenesis. A crucial role in mediating the effect of Far1 is played by the Sfp1 protein, whose presence is mandatory to allow coordinated increase in both RNA and protein in ethanol-grown cells.

Legends of Figures

Fig. 1 The Far1 interaction network.

(A) Proteins interacting with Far1 by direct physical interaction (solid lines), genetic interactions (dotted lines) or that are present within Far1-containing complexes (no Far1-connecting lines) are shown. Nodes are color-coded according to function. Four proteins (MLF3, UBX6, DMA2 and YHR033W) are omitted since they are of unknown function or their functional group has no known direct interaction with FAR1. (B) Far1-containing protein complexes are depicted. Two further complexes have been found, but they are not represented in the picture since they are two subsets of the complexes **2** and **8** respectively. Complex **8** also contains the protein encoded by ORF YHR033W. It has been omitted since its function is unknown. Genetic and direct physical connections were obtained from the *Saccharomyces* Genome Database (http://www.yeastgenome.org/), complex composition from the Database of Interacting Proteins (http://dip.doe-mbi.ucla.edu/).

Fig. 2 Overall transcriptional effect induced by the *FAR1* dosage

Principal Component Analysis (PCA) performed with data from ethanol- (A) and glucose (B) grown cells individually. The two axes indicate Principal Component 1 (PC1) and Principal Component 2 (PC2). Each symbol represents a replicate experiment. (C) Global heat map of the 487 genes mostly contributing to differential gene expression in our experimental set-up. Clusters have been ordered based on Pearson correlation. Each column is a replicate-averaged microarray experiment. In the heat map, red indicates high and green indicates low expression values.

Fig. 3 Pathways and ontologies affected by *FAR1* dosage.
Pie charts summarize statistically significant results (p-value ≤ 0.05) obtained by analysis of transcriptomics data with different tools: MIPS (A), GO terms (B), KEGG (C), and transcription factor, regulator (D). The complete analytical results, without p-value filtering are reported in Table S3.

Fig. 4 Mapping of gene expression data on the yeast interactome
(A) After mapping of gene expression data on the yeast interactome, a network containing 559 proteins and 1309 PPIs was obtained. Sub-networks were extracted through the MCODE algorithm. (B) The four panels represent pair-wise comparisons (*far1Δ vs* wild type and $FAR1^{OE}$ *vs wild type* in cells grown in media supplemented with ethanol (left) and glucose (right)) showing differences in gene expression color-coded as indicated in the legend.

Fig. 5 *FAR1* overexpression alters transcription of several genes encoding proteins involved in nutrient sensing pathways.
A simplified view of several nutrient sensing pathways in yeast (modified from Busti et al., 2010). Elements whose transcription is affected by *FAR1* overespression during growth in either ethanol or glucose (or both) are shaded in grey. Colored squares provide a graphical comparison between the wild type and either the *far1Δ* (left squares) or the *FAR1* overespressing strains (right squares). The fold change values in each pair-wise combination are color-coded as indicated in the legend.

Fig. 6 *FAR1* overespression enhances oxidative stress resistance during growth on ethanol medium and the expression of a STRE-driven reporter gene.
(A) Stress resistance of the wild type and *FAR1* overespressing strains. Aliquots ($2*10^8$) of growing cells were exposed to the indicated stress conditions. Cells were then serially diluted and spotted on YPD plates. Photographs were taken after 48h incubation at 30°C. (B) Oxidative stress resistance of the wild type and *FAR1*-overespressing strains. Cells were treated with 2mM (glucose cultures) or 100mM hydrogen peroxide (ethanol cultures). At the indicated time points, samples were taken to evaluate the cellular viability of the cultures. (C) Glutathione content in wild type and *FAR1* overespressing strains. Glutathione level was measured in cells growing in either glucose or ethanol. (D) Reduced/oxidized glutathione ratio (GSH/GSSG) in wild type and *FAR1* overespressing strains. Where indicated, cells were treated for 1h with sub-lethal doses of H_2O_2 (1mM for glucose grown-cells and 10mM for

ethanol grown cells) before the analysis. (E) The activity of the *GUS* reporter under the control of the stress-responsive *HSP12* promoter was evaluated in wild type (grey bars) and *FAR1*-overespressing (white bars) cells during growth on either glucose or ethanol. Values reported are means ± standard errors of three independent experiments. The asterisk indicates that the differences between the wild type and the *FAR1*-overespressing strains are statistically significant ($p \leq 0.05$ for ethanol and $p \leq 0.1$ for glucose, respectively). (F) Effects of *FAR1* overespression on invasivity and pseudohyphal growth. Left panel: invasive growth of the Neph8 haploid strain. Cells were spotted on YPD plates and incubated for 5 days at 30°C (upper image). Following incubation the plate was gently washed with water and immediately photographed again (bottom image): only cells which had invaded the agar remained on plate after the wash. Right panel: pseudohyphal growth of the Nephtlys886 diploid strain. Representative microcolonies grown on SLAD plates were photographed after 5 days at 30°C. (G) Zymolyase sensitivity of the wild type and *FAR1*-overespressing strains. Aliquots ($1*10^8$) of growing cells were resuspended in zymolyase digestion buffer. At the indicated time points, samples were diluted in distilled water and the turbidity of the cellular suspension was measured at 600 nm. Values reported are relative to the value measured at time 0.

Fig. 7 *FAR1* overexpression releases control of invertase expression

(A) Glucose consumption and ethanol production in wild type and *FAR1* overespressing cells. Cells were grown overnight in 2% glucose, harvested and resuspended in fresh medium containing 50mM glucose at a final cellular density of about $4*10^6$cells/mL. At the indicated time points samples were collected to evaluate the glucose (squares) and the ethanol (triangles) levels in the medium. The experiment was repeated twice with identical results. (B) Ethanol consumption in wild type and *FAR1* overespressing cells. Cells were grown overnight in 2% ethanol and resuspended in fresh 1% ethanol medium at a final cellular density of about $5*10^6$cells/mL. At the indicated time points samples were taken to evaluate the cellular density of the cultures (squares) and the residual ethanol content (triangles) in the medium. Data reported are representative of two independent experiments. (C) Invertase activity in the wild type and *FAR1* overespressing strains. Cells were grown overnight in 2% ethanol supplemented medium, harvested and resuspended either in the same ethanol medium or in media containing the indicated amount of glucose. After an incubation of 5 hours at 30°C, invertase activity was determined using whole cells as described in Materials and Methods. Data reported are means ± standard errors of two independent experiments. The asterisk indicates that the difference in invertase activity between the wild type (grey bars) and *FAR1* overespressing (white bars) strains is statistically significative ($p \leq 0.05$ during growth in ethanol, ($p \leq 0.1$ for growth in glucose).

Fig. 8 *FAR1* overexpression fails to upregulate the cellular RNA content in the absence of Sfp1 but not of Sch9.

Protein and RNA total contents (as determined by cytofluorimetric analysis) for wild type (left panel) *sch9Δ* (center panel) and *sch9Δ* (right panel) strains cultivated in either ethanol (upper panels) or glucose (lower panels). Protein and RNA scale for the different strains are not directly comparable, since they have been chosen in order to allow differences between mock-transformed and Far1-oberexprrssing strains to be better appreciated.

References

Alberghina FA, Sturani E, Gohlke JR. Levels and rates of synthesis of ribosomal ribonucleic acid, transfer ribonucleic acid, and protein in Neurospora crassa in different steady states of growth. J Biol Chem. 1975;250:4381-8.

Alberghina L, Coccetti P, Orlandi I. Systems biology of the cell cycle of Saccharomyces cerevisiae: From network mining to system-level properties. Biotechnol Adv. 2009;27:960-78.

Alberghina L, Rossi RL, Querin L, Wanke V, Vanoni M. A cell sizer network involving Cln3 and Far1 controls entrance into S phase in the mitotic cycle of budding yeast. J Cell Biol. 2004;167:433-43.

Amoros M, Estruch F. Hsf1p and Msn2/4p cooperate in the expression of Saccharomyces cerevisiae genes HSP26 and HSP104 in a gene- and stress type-dependent manner. Mol Microbiol. 2001;39:1523-32.

Aoki-Kinoshita KF, Kanehisa M. Gene annotation and pathway mapping in KEGG. Methods Mol Biol. 2007;396:71-91.

Bader GD, Hogue CW. An automated method for finding molecular complexes in large protein interaction networks. BMC Bioinformatics. 2003;4:2.

Barberis M, Klipp E, Vanoni M, Alberghina L. Cell size at S phase initiation: an emergent property of the G1/S network. PLoS Comput Biol. 2007;3:e64.

Bardwell L. A walk-through of the yeast mating pheromone response pathway. Peptides. 2005;26:339-50.

Bernstein KA, Bleichert F, Bean JM, Cross FR, Baserga SJ. Ribosome biogenesis is sensed at the Start cell cycle checkpoint. Mol Biol Cell. 2007;18:953-64.

Blondel M, Galan JM, Chi Y, Lafourcade C, Longaretti C, Deshaies RJ, et al. Nuclear-specific degradation of Far1 is controlled by the localization of the F-box protein Cdc4. EMBO J. 2000;19:6085-97.

Breitkreutz A, Boucher L, Tyers M. MAPK specificity in the yeast pheromone response independent of transcriptional activation. Curr Biol. 2001;11:1266-71.

Busti S, Coccetti P, Alberghina L, Vanoni M. Glucose Signaling-Mediated Coordination of Cell Growth and Cell Cycle in Saccharomyces Cerevisiae. Sensors. 2010;10:6195-240.

Butty AC, Pryciak PM, Huang LS, Herskowitz I, Peter M. The role of Far1p in linking the heterotrimeric G protein to polarity establishment proteins during yeast mating. Science. 1998;282:1511-6.

Chang F, Herskowitz I. Identification of a gene necessary for cell cycle arrest by a negative growth factor of yeast: FAR1 is an inhibitor of a G1 cyclin, CLN2. Cell. 1990;63:999-1011.

Chang F, Herskowitz I. Phosphorylation of FAR1 in response to alpha-factor: a possible requirement for cell-cycle arrest. Mol Biol Cell. 1992;3:445-50.

Chou S, Zhao S, Song Y, Liu H, Nie Q. Fus3-triggered Tec1 degradation modulates mating transcriptional output during the pheromone response. Mol Syst Biol. 2008;4:212.

Cimini D, Patil KR, Schiraldi C, Nielsen J. Global transcriptional response of Saccharomyces cerevisiae to the deletion of SDH3. BMC Syst Biol. 2009;3:17.

Cipollina C, Alberghina L, Porro D, Vai M. SFP1 is involved in cell size modulation in respiro-fermentative growth conditions. Yeast. 2005;22:385-99.

Cipollina C, van den Brink J, Daran-Lapujade P, Pronk JT, Porro D, de Winde JH. Saccharomyces cerevisiae SFP1: at the crossroads of central metabolism and ribosome biogenesis. Microbiology. 2008a;154:1686-99.

Cipollina C, van den Brink J, Daran-Lapujade P, Pronk JT, Vai M, de Winde JH. Revisiting the role of yeast Sfp1 in ribosome biogenesis and cell size control: a chemostat study. Microbiology. 2008b;154:337-46.

Cline MS, Smoot M, Cerami E, Kuchinsky A, Landys N, Workman C, et al. Integration of biological networks and gene expression data using Cytoscape. Nat Protoc. 2007;2:2366-82.

Coccetti P, Rossi RL, Sternieri F, Porro D, Russo GL, di Fonzo A, et al. Mutations of the CK2 phosphorylation site of Sic1 affect cell size and S-Cdk kinase activity in Saccharomyces cerevisiae. Mol Microbiol. 2004;51:447-60.

Di Talia S, Skotheim JM, Bean JM, Siggia ED, Cross FR. The effects of molecular noise and size control on variability in the budding yeast cell cycle. Nature. 2007;448:947-51.
Eilers M, Eisenman RN. Myc's broad reach. Genes Dev. 2008;22:2755-66.
Ferguson SB, Anderson ES, Harshaw RB, Thate T, Craig NL, Nelson HC. Protein kinase A regulates constitutive expression of small heat-shock genes in an Msn2/4p-independent and Hsf1p-dependent manner in Saccharomyces cerevisiae. Genetics. 2005;169:1203-14.
Fingerman I, Nagaraj V, Norris D, Vershon AK. Sfp1 plays a key role in yeast ribosome biogenesis. Eukaryot Cell. 2003;2:1061-8.
Forster J, Famili I, Fu P, Palsson BO, Nielsen J. Genome-scale reconstruction of the Saccharomyces cerevisiae metabolic network. Genome Res. 2003;13:244-53.
Fu X, Ng C, Feng D, Liang C. Cdc48p is required for the cell cycle commitment point at Start via degradation of the G1-CDK inhibitor Far1p. J Cell Biol. 2003;163:21-6.
Gartner A, Jovanovic A, Jeoung DI, Bourlat S, Cross FR, Ammerer G. Pheromone-dependent G1 cell cycle arrest requires Far1 phosphorylation, but may not involve inhibition of Cdc28-Cln2 kinase, in vivo. Mol Cell Biol. 1998;18:3681-91.
Gimeno CJ, Ljungdahl PO, Styles CA, Fink GR. Unipolar cell divisions in the yeast S. cerevisiae lead to filamentous growth: regulation by starvation and RAS. Cell. 1992;68:1077-90.
Gomez-Roman N, Felton-Edkins ZA, Kenneth NS, Goodfellow SJ, Athineos D, Zhang J, et al. Activation by c-Myc of transcription by RNA polymerases I, II and III. Biochem Soc Symp. 2006:141-54.
Grant CM, Perrone G, Dawes IW. Glutathione and catalase provide overlapping defenses for protection against hydrogen peroxide in the yeast Saccharomyces cerevisiae. Biochem Biophys Res Commun. 1998;253:893-8.
Hall DD, Markwardt DD, Parviz F, Heideman W. Regulation of the Cln3-Cdc28 kinase by cAMP in Saccharomyces cerevisiae. EMBO J. 1998;17:4370-8.
Henchoz S, Chi Y, Catarin B, Herskowitz I, Deshaies RJ, Peter M. Phosphorylation- and ubiquitin-dependent degradation of the cyclin-dependent kinase inhibitor Far1p in budding yeast. Genes Dev. 1997;11:3046-60.
Jeoung DI, Oehlen LJ, Cross FR. Cln3-associated kinase activity in Saccharomyces cerevisiae is regulated by the mating factor pathway. Mol Cell Biol. 1998;18:433-41.
Jin R, Dobry CJ, McCown PJ, Kumar A. Large-scale analysis of yeast filamentous growth by systematic gene disruption and overexpression. Mol Biol Cell. 2008;19:284-96.
Johnston GC. Cell size and budding during starvation of the yeast Saccharomyces cerevisiae. J Bacteriol. 1977;132:738-9.
Johnston GC, Ehrhardt CW, Lorincz A, Carter BL. Regulation of cell size in the yeast Saccharomyces cerevisiae. J Bacteriol. 1979;137:1-5.
Jones S, Vignais ML, Broach JR. The CDC25 protein of Saccharomyces cerevisiae promotes exchange of guanine nucleotides bound to ras. Mol Cell Biol. 1991;11:2641-6.
Jorgensen P, Nishikawa JL, Breitkreutz BJ, Tyers M. Systematic identification of pathways that couple cell growth and division in yeast. Science. 2002;297:395-400.
Jorgensen P, Rupes I, Sharom JR, Schneper L, Broach JR, Tyers M. A dynamic transcriptional network communicates growth potential to ribosome synthesis and critical cell size. Genes Dev. 2004;18:2491-505.
Jorgensen P, Tyers M. How cells coordinate growth and division. Curr Biol. 2004;14:R1014-27.
Kuchin S, Vyas VK, Carlson M. Snf1 protein kinase and the repressors Nrg1 and Nrg2 regulate FLO11, haploid invasive growth, and diploid pseudohyphal differentiation. Mol Cell Biol. 2002;22:3994-4000.
Lamb TM, Mitchell AP. The transcription factor Rim101p governs ion tolerance and cell differentiation by direct repression of the regulatory genes NRG1 and SMP1 in Saccharomyces cerevisiae. Mol Cell Biol. 2003;23:677-86.
Lee P, Cho BR, Joo HS, Hahn JS. Yeast Yak1 kinase, a bridge between PKA and stress-responsive transcription factors, Hsf1 and Msn2/Msn4. Mol Microbiol. 2008;70:882-95.

Lempiainen H, Shore D. Growth control and ribosome biogenesis. Curr Opin Cell Biol. 2009;21:855-63.
Lempiainen H, Uotila A, Urban J, Dohnal I, Ammerer G, Loewith R, et al. Sfp1 interaction with TORC1 and Mrs6 reveals feedback regulation on TOR signaling. Mol Cell. 2009;33:704-16.
Lorincz A, Carter BLA. Control of Cell Size at Bud Initiation in Saccharomyces cerevisiae. J Gen Microbiol. 1979;113:287-95.
Madhani HD, Fink GR. Combinatorial control required for the specificity of yeast MAPK signaling. Science. 1997;275:1314-7.
Magherini F, Busti S, Gamberi T, Sacco E, Raugei G, Manao G, et al. In Saccharomyces cerevisiae an unbalanced level of tyrosine phosphorylation down-regulates the Ras/PKA pathway. Int J Biochem Cell Biol. 2006;38:444-60.
Marion RM, Regev A, Segal E, Barash Y, Koller D, Friedman N, et al. Sfp1 is a stress- and nutrient-sensitive regulator of ribosomal protein gene expression. Proc Natl Acad Sci U S A. 2004;101:14315-22.
McKinney JD, Chang F, Heintz N, Cross FR. Negative regulation of FAR1 at the Start of the yeast cell cycle. Genes Dev. 1993;7:833-43.
McKinney JD, Cross FR. FAR1 and the G1 phase specificity of cell cycle arrest by mating factor in Saccharomyces cerevisiae. Mol Cell Biol. 1995;15:2509-16.
Mitchison JM. The biology of the cell cycle. New York: Cambridge University Press; 1971.
Moriya H, Shimizu-Yoshida Y, Kitano H. In vivo robustness analysis of cell division cycle genes in Saccharomyces cerevisiae. PLoS Genet. 2006;2:e111.
Nern A, Arkowitz RA. A Cdc24p-Far1p-Gbetagamma protein complex required for yeast orientation during mating. J Cell Biol. 1999;144:1187-202.
Oehlen LJ, McKinney JD, Cross FR. Ste12 and Mcm1 regulate cell cycle-dependent transcription of FAR1. Mol Cell Biol. 1996;16:2830-7.
Oliveira AP, Patil KR, Nielsen J. Architecture of transcriptional regulatory circuits is knitted over the topology of bio-molecular interaction networks. BMC Syst Biol. 2008;2:17.
Palecek SP, Parikh AS, Kron SJ. Sensing, signalling and integrating physical processes during Saccharomyces cerevisiae invasive and filamentous growth. Microbiology. 2002;148:893-907.
Park SH, Koh SS, Chun JH, Hwang HJ, Kang HS. Nrg1 is a transcriptional repressor for glucose repression of STA1 gene expression in Saccharomyces cerevisiae. Mol Cell Biol. 1999;19:2044-50.
Peter M, Gartner A, Horecka J, Ammerer G, Herskowitz I. FAR1 links the signal transduction pathway to the cell cycle machinery in yeast. Cell. 1993;73:747-60.
Peter M, Herskowitz I. Direct inhibition of the yeast cyclin-dependent kinase Cdc28-Cln by Far1. Science. 1994;265:1228-31.
Roberts RL, Fink GR. Elements of a single MAP kinase cascade in Saccharomyces cerevisiae mediate two developmental programs in the same cell type: mating and invasive growth. Genes Dev. 1994;8:2974-85.
Robinson LC, Tatchell K. TFS1: a suppressor of cdc25 mutations in Saccharomyces cerevisiae. Mol Gen Genet. 1991;230:241-50.
Rossi RL, Zinzalla V, Mastriani A, Vanoni M, Alberghina L. Subcellular localization of the cyclin dependent kinase inhibitor Sic1 is modulated by the carbon source in budding yeast. Cell Cycle. 2005;4:1798-807.
Swinnen E, Wanke V, Roosen J, Smets B, Dubouloz F, Pedruzzi I, et al. Rim15 and the crossroads of nutrient signalling pathways in Saccharomyces cerevisiae. Cell Div. 2006;1:3.
Tamaki H, Yun CW, Mizutani T, Tsuzuki T, Takagi Y, Shinozaki M, et al. Glucose-dependent cell size is regulated by a G protein-coupled receptor system in yeast Saccharomyces cerevisiae. Genes Cells. 2005;10:193-206.
Toda T, Cameron S, Sass P, Zoller M, Wigler M. Three different genes in S. cerevisiae encode the catalytic subunits of the cAMP-dependent protein kinase. Cell. 1987;50:277-87.

Tyson CB, Lord PG, Wheals AE. Dependency of size of Saccharomyces cerevisiae cells on growth rate. J Bacteriol. 1979;138:92-8.
Urban J, Soulard A, Huber A, Lippman S, Mukhopadhyay D, Deloche O, et al. Sch9 is a major target of TORC1 in Saccharomyces cerevisiae. Mol Cell. 2007;26:663-74.
Varela JC, Praekelt UM, Meacock PA, Planta RJ, Mager WH. The Saccharomyces cerevisiae HSP12 gene is activated by the high-osmolarity glycerol pathway and negatively regulated by protein kinase A. Mol Cell Biol. 1995;15:6232-45.
Vinod PK, Sengupta N, Bhat PJ, Venkatesh KV. Integration of global signaling pathways, cAMP-PKA, MAPK and TOR in the regulation of FLO11. PLoS One. 2008;3:e1663.
Vinod PK, Venkatesh KV. Specificity of MAPK signaling towards FLO11 expression is established by crosstalk from cAMP pathway. Syst Synth Biol. 2007;1:99-108.
Vyas VK, Berkey CD, Miyao T, Carlson M. Repressors Nrg1 and Nrg2 regulate a set of stress-responsive genes in Saccharomyces cerevisiae. Eukaryot Cell. 2005;4:1882-91.
Vyas VK, Kuchin S, Carlson M. Interaction of the repressors Nrg1 and Nrg2 with the Snf1 protein kinase in Saccharomyces cerevisiae. Genetics. 2001;158:563-72.
Waldron C, Jund R, Lacroute F. Evidence for a high proportion of inactive ribosomes in slow-growing yeast cells. Biochem J. 1977;168:409-15.
Wei Y, Zheng XF. TORC1 association with rDNA chromatin as a mechanism to co-regulate Pol I and Pol III. Cell Cycle. 2009;8:3802-3.
Wiget P, Shimada Y, Butty AC, Bi E, Peter M. Site-specific regulation of the GEF Cdc24p by the scaffold protein Far1p during yeast mating. EMBO J. 2004;23:1063-74.
Zaman S, Lippman SI, Zhao X, Broach JR. How Saccharomyces responds to nutrients. Annu Rev Genet. 2008;42:27-81.
Zara G, Zara S, Pinna C, Marceddu S, Budroni M. FLO11 gene length and transcriptional level affect biofilm-forming ability of wild flor strains of Saccharomyces cerevisiae. Microbiology. 2009;155:3838-46.
Zeller CE, Parnell SC, Dohlman HG. The RACK1 ortholog Asc1 functions as a G-protein beta subunit coupled to glucose responsiveness in yeast. J Biol Chem. 2007;282:25168-76.
Zhou H, Winston F. NRG1 is required for glucose repression of the SUC2 and GAL genes of Saccharomyces cerevisiae. BMC Genet. 2001;2:5.

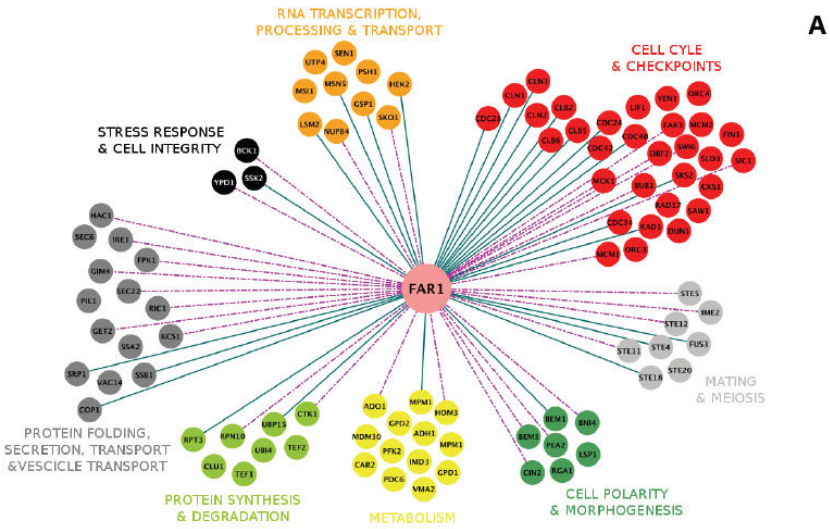
A
RNA TRANSCRIPTION,
PROCESSING & TRANSPORT
CELL CYLE
& CHECKPOINTS
STRESS RESPONSE
& CELL INTEGRITY
FAR1
MATING
& MEIOSIS
PROTEIN FOLDING,
SECRETION, TRANSPORT
&VESCICLE TRANSPORT
PROTEIN SYNTHESIS
& DEGRADATION
METABOLISM
CELL POLARITY
& MORPHOGENESIS

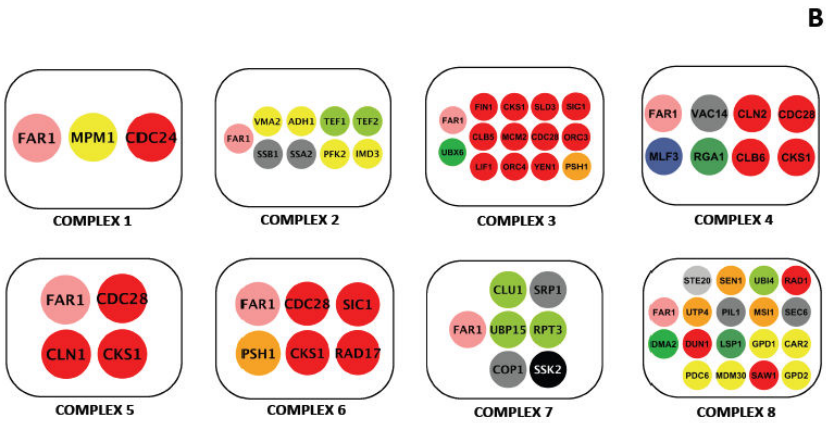
B
FAR1 MPM1 CDC24
COMPLEX 1
FAR1 VMA2 ADH1 TEF1 TEF2 SSB1 SSA2 PFK2 IMD3
COMPLEX 2
FAR1 FIN1 CKS1 BLD3 SIC1 CLB5 MCM2 CDC28 ORC3 UBX6 LIF1 ORC4 YEN1 PSH1
COMPLEX 3
FAR1 VAC14 CLN2 CDC28 MLF3 RGA1 CLB6 CKS1
COMPLEX 4
FAR1 CDC28 CLN1 CKS1
COMPLEX 5
FAR1 CDC28 SIC1 PSH1 CKS1 RAD17
COMPLEX 6
CLU1 SRP1 FAR1 UBP15 RPT3 COP1 SSK2
COMPLEX 7
STE20 SEN1 UBI4 RAD1 FAR1 UTP4 PIL1 MSI1 SEC6 DMA2 DUN1 LSP1 GPD1 CAR2 PDC6 MDM30 SAW1 GPD2
COMPLEX 8

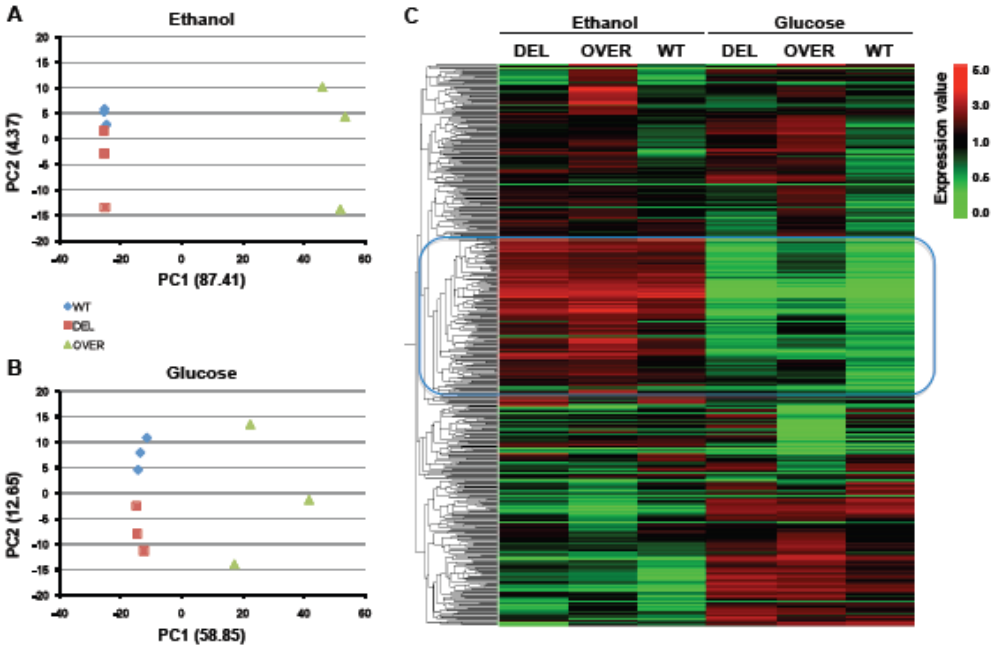
A
Ethanol
PC2 (4.37)
PC1 (87.41)
WT
DEL
OVER
B
Glucose
PC2 (12.65)
PC1 (58.85)
C
Ethanol
Glucose
DEL
OVER
WT
DEL
OVER
WT
Expression value
5.0
3.0
1.0
0.5
0.0

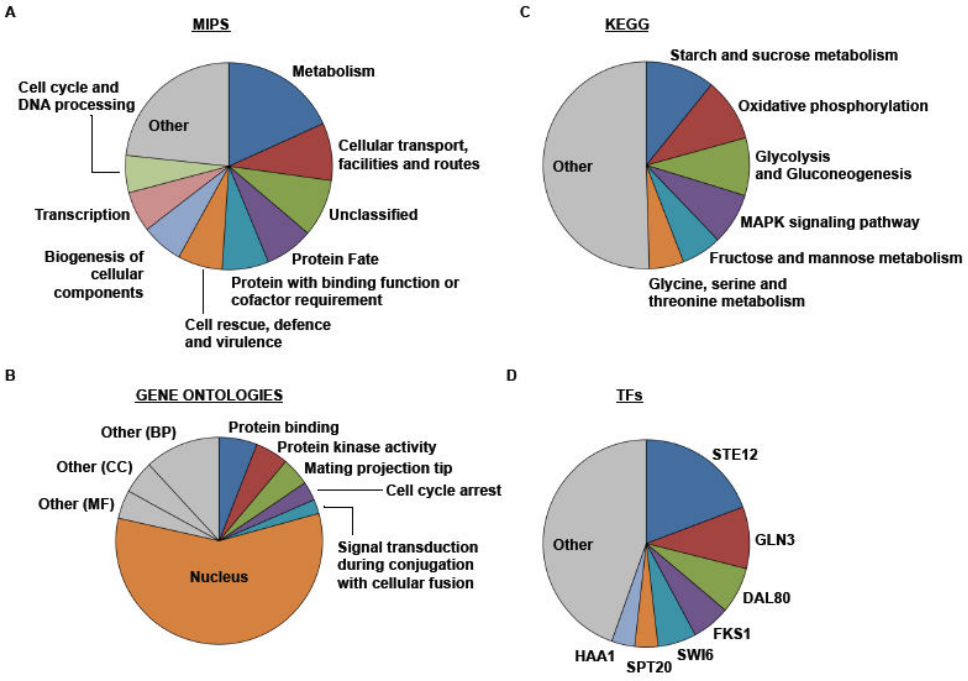
A
MIPS
Metabolism
Cellular transport, facilities and routes
Unclassified
Protein Fate
Protein with binding function or cofactor requirement
Cell rescue, defence and virulence
Biogenesis of cellular components
Transcription
Cell cycle and DNA processing
Other
C
KEGG
Starch and sucrose metabolism
Oxidative phosphorylation
Glycolysis and Gluconeogenesis
MAPK signaling pathway
Fructose and mannose metabolism
Glycine, serine and threonine metabolism
Other
B
GENE ONTOLOGIES
Protein binding
Protein kinase activity
Mating projection tip
Cell cycle arrest
Signal transduction during conjugation with cellular fusion
Nucleus
Other (BP)
Other (CC)
Other (MF)
D
TFs
STE12
GLN3
DAL80
FKS1
SWI6
SPT20
HAA1
Other

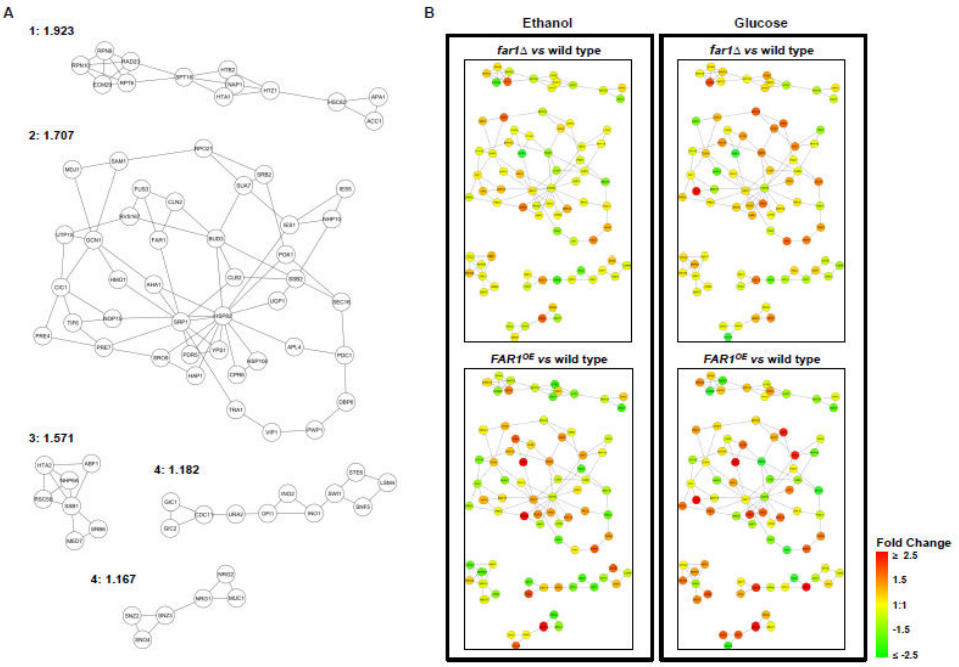
A
1: 1.923
2: 1.707
3: 1.571
4: 1.182
4: 1.167
B
Ethanol
Glucose
far1Δ vs wild type
far1Δ vs wild type
FAR1OE vs wild type
FAR1OE vs wild type
Fold Change
≥ 2.5
1.5
1:1
-1.5
≤ -2.5

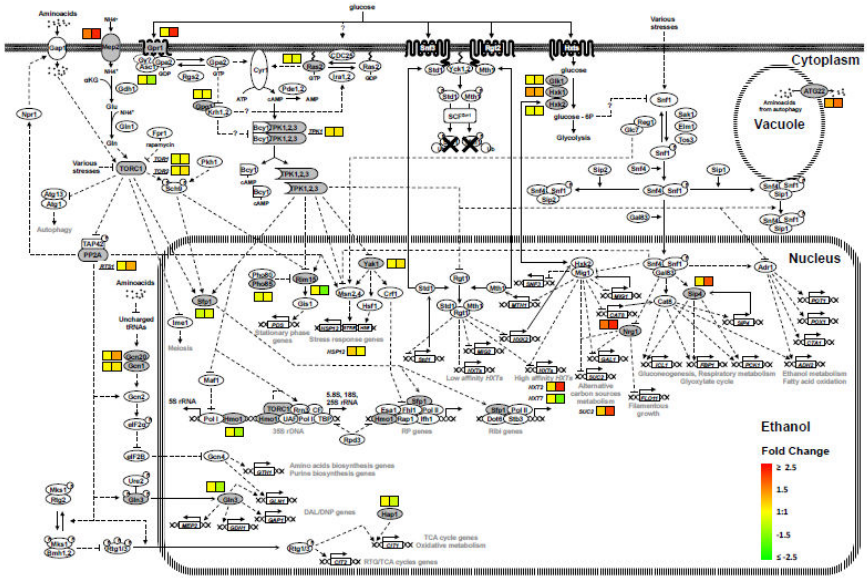
Cytoplasm
Vacuole
Nucleus
Ethanol
Fold Change
≥ 2.5
1.5
1:1
-1.5
≤ -2.5

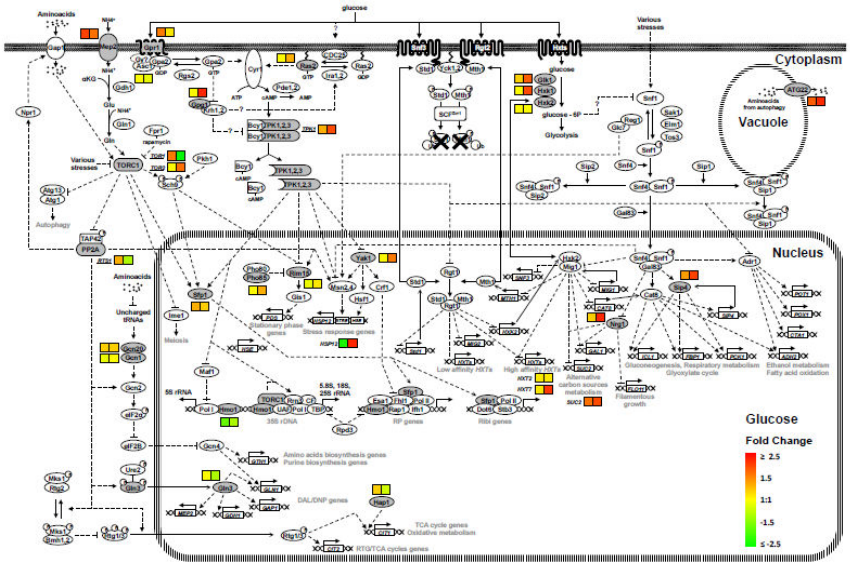
Cytoplasm
Vacuole
Nucleus
Glucose
Fold Change
≥ 2.5
1.5
1:1
-1.5
≤ -2.5

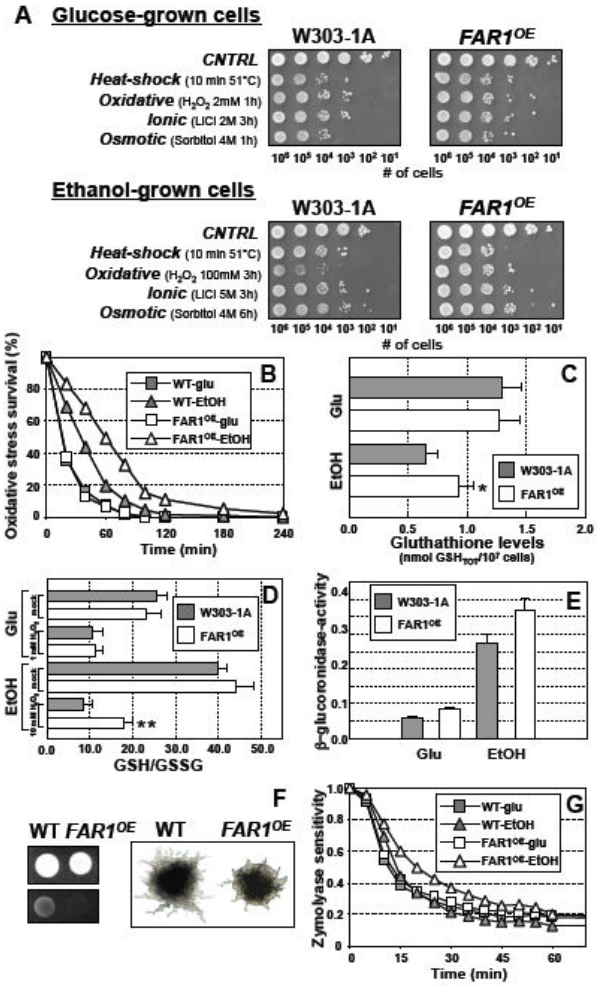
A
Glucose-grown cells
W303-1A
FAR1OE
CNTRL
Heat-shock (10 min 51°C)
Oxidative (H2O2 2mM 1h)
Ionic (LICl 2M 3h)
Osmotic (Sorbitol 4M 1h)
10⁶ 10⁵ 10⁴ 10³ 10² 10¹
# of cells
Ethanol-grown cells
W303-1A
FAR1OE
CNTRL
Heat-shock (10 min 51°C)
Oxidative (H2O2 100mM 3h)
Ionic (LICl 5M 3h)
Osmotic (Sorbitol 4M 6h)
10⁶ 10⁵ 10⁴ 10³ 10² 10¹
# of cells
B
Oxidative stress survival (%)
WT-glu
WT-EtOH
FAR1OE-glu
FAR1OE-EtOH
Time (min)
C
Glu
EtOH
W303-1A
FAR1OE
Gluthathione levels
(nmol GSHtot/10⁷ cells)
D
Glu
EtOH
W303-1A
FAR1OE
GSH/GSSG
E
β-glucoronidase-activity
W303-1A
FAR1OE
Glu
EtOH
F
WT FAR1OE
WT
FAR1OE
G
Zymolyase sensitivity
WT-glu
WT-EtOH
FAR1OE-glu
FAR1OE-EtOH
Time (min)

Figure 6

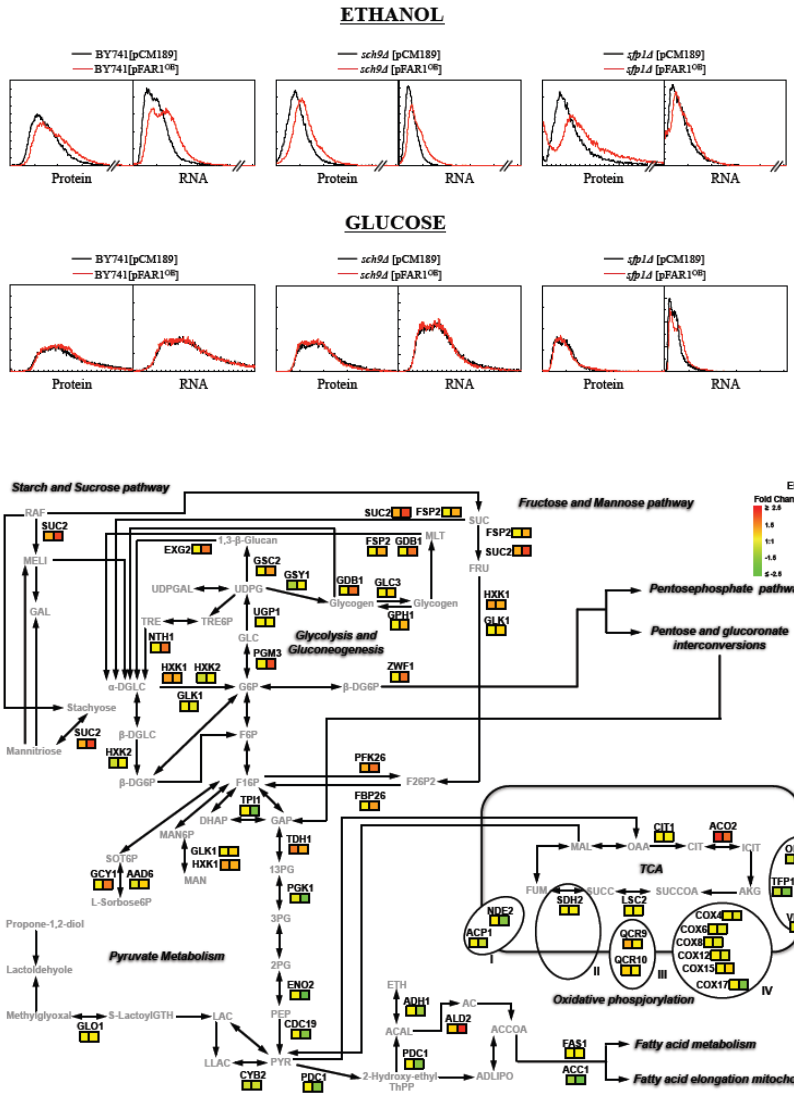
ETHANOL
BY741[pCM189]
BY741[pFAR1OE]
sch9Δ [pCM189]
sch9Δ [pFAR1OE]
sfp1Δ [pCM189]
sfp1Δ [pFAR1OE]
Protein
RNA
GLUCOSE
Starch and Sucrose pathway
Fructose and Mannose pathway
Glycolysis and Gluconeogenesis
Pentosephosphate pathway
Pentose and glucoronate interconversions
Pyruvate Metabolism
TCA
Oxidative phosphorylation
Fatty acid metabolism
Fatty acid elongation mitochondria
Ethanol
Fold Change

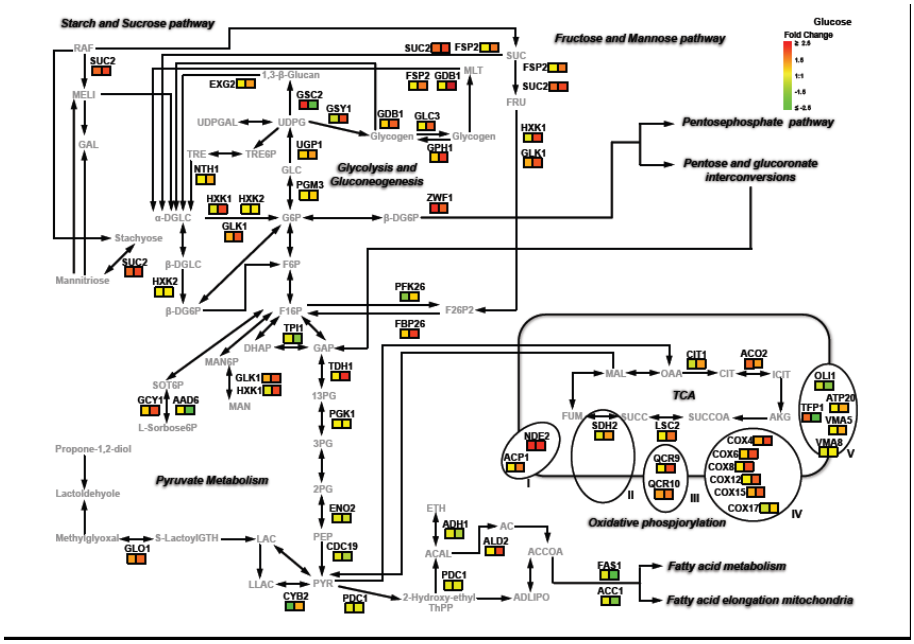
Starch and Sucrose pathway
Fructose and Mannose pathway
Glucose
Fold Change
Pentosephosphate pathway
Pentose and glucoronate interconversions
Glycolysis and Gluconeogenesis
TCA
Pyruvate Metabolism
Oxidative phospjorylation
Fatty acid metabolism
Fatty acid elongation mitochondria
RAF
MELI
GAL
Mannitriose
Stachyose
α-DGLC
β-DGLC
β-DG6P
G6P
F6P
F16P
F26P2
β-DGGP
DHAP
GAP
MAN6P
SOT6P
MAN
L-Sorbose6P
13PG
3PG
2PG
PEP
PYR
LAC
LLAC
S-LactoylGTH
Methylglyoxal
Lactoldehyole
Propone-1,2-diol
UDPGAL
UDPG
Glycogen
TRE
TRE6P
GLC
SUC
FRU
MLT
1,3-β-Glucan
ETH
ACAL
AC
ACCOA
ADLIPO
2-Hydroxy-ethyl ThPP
MAL
OAA
CIT
ICIT
AKG
SUCCOA
SUCC
FUM
SUC2
FSP2
GDB1
GLC3
GPH1
EXG2
GSC2
GSY1
UGP1
NTH1
PGM3
HXK1
HXK2
GLK1
ZWF1
PFK26
FBP26
TPI1
TDH1
PGK1
ENO2
CDC19
PDC1
CYB2
ADH1
ALD2
FAS1
ACC1
CIT1
ACO2
NDE2
ACP1
SDH2
LSC2
QCR9
QCR10
COX4
COX6
COX8
COX12
COX13
COX17
OLI1
ATP20
TFP1
VMA5
VMA8
V
I
II
III
IV
GCY1
AAD6
GLO1
PDC1

Nel lievito gemmante *Saccharomyces cerevisiae*, organismo modello per gli studi sul ciclo cellulare, la precisa coordinazione tra crescita e divisione cellulare ha luogo a Start, un'area di regolazione del ciclo cellulare posizionata prima della fase S, tra G_1-S. Subito dopo Start la cellula può cominciare un nuovo ciclo mitotico. L'esecuzione di Start richiede che la cellula abbia raggiunto un volume cellulare critico (contenuto proteico per l'inizio della replicazione del DNA, Ps) richiesto per entrare in fase S. Ps aumenta in relazione alla ploidia ed è modulato dai nutrienti. Studi condotti nel nostro laboratorio hanno suggerito che Far1, l'inibitore delle chinasi ciclina-dipendente (Cki), e Cln3, una ciclina di fase G_1, potrebbero costituire una soglia che controlla l'entrata in fase S. L'overespressione del gene *FAR1* induce un aumento cellulare modulato dai nutrienti (Alberghina et al., 2004). Mediante un'analisi di trascrittomica genome-wide di cellule overesprimenti il gene *FAR1* e cellule *far1Δ* cresciute in terreno contenente o etanolo oppure glucosio, il nostro gruppo ha dimostrato che l'overespressione di Far1 induce un grande rimodellamento trascrizionale in grado di influenzare pathways coinvolti nel controllo della crescita cellulare, incluso il pathway deputato al sensing del glucosio (che influenza il tasso di crescita cellulare) e PKA e TOR che sono i maggiori pathways deputati alla regolazione della crescita cellulare nel lievito. Sch9 ed Sfp1 sono due proteine *targets* che si trovano a monte del pathway di Tor, pathway richiesto per il controllo della crescita cellulare mediante la regolazione della sintesi proteica. Entrambe queste proteine sono state identificate in uno screening genome-wide per mutanti di ridotte dimensioni (*whi*). Perciò eravamo interessati a vedere se l'aumento in dimensioni cellulari (RNA e proteine) mediato dall'overespressione di *FAR1* era mediato da Sfp1 e Sch9. L'effetto dell'overespressione di *FAR1* sui parametri riguardanti la massa cellulare dei ceppi wild type BY4741 (ceppo isogenico, mutanti *sch9Δ* e *sfp1Δ*), cresciuti in terreno sintetico addizionato o di etanolo o di glucosio come fonte di carbonio, sono risultati molto simili a quelli ottenuti con il ceppo nel *background* W303. I deleti *sfp1Δ* e *sch9Δ* son molto più piccoli del wild type sia in glucosio (Jorgensen et al., 2002; Jorgensen et al., 2004) che in etanolo. Come già osservato in cellule wild type, in entrambi i mutanti l'overespressione di *FAR1* ha solo effetti minori sulle dimensioni cellulari quando le cellule crescono in glucosio.

L'overespressione di *FAR1* non induce una variazione nel tempo di duplicazione nel ceppo *sch9Δ* cresciuto in glucosio, diversamente *sfp1Δ* overesprimente il gene *FAR1* risulta "malaticcio" con un aumento notevole nel tempo di duplicazione. Complessivamente l'aumento nel volume cellulare risulta drammatico in etanolo, mentre nel ceppo wild type ed *sch9Δ* l'aumento del volume dipende da un aumento bilanciato in RNA e proteine, nel ceppo *sfp1Δ* l'aumento in contenuto proteico non è accompagnato da un concomitante aumento in RNA, come ben dimostrato dalle analisi al FACS e dosaggi chimici.

Questo dato sta ad indicare che Sfp1 è richiesto per mantenere il giusto accoppiamento RNA e sintesi proteica quando Far1 è overespresso in cellule cresciute in etanolo.

Il lievito *S. cerevisiae* necessita di regolare la crescita ed il ciclo cellulare a seguito di cambiamenti nelle condizioni di crescita, quindi proliferando rapidamente se dispone di nutrienti, e cessando o rallentando la crescita in caso contrario. Nutrienti come il glucosio devono quindi generare segnali che vengano ricevuti ed elaborati dal complesso macchinario che governa crescita e progressione del ciclo cellulare.
Di conseguenza, il lievito ha evoluto molti meccanismi per monitorare il livello di glucosio: i pathways cAMP-PKA (che coinvolgono Ras ed il modulo Gpr1-Gpa2), Rgt2/Snf3-Rgt1 pathway e il "*main repression pathway*" che vede coinvolta la chinasi Snf1. Per poter capire se l'effetto del glucosio sul dimensioni cellulari era dovuto alla sua funzione di nutriente, che richiede il suo stesso metabolismo, oppure alla sua natura di molecola segnale, abbiamo analizzato ceppi di lievito in cui uno o più *pathways* deputati al *sensing* del glucosio erano modificati a causa di delezioni di uno o più geni codificanti recettori. Abbiamo quindi deletato *GPR1* che codifica per un sensore dell'alto glucosio, *SNF3* codificante un sensore del basso glucosio ed *RGT2* codificante recettore per l'alto glucosio. Il ceppo *gpa2Δ gpr1Δ* non mostra sostanziali modifiche nel tempo di duplicazione se confrontato con il ceppo isogenico nelle stesse condizioni di crescita, mentre il contenuto proteico è decisamente inferiore. In entrambi i ceppi *snf3Δ rgt2Δ* e *snf3Δ rgt2Δ gpa2Δ gpr1Δ* il basso contenuto proteico è accompagnato da un aumento nel tempo di duplicazione, se confrontato con il ceppo wild type. In quest'ultimo esiste una forte correlazione tra contenuto proteico e tempo di duplicazione in cellule cresciute in glucosio, mentre quando le cellule vengono fatte crescere in etanolo, esiste un drammatico aumento nel tempo di duplicazione, non accompagnato però da una diminuzione cosi forte in contenuto proteico. Lo stesso *trend* si può osservare nei mutanti deleti nei sensori per il glucosio, che perciò mantengono, almeno in parte, la capacità di modulare le dimensioni cellulari. Anche se i dettagli più sottili del metabolismo potrebbero differire tra wild type e mutanti, il tipo di metabolismo rimane uguale (ex. tutti i mutanti crescono in glucosio usando un metabolismo di tipo fermentativo). Questi risultati suggeriscono che, in condizioni di crescita esponenziale bilanciata, la dimensione cellulare è *guidata* dal metabolismo, ma gli *aggiustamenti fini,* del contenuto proteico sono settati in accordo con la percezione del glucosio extracellulare. In conclusione, questo lavoro mette in luce che gli elementi coinvolti nella determinazione delle dimensioni cellulari sono molteplici, ed interconnessi. Notevoli alterazioni nelle dimensioni e nel contenuto proteico cellulare possono derivare non solo da alterazioni nel dosaggio di geni coinvolti nel meccanismo molecolare della soglia che controlla il Ps, ma anche dalle condizioni ambientali. Di particolare rilevanza risulta l'osservazione che l'effetto esercitato dal glucosio è dovuto non solo alle sue funzioni di molecola segnale, ma anche come modulatore molecolare.